DISSERTATION

CROP DOMESTICATION IMPACTS ON RHIZOSPHERE INTERACTIONS AND NITROGEN ACQUISITION

Submitted by

Siwook Hwang

Graduate Degree Program in Ecology

In partial fulfillment of the requirements

For the Degree of Doctor of Philosophy

Colorado State University

Fort Collins, Colorado

Fall 2024

Doctoral Committee:

Advisor: Steven J. Fonte

Megan B. Machmuller
Timothy E. Crews
Kelly C. Wrighton
Claudia M. Boot

ABSTRACT

CROP DOMESTICATION IMPACTS ON RHIZOSPHERE INTERACTIONS

AND NITROGEN ACQUISITION

Synthetic nitrogen (N) fertilizer is an essential pillar of modern industrial agriculture. Production and application of synthetic N fertilizer, however, are two of the most expensive, energy intensive, and environmentally deleterious processes in agriculture. Therefore, alternative means of providing N in an agroecosystem are of great interest in sustainable agriculture. While many solutions – from cover cropping to intercropping – have been suggested over time it remains unclear if the modern high-yielding crops can thrive in these alternative N conditions. Decades of breeding under high synthetic N input as well as the inherently annual nature of these modern cereal crops may prevent them from fully taking advantage of these alternative N sources. In this dissertation, I explored the impact of domestication on crop rhizosphere interactions and N acquisition, in both retrospective and prospective terms.

First, I investigated how modern maize (*Zea mays* subsp. *mays*), and its wild relative Teosinte (*Zea mays* subsp. *parviglumis*) differed in their ability to adapt to, and take up, cover crop residue N and synthetic N inputs. We designed a ^{13}C (carbon)/^{15}N dual isotope labeling experiment in which we compared the C allocation patterns of modern maize and teosinte in response to synthetic (urea) and organic (cover crop residue) forms of N. Teosinte responded to organic N by increasing its biomass root-to-shoot (R:S) ratio by 50% compared to synthetic N, while modern maize maintained the same biomass R:S ratios in

both N treatments. Recent photosynthate R:S ratio (measured using ^{13}C-CO_2, 7 weeks after establishment) was greater in organic N than in synthetic N treatments for both modern maize and teosinte (91% and 37%; respectively). Label-derived dissolved organic C (DOC), representing recent rhizodeposits, was 2.5 times greater in the organic N treatments for both genotypes. Modern maize took up a similar amount of organic N as teosinte using different C allocation strategies. Our findings suggest that intensive breeding under high N input conditions has not affected this modern maize hybrid's access to organic N sources while improving its ability to take up synthetic N.

Next, I shifted my focus to the novel perennial grains Kernza and perennial wheat. Kernza® is a domesticated intermediate wheatgrass (IWG, *Thinopyrum intermedium*). Perennial wheat is a hybrid between Kernza/IWG and modern annual durum wheat (*Triticum turgidum* subsp. *durum*). Kernza, in addition to being a perennial, may still possess beneficial belowground traits that may have been lost in modern cereals through millennia of aboveground-focused plant breeding. If so, such traits may be passed down to perennial wheat.

To characterize root architecture, exudate profiles, and microbial communities of Kernza and perennial wheat in relation to annual wheat, I conducted a greenhouse experiment. We grew three genotypes/species (Kernza, perennial wheat, annual wheat) and collected their root exudates after 8 weeks of growth. The exudates were analyzed via LC-MS/MS for their chemical composition. We extracted DNA from rhizosphere soils and sequenced them for 16S and ITS profiles. Lastly, we scanned the roots to analyze root distribution across different diameter classes. We found that perennial wheat invested more heavily into very

fine (< 250 µm) roots compared to annual wheat and Kernza. Perennial wheat also exuded at a greater rate of exudates per amount of root biomass. We suspect that the greater proportion of very fine roots in perennial wheat led to greater surface area and greater specific exudation rate, and that this may be related to hybrid vigor. We did not find evidence of a genotype effect on root exudate or microbial community composition. However, root exudates (overall metabolite profiles) significantly correlated with root architecture (distribution of root volume over different diameter classes) and the microbial community composition. These interactions represent a potential pathway through which plants can exert influence over the rhizosphere microbial community. Overall, these results emphasize the importance of root architecture in mediating belowground interactions. Understanding rhizosphere dynamics and the response to domestication and hybridization can guide further development of robust perennial cereal crops.

In a third experiment, I studied how Kernza, perennial wheat, and annual responded to cereal-legume intercropping (biculture) in the field. To do so, we planted each of the three genotypes in monoculture or in biculture with alfalfa (*Medicago sativa*). We sampled their rhizosphere over two growing seasons and extracted soil DNA to construct rhizosphere 16S and ITS profiles. We hypothesized that 1) rhizosphere microbial community composition of annual wheat and Kernza will be most dissimilar from each other with perennial wheat intermediate, and 2) microbial community composition will shift in biculture, with the greatest change in Kernza and the smallest in annual wheat. We found that the rhizosphere 16S profiles differed significantly from the other two genotypes but the 16S profile of perennial wheat did not differ from that of annual wheat. Perennial wheat seemingly

inherited microbial recruitment traits of its annual parent more so than its perennial parent's. Interestingly, inclusion of legumes led to the convergence, rather than divergence, of 16S profiles among genotypes. We postulate that the competitive pressure of alfalfa may have led to this convergence of 16S profiles across genotypes. The fungal community did not show evidence of genotype effect. However, the fungal community composition changed over two years in monoculture but not in biculture. This result implies that fungal community may become distinct over time if it is influenced by only one genotype (i.e., monoculture) rather than two (i.e., biculture). In conclusion, we found evidence of genotype-driven microbial community assembly that changed with legume's competitive pressure. The inheritability of microbial assembly was present but skewed towards the annual parent. Our study demonstrates the importance of including rhizosphere interactions in our evaluation of novel cereal crops in and out of cereal-legume biculture.

In a final study, I investigated how rhizosphere microbial ecology of these three genotypes (Kernza, annual wheat, and perennial wheat) could be linked to their ability to acquire N from neighboring alfalfa plants. We designed a greenhouse study in which we planted all three cereals in monoculture or in biculture with alfalfa and used ^{15}N leaf feeding technique to track the movement of N from alfalfa to cereals. In addition, we also extracted DNA from the soil and sequenced it for 16S rRNA profiles. Arbuscular mycorrhizal fungi (AMF) infection rate was also measured on all cereals and legumes. We hypothesized that: 1) annual wheat would produce the greatest biomass but Kernza would have highest proportion of legume derived N in its biomass, 2) all microbial communities will shift in biculture, with the greatest change in Kernza and the smallest in annual wheat, and 3)

Kernza would have the highest rate of infection from AMF, especially in biculture. Surprisingly, we found no evidence of genotype or cropping system (monoculture or biculture) effect on either proportion or absolute amount of N derived from legume. We did find, however, that DOC concentration was higher in cereal rhizosphere grown in biculture than in monoculture, suggesting greater belowground investment in exudates when the grasses are grown with a legume. Despite this trend, annual wheat had much lower microbial biomass carbon (MBC) level in its rhizosphere compared to the perennials, in biculture. We contended that this may be due to substrate suitability of annual wheat's rhizodeposit. We also found that AMF infection rate was in fact the lowest in Kernza. Lastly, we found that 16S profiles of all three cereals shifted towards that of alfalfa in biculture. This trend might suggest microbial spillover, wherein rhizosphere microbial community of one genotype colonizes that of a neighboring plant, from alfalfa rhizosphere. Overall, we demonstrated that quantifying the N transfer in the rhizosphere can provide important insight into how these genotypes may be inducing changes in soil biogeochemistry in response to neighboring legumes.

In summation, this dissertation provides links between crop genotype, root exudate chemistry and rate, microbial community assembly, and their biogeochemical consequences, in alternative N environments. Deepened understanding of how complex rhizosphere interactions may affect internal N cycling could be leveraged to further optimize these unique systems such as perennial cereal-legume biculture. In doing so, we will be one step closer to a more sustainable future, that is less reliant on synthetic N fertilizers.

ACKNOWLEDGEMENTS

First and foremost, I must thank Steve Fonte for being the best PhD advisor one could ask for, often putting his students' success and wellbeing ahead of everything else. I must also thank my committee members, Megan Machmuller, Tim Crews, Kelly Wrighton, and Claudia Boot for supporting me and pushing me to become a better scientist. The staff members at Agriculture Research Development and Education Center (ARDEC), Plant Growth Facility (PGF), and EcoCore all went above and beyond to help an unexperienced PhD student realize their (often lofty) ideas. Of course, this dissertation would not have happened without contribution from my other coauthors; Amélie Gaudin, who supported me from afar through my tumultuous first manuscript (Chapter 2 of this dissertation); Joe Brummer, who cared for my research plots like they were his own; Lady Grant, Bridget McGivern, and Laura Mason who made me look like a competent microbial ecologist; Paul Mathews, who made me look like a competent analytical chemist; Liz Koziol, who took on the tedious task of counting mycorrhizal hyphae. Lastly, I thank those who have endured hours of weeding, sieving, griding, and washing alongside me: Sarah Harper, Bo Collins, Carolita Landers, Cole Goldman, Oliver Hoffman, Lexee Wilson, Jonathan Asphaug, Tad Trimarco, Tayin Wang, and Hannah Mitchell. I also thank those who provided funds for this project as well as my time through graduate school. The Foundation for Food and Agriculture Research, along with the Perennial Agriculture Project (joint project of the Land Institute and the Malone Family Land Preservation Foundation), put their trust in me, and for that I am eternally grateful. The second chapter of this dissertation was also supported by USDA NIFA postdoctoral fellowship grant awarded to Megan Machmuller (award# 2017-

67012-26112). This research was performed on the land belonging to Arapaho, Cheyenne, Lakota, and Ute people.

DEDICATION

To Quinn, to my parents, and to all those that came before me who dared to ask, "our bodies make soil of the ground, but what about what we do now?"

TABLE OF CONTENTS

CHAPTER 1: INTRODUCTION

1.1. The nitrogen problem

Decades of technological leaps following the Green Revolution have birthed a behemoth that is modern industrial agriculture. Synthetic N fertilizer is an integral part of this machinery and has contributed greatly to its development. The Haber-Bosch process has allowed humanity to artificially fix N from the atmosphere and manufacture synthetic N fertilizer at industrial scale, which in turn contributed to a sharp increase in food production (Smil, 2001). As Smil (2001) famously put, 40% of humanity now owe their existence to the Haber-Bosch process.

However, this awe-inspiring development comes with some heavy costs. These costs all originate from the energy-intensive nature of artificial N fixation. Production of synthetic fertilizer is an energetically demanding process that make up around 30% of all annual agriculture related energy expenditure in the US (based on 2014 data; Hitaj and Suttles, 2016). This high energetic cost often translates to high financial costs. In 2023, fertilizers and other soil amendments amounted to about 12% of all on-farm operating costs in the United States (USDA National Agricultural Statistics Service, 2024).

The energy-intensive nature of fertilizer production also means it contributes greatly to greenhouse gas (GHG) emissions. In 2018, production of N fertilizer emitted around 440 Mt CO_2e globally, which is nearly 5% of all GHG emission attributed to agriculture for that year (Food and Agriculture Organization, 2018; Menegat *et al.*, 2022).

Even though we invest vast amount of energy and money into manufacturing N fertilizers, around half of this N is lost before being taken up by crops (Coskun *et al*., 2017). Not only does this loss of N represent an enormous waste of energy, but it also leads to further environmental harm. Fertilizer N lost via leaching (often in the form of nitrate (NO_3^-), can cause eutrophication downstream and cause health issues if found in drinking water in high concentration (Vitousek *et al*., 1997; Townsend *et al*., 2003; Coskun *et al*., 2017). Fertilizer N can also be lost in the form of N_2O, a powerful GHG, further adding to the overall GHG emission attributed to fertilizer use (Coskun *et al*., 2017). In 2018, such gaseous loss was estimated to be around 450 Mt CO_2-eq globally, and amounted to yet another 5% of all agriculture related GHG emissions that year (Food and Agriculture Organization, 2018; Menegat *et al*., 2022).

Given its reliance on energy-intensive manufacturing process, detrimental environmental impacts, and lingering efficiency issues, alternative sources of N have been a focal point of efforts to achieve more sustainable agricultural systems through the years.

1.2. Legumes as an N source

Some of the solutions rely on the increased use of legumes (Crews and Peoples, 2004). Legumes recruit and foster microbes that can fix N from the atmosphere (biological N fixation; BNF), but without reliance on fossil fuels (Crews and Peoples, 2004). Humanity has been leveraging BNF for soil fertility for a very long time, and some of those practices are still common today.

One such example is cover cropping. Cover cropping involves growing non-crop plant species between periods of main crop cultivation (Parr *et al*., 2011). Cover crops often include legume species to provide N for subsequent crops in the rotation. Though amount of legume-derived N available to the following cash crop can vary widely, one study estimates that up to 170 kg N ha^{-1} was biologically fixed by hairy vetch cover crop (Parr *et al*., 2011), indicating that N-fixing cover crops can provide most if not all the N required by the subsequent cash crop.

Another solution involving legumes is intercropping. If cover cropping incorporates legumes in time, intercropping incorporates legumes in space. In intercropped plots, one crop is planted next to another crop, often in alternating rows. When one of the planted crops is a legume, it can act as a N source for the neighboring cereal, with one study reporting that up to 30% of legume N ended up in neighboring grass 60 days later (Rasmussen et al., 2019a).

1.3. Domestication and breeding problem

One aspect of modern industrial agriculture may complicate the implementation of these solutions. Recent breeding efforts for many modern crops have occurred in high-input (including synthetic N) systems and thus newer varieties may be optimized for those systems. As a result, modern crops boast higher yield compared to their progenitors but they may have also lost traits that would allow better access to alternative forms of N (e.g., from cover crops or manure) that likely dominated before the green revolution (Isaac *et al*., 2021).

For example, taking up cover crop residue N requires depolymerization and mineralization of these larger organic molecules into smaller monomers or inorganic forms of N (Daly *et al.*, 2021). These processes are performed by soil microbes, whom plants can recruit and assemble by modulating root exudate rate or chemistry (Zhalnina *et al.*, 2018; Daly *et al.*, 2021). Some have questioned to what extent modern crop varieties can still recruit beneficial microbes able to mineralize cover crop residue into plant available N (Pérez-Jaramillo *et al.*, 2016). Furthermore, rhizodeposits by plants have been shown to increase microbial degradation of soil organic matter (SOM) leading to greater N availability (de Graaff *et al.*, 2009). Since modern breeding has focused its attention on maximizing aboveground biomass/yield, it is possible that we inadvertently selected against belowground resource allocation that would increase soil N availability (Isaac *et al.*, 2021).

Acquiring N from an intercropped legume is yet another matter. There exists a myriad of different pathways that N could take from legumes into neighboring cereals (Høgh-Jensen, 2006). One indirect pathway is through depolymerization, mineralization, and uptake of N from legume above and belowground residues (Høgh-Jensen, 2006). Other pathways are a bit more direct, such as direct root-to-root transfer, wherein small, N-rich compounds are exuded by legume roots and quickly taken up by nearby cereal roots (Høgh-Jensen, 2006). Another is through common mycorrhizal networks (CMNs), wherein the same arbuscular mycorrhizal fungi infect both legumes and cereals and facilitate movement of N between the two plants (He *et al.*, 2003). Taking advantage of these two direct pathways would be predicated by certain rhizosphere traits – different root morphology to better reach legume roots for root-to-root transfer or greater arbuscular mycorrhizal fungi symbiosis leading to

greater chance of CMN-mediated N acquisition (He *et al*., 2003; Høgh-Jensen, 2006). Again, selective pressure for greater yield under high synthetic N input system could have inadvertently selected against the beneficial rhizosphere traits (Pérez-Jaramillo *et al*., 2016; Isaac *et al*., 2021).

Indeed, there is evidence to suggest domestication and/or intensive breeding affect root architecture (Gioia *et al*., 2015; Isaac *et al*., 2021), root exudate chemistry (Iannucci *et al*., 2017), and microbial community assembly (Pérez-Jaramillo *et al*., 2016; Brisson *et al*., 2019)., but the overall impact on rhizosphere processes and crop N nutrition remains poorly understood.

1.4. Wild crop relatives and novel perennial crops

Exploring how domestication and breeding interact with these alternative N sources (i.e., cover crop and cereal-legume biculture) is the main objective of the following chapters. In chapter 2, I compare modern maize with teosinte, its wild crop relative. Since teosinte has survived in the wild for the past 10,000 years, there is reason to believe that it would be better adapted to low synthetic N, high organic N environments (Doebley, 2004). In this experiment I used both ^{13}C and ^{15}N stable isotopes to track the movement of C (plant resource allocation pattern) and N (nutrient acquisition pattern).

Next, I consider newly developed perennial grain crops and examine to what extent they can manipulate their rhizosphere communities to take advantage of intercropped legume N. Kernza® and perennial wheat are both novel perennial cereal crops with great agroecological promise. The former is domesticated intermediate wheatgrass (IWG,

Thinopyrum intermedium) and the latter is a hybrid between IWG and an annual durum wheat (*Triticum turgidum* subsp. *durum*) (DeHaan *et al*., 2023). Kernza, only recently domesticated, may still possess beneficial root traits that allow for greater N uptake in cereal-legume intercrops. Perennial wheat, being a hybrid of IWG and annual wheat, may have inherited some of these beneficial traits. It is worth noting that perennial cereal grains hold promise for ecological benefits far beyond the realm of N uptake. They have potential to regenerate soil health across agricultural landscapes through reduced/eliminated need for tillage and extensive root systems that can rebuild SOM (Crews *et al*., 2016).

For Chapter 3, I examined Kernza, perennial wheat, and annual durum wheat in monoculture. This experiment was performed in a greenhouse under a more controlled environment that allowed me to gain a mechanistic understanding of plant-rhizosphere interactions. I analyzed root architecture, exudation rate and chemical composition, and soil microbial communities to understand how these traits may influence one another.

Chapter 4 describes results from a field trial in which I planted the three cereals in and out of cereal-legume intercrops. I analyzed microbial community composition to evaluate how cereal genotype modulates soil microbial communities under more realistic field conditions.

Lastly, in Chapter 5, I report on another greenhouse experiment in which I examine the flow of N transferred from a legume (alfalfa) into perennial cereals (Kernza, perennial wheat). I measured the rhizosphere microbial community composition to ascertain whether microbial community affects amount of N transferred from legume to cereals.

CHAPTER 2: A TEOSINTE AND MODERN MAIZE HYBRID USE DIFFERENT CARBON ALLOCATION STRATEGIES IN RESPONSE TO COVER CROP RESIDUE NITROGEN[1]

2.1. Introduction

Modern maize (*Zea mays* subsp. *mays)* and one of its wild relatives, Balsas teosinte (*Zea mays* subsp. *parviglumis*; hereinafter referred to as 'teosinte'), diverged in their evolutionary paths approximately 10,000 years ago (Doebley, 1990, 2004). Teosinte remained wild, evolving in the similar environments of Mesoamerica that their common ancestors lived in (Doebley, 1990, 2004). On the other hand, modern maize has undergone dramatic changes through continued selection by farmers and plant breeders, thus increasing its yield dramatically (Ranum *et al*., 2014; USDA National Agricultural Statistics Service, 2017). With the onset of the Green Revolution, modern maize development largely occurred under a regime of high synthetic fertilizer inputs and frequent mechanical soil tillage (York *et al*., 2015; Schmidt, 2020). Higher yields in modern maize varieties have been associated with higher nitrogen (N) requirements (Taylor, 1994; USDA National Agricultural Statistics Service, 2017). High synthetic N inputs to meet this demand have contributed to multiple negative environmental outcomes, such as groundwater pollution and climate change (Galloway *et al*., 2008; Bobbink *et al*., 2010). In response to these threats, alternative nutrient management strategies have been promoted, including the use of organic N sources such as cover crops (Dabney *et al*., 2001). Leguminous cover crops can

[1] Published as: Hwang, S., Machmuller, M.B., Gaudin, A.C.M., Fonte, S.J., 2024. A teosinte and modern maize hybrid use different carbon allocation strategies in response to cover crop residue nitrogen. Plant and Soil. doi:10.1007/s11104-024-06494-0

provide large quantities of N and contribute to a suite of other ecosystem services (Blanco-Canqui *et al*., 2015; Abdalla *et al*., 2019). However, N uptake from organic sources, such as cover crops residue is more complex, and further study is needed to optimize plant N uptake and supply from these sources (Grandy *et al*., 2022).

Modern maize and teosinte evolved in distinct environments that are synthetic- and organic-N dominated, respectively (Doebley, 1990; Gaudin *et al*., 2011). Thus, the two genotypes may differ in their abilities to utilize synthetic and organic sources of N. This may be mediated by differences in belowground carbon (C) allocation in biomass and rhizodeposits to support organic N cycling for uptake. Additionally, plants' ability to take up organic monomers such as amino acids could impact organic N uptake (Näsholm *et al*., 2009).

Organic N (e.g., from compost, manure, decomposing plant residues) requires depolymerization to organic monomers and/or further mineralization to inorganic N forms to be plant-available (Daly *et al*., 2021). This process is carried out by soil microbial communities and the exoenzymes they produce (Weintraub *et al*., 2007). Because synthesizing exoenzymes comes with metabolic costs, microbial communities receiving a greater amount of labile C from nearby plant roots may be able to synthesize more N-cycling enzymes(Weintraub *et al*., 2007; Meier *et al*., 2017). This, in turn, would lead to a greater rate of N mineralization (Weintraub *et al*., 2007; Meier *et al*., 2017; Kelly *et al*., 2022b) and plant N supply. Given its continued evolution in natural environments, wherein N supply is scarce, teosinte may have better-retained traits that facilitate microbial N cycling from organic N sources, possibly through a greater investment of its photosynthate

C belowground (Gaudin *et al*., 2011; York *et al*., 2015). At the same time, high levels of synthetic N input (e.g. urea fertilizer) may have selected against this N acquisition strategy in modern maize, in favor of greater C allocation aboveground (York *et al*., 2015; Schmidt, 2020).

Even though modern maize and teosinte differ vastly in physiology, little is known about how these traits affect organic N uptake. Modern maize and teosinte can modify their root structure in response to different levels of synthetic N inputs (Gaudin *et al*., 2011). It has also been shown that the two genotypes support distinct rhizosphere microbial communities (Brisson *et al*., 2019) and microbial enzyme activities involved with N-cycling (Schmidt *et al*., 2020). An *et al*. (2015) found that modern maize increases its belowground C allocation (in both root biomass and rhizosphere soil) in response to increasing organic N addition (manure). Still, there remains a need to concretely link the C allocation plasticity of each genotype to N uptake patterns for both synthetic and organic forms of N.

We examined the response of a modern maize hybrid and a teosinte (subsp. *parviglumis*) to both synthetic and organic N amendments. We used ^{15}N isotopic enrichment of N sources to evaluate the uptake of synthetic (urea) vs organic N (cover crop residue). We also utilized ^{13}C-CO_2 pulse labeling to track short-term C allocation in modern maize vs teosinte in response to distinct N environments. We hypothesized that compared to modern maize, teosinte will (1) allocate a greater proportion of its photosynthate C belowground when provided with organic N, resulting in (2) greater recent C assimilation into the microbial pools, and subsequently, (3) greater uptake of organic (cover crop-derived) N. Understanding how modern maize and its wild relative differ in their access to cover crop N

is important for developing new maize varieties adapted to more sustainable systems, especially in the context of evolving agroecosystem paradigms that aim to rely on organic N sources for meeting crop nutrient demands.

2.2. Methods

2.2.1. Experimental Design

This research was conducted in a greenhouse at the Plant Growth Facility at Colorado State University, in Fort Collins, Colorado, USA. We used soil mesocosms and dual stable isotope (^{13}C and ^{15}N) labeling to understand how distinct *Zea mays* genotypes respond to different sources of added N. A modern variety (*Zea mays* subsp. *mays,* DKC64-69, DeKalb Genetics Corporation, IL) and teosinte (*Zea mays* subsp. *parviglumis*, PI 566691, North Central Regional Plant Introduction Station, IA) were chosen among many other *Zea mays* subspecies to represent distinct ends of the domestication spectrum for this proof-of-concept study. We established four treatments, using two *Zea* mays genotypes and two N sources - synthetic (S) vs. organic (O) N, in a full factorial, randomized complete block design with five replicate blocks. Each block was planted one week apart, to facilitate a detailed time-consuming ^{13}C labeling procedure at the end of the experimental growing period. Additionally, we included natural abundance controls, with five replicates of both genotypes that did not receive any isotopic enrichment of C or N, for a total of 30 mesocosms.

Mesocosms consisted of a 30 cm section of PVC pipe (15 cm diameter), with wire mesh installed on the bottom to hold the soil in place and allow for drainage. Mesocosm size was chosen to allow adequate root growth and facilitate transport for ^{13}C labelling. The soil

used in the experiment was collected from a depth of 15 cm in a dryland wheat field at USDA-ARS Central Great Plains Research Station near Akron, CO (40°09'22"N 103°08'26"W). The site is located at an elevation of 1,384 m and the soil is classified as a Weld silt loam (fine, smectitic, mesic Aridic Argiustoll). Despite a relatively neutral pH of 7.2 the soil was confirmed to be carbonate-free to avoid potential issues with ^{13}C calculations (Kelly *et al*., 2022b). The soil was air-dried, sieved to 2 mm, homogenized, and mixed with sand (1:1, soil:sand ratio by volume), and roughly 4.5 kg (dry weight) of the soil-sand mixture was added to each mesocosm. Seeds of both genotypes were germinated for three days on a damp piece of paper towel before being transplanted into the mesocosms at a depth of 1 cm.

Nitrogen was provided as ^{15}N labeled urea solution (synthetic N treatment; 10 atom% ^{15}N) or as ^{15}N labeled cover crop residue. The cover crop residue was a mixture of triticale (×*Triticosecale* Wittmack) and hairy vetch (*Vicia villosa*) that was grown with isotopically enriched ^{15}N Hoagland solution. The final N concentration and isotopic enrichment of the residue mixture were 18.0 mg N g^{-1} and 7.5 atom% ^{15}N, respectively. The cover crop residue was oven-dried at 60 °C, cut into pieces (3-5 mm long), and mixed in with the soil prior to planting at a rate of 18.4 g of dry cover crop residue per mesocosm. Early N mineralization was prevented by keeping the mesocosms dry until the day of transplanting, five days later. For the synthetic N treatment, ^{15}N-labeled urea solution was added to the soil surface 4 weeks after transplanting. Both N treatments received a similar total amount of N (330 mg N per mesocosm, ~181 kg N ha^{-1}). Immediately after transplanting, all plants were also

fertilized with triple super phosphate at a rate of 36 mg P per mesocosm (equivalent to 19.7 kg P ha^{-1}).

The temperature inside the Plant Growth Facility averaged 19.4 °C night/23.9 °C day. Supplementary light was provided to achieve a standard day length of 16 hr. Throughout the experiment, the plants were manually watered to approximately 80% field capacity to avoid leaching. The amount of water added to each mesocosm was determined by weight difference, disregarding plant biomass. Seven weeks after transplanting, plants were pulse labeled with ^{13}C-CO_2 and destructively harvested. We processed one plant per day due to the time-consuming nature of the pulse labeling procedure (described below). All treatments in each block were processed within the same week, and the order of processing was randomized each week. Thus, plants grew for 44 days $\pm$ 2 days after transplanting.

2.2.2. ^{13}C Labeling

To assess differences in plant C allocation between genotypes and in response to the N environment, we used a ^{13}C-CO_2 pulse-labeling method adapted from Cheng *et al* (1993) and Hafner *et al*. (2012). The labeling chamber was constructed of transparent polycarbonate and acrylic sheets (Fig. 2.1). The chamber floor was designed to cap over the PVC soil column, with the rest of the chamber designed to fit on top of the chamber floor, separating the soil from the plant shoots (Figs. 2.1b, c). The chamber itself was 30 cm x 30 cm x 66 cm (56 L; Fig. 2.1) and included four ports through which we added ^{13}C-CO_2 and monitored $\delta^{13}C$-CO_2 isotopic composition and CO_2 concentration using a cavity ring-down spectrometer (CRDS; G2101-I, Picarro, Inc. Santa Clara, CA). A small fan within the

chamber was run during the labeling operation to circulate the air. Soil CO_2 flux was measured from the headspace of the bottom cap, a PVC cap with two ports (gas inlet and outlet) attached to the bottom of the soil column (Fig. 2.1).

Labeling took place on the seventh week after transplanting (modern maize growth stage V8-9 for synthetic N treatment and V6 for organic N treatment), based on when the N uptake would likely be the highest. Before harvest, individual mesocosms were transferred to a constant temperature room (25 °C) with one grow light (Sun Blaze® T5HO-44, Sunlight Supply®, Inc. Vancouver WA) as the sole light source to minimize environmental variation throughout the process. At the start of the labeling procedure the mesocosm soil was adjusted to 80% of field capacity if needed.

The labeling procedure consisted of four distinct phases (Fig. S2.1). In the first phase (Fig. S2.1a), the chamber floor was affixed to the soil column (Fig. 2.1c). The aboveground portion of each plant was then isolated from the soil by wrapping parafilm as well as a rubber sheet with a slit around the stalk and extending to the edges of the chamber floor to create an airtight seal between the chamber and soil column. Next, the chamber was attached to the top of the chamber floor. Immediately after a seal was created, we measured plant C uptake via the drawdown of CO_2 inside the chamber until CO_2 concentrations dropped below 50 ppm.

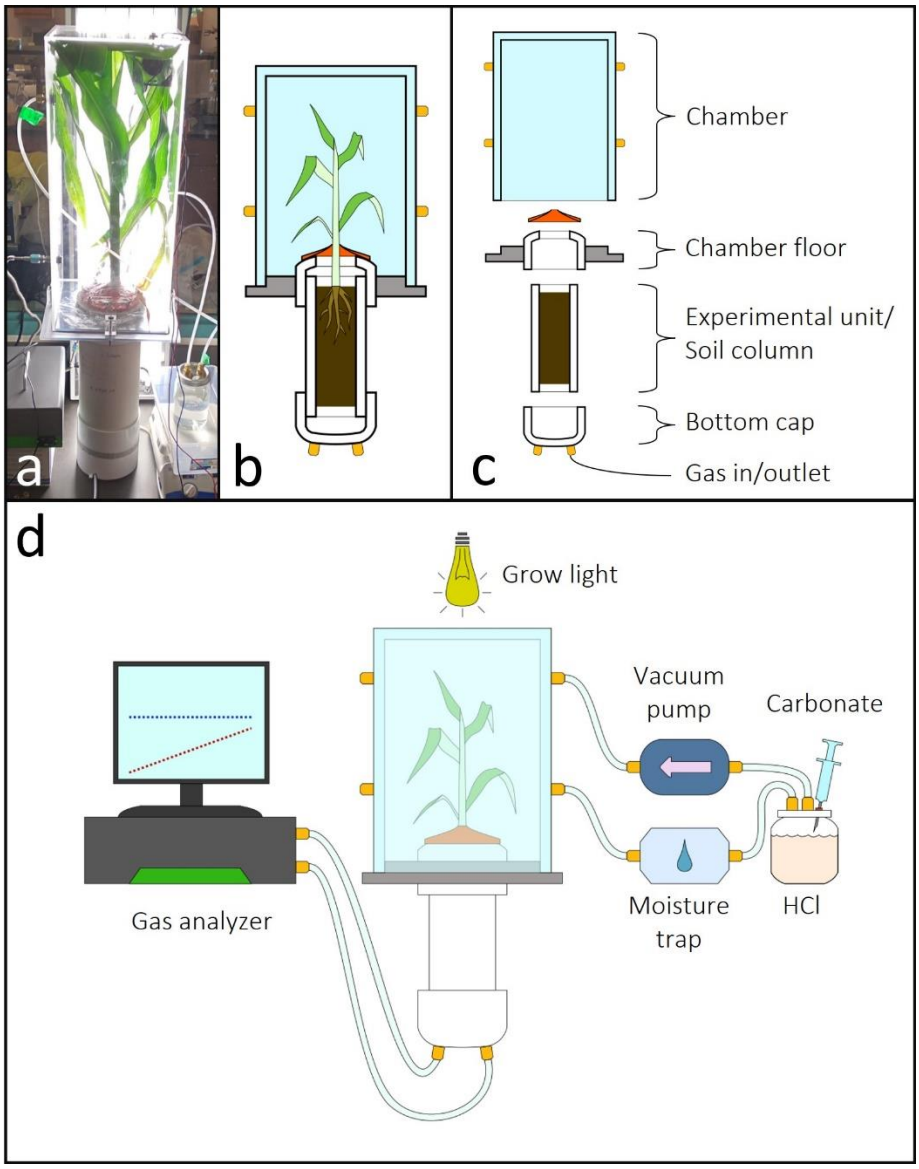

Figure. 2.1 Pulse labeling chamber and the related set up. **(a)** Picture of the chamber set up with a plant inside. **(b)** Cross-section diagram showing what is inside the chamber and the soil column. **(c)** The component parts. **(d)** The pulse labeling apparatus set up with the CRDS and CO_2 generation loop (not shown: stir plate under the container of HCl, vacuum pump that facilitates circulation to and from the CRDS, the small fan inside the shoot chamber used for circulation).

In the second phase (Fig. S2.1b), a natural abundance CO_2 pulse was generated by injecting sodium carbonate solution (100 mg mL^{-1}, 2.24 mmol) into an airtight container containing 1 M HCl. The carbonate solution was constantly stirred on a stir plate and the

CO_2 generated was injected into the chamber via a vacuum pump (Fig. 2.1d). Following the initial CO_2 pulse, we monitored CO_2 concentration within the chamber until the majority of CO_2 was utilized by the plant (i.e., [CO_2] < 50 ppm) which took 97 minutes on average. The amount of time required for each plant to utilize all the injected CO_2 varied between 37 and 163 min, likely due to the differences in aboveground biomass, and thus the total plant photosynthetic capacity. The assimilation time observed in this phase was used to time the enriched CO_2 labeling in the next phase.

In the third phase (Fig. S2.1c), the CRDS was disconnected from the chamber and attached to the bottom cap of the soil column to measure soil CO_2 efflux (root and soil microbial respiration). We then injected 98 atom% ^{13}C-CO2 into the chamber following the same protocol as described in the second phase (except using ^{13}C-enriched sodium carbonate) (100 mg mL^{-1}, 2.24 mmol). Since the instrument did not allow for accurate CO_2 concentration measurements with high ^{13}C enrichment, we could not directly measure the CO_2 concentration of the chamber portion after introducing the labeled CO_2 in the system. We instead used the time elapsed for the previous natural abundance pulse (second phase) to estimate when the plant would have taken up all the ^{13}C enriched CO_2.

In the last phase (Fig. S2.1d), the soil column CO_2 level was continuously monitored, and the soil column was flushed with ambient air intermittently, when the CO_2 level reached 4,000 ppm. Once the predetermined time had elapsed, based on the earlier natural abundance pulse, we removed the chamber from the chamber floor and allowed the plant to continue photosynthesizing with the ambient air. When enriched CO_2 was first detected in the soil column, it was flushed again with ambient air. We then monitored the change in

CO_2 concentration and $\delta^{13}C$-CO_2 in the soil column until we observed a consistent, linear increase in both. On average, we observed these constant $\delta^{13}C$ and CO_2 fluxes 160 min after we added the ^{13}C enriched carbonate. The data obtained during this period was used to calculate the $\delta^{13}C$ signature of soil CO_2 efflux using Keeling plots (see "Isotope Calculations" section below).

2.2.3. Sampling Process

Immediately after pulse labeling, the aboveground biomass was cut at the base of the stem and oven-dried at 60 °C until constant weight. Following this, roots were extracted from the soil by first gently massaging the roots to separate them from clumps of soil. Afterwards, the root system was shaken to remove soil further, thoroughly washed, then oven-dried at 60 °C. When dried, all plant components were weighed and finely ground for elemental and isotopic analysis (see below).

A representative subsample of moist soil (~1 kg subsample from ~6 kg total) was collected from each mesocosm and passed through a 2 mm sieved to remove any large plant debris and homogenize the soil. Based on the root system size, we assumed that all soil was influenced by the plant rhizosphere, if not in direct contact with the roots. Therefore, we did not distinguish rhizosphere from bulk soil. All soil samples were kept frozen at -20 °C until further analysis.

A subsample of the sieved soil was weighed before and after drying at 60 °C to calculate its gravimetric water content. The dried soil was then ground for analysis of total C and N content as well as the $\delta^{13}C$ and $\delta^{15}N$ isotopic signatures.

2.2.4. Microbial Biomass

Soil microbial biomass was extracted using the method described by Rinkes *et al*. (2011). Briefly, the frozen soil was thawed, and two subsamples (10 g, moist weight) were collected from each sample. Chloroform (4 ml) was added to one of the samples to lyse the microbial cells ('fumigated'), while no chloroform was added to the other subsamples ('non-fumigated'). Both subsamples were then incubated for 24 hours. Three negative control (no soil) samples were run with each batch of samples to detect and account for any C and N contamination that could be introduced during the extraction process. After incubation, all subsamples received 50 mL of 0.05 M K_2SO_4 solution, were shaken for one hour, then filtered using Whatman® Grade 1 cellulose filter paper (pore size = 0.11 um; Cytiva, Marlborough, MA). The resulting solution was divided into two aliquots. One aliquot was kept refrigerated until it was analyzed on a TOC-L TNM-L (Shimadzu Corp, Kyoto, Japan) to measure C and N concentrations. The C and N concentration of non-fumigated subsamples was used to determine dissolved organic C (DOC) and total dissolved N (TDN). These values were then subtracted from the C and N concentration of the fumigated subsamples (including both dissolved CN and lysed microbial cell contents) to calculate microbial biomass C and N (MBC, MBN). The remaining aliquots were freeze-dried and analyzed for $\delta^{13}C$ and $\delta^{15}N$ (see below).

2.2.5. Isotope Analyses and Calculations

Total C and N content as well as $\delta^{13}C$ and $\delta^{15}N$ in plant biomass, soil samples, MBC, MBN, DOC, and TDN were measured using an EA-IRMS (elemental analyzer coupled with Delta V

Advantage isotope ratio mass spectrometer; Costech Analytical Technologies, Inc., Valencia, CA and Thermo Fisher Scientific Inc., Waltham, MA, respectively).

The labeled plant CO_2 efflux and corresponding $\delta^{13}C$ were calculated as described by Lynch *et al*. (2018). We extracted a section of the data with concurrent, linear increase in both CO_2 concentration and ^{13}C. We ensured that these sections included a minimum increase of 100 ppm CO_2 and 100 per mil $\delta^{13}C$. The Keeling plots (Keeling, 1960) were then used to calculate the $\delta^{13}C$ isotopic signature of the CO_2 efflux from the soil column using the y-intercept of the linear regression between the $\delta^{13}C$ signature and the inverse of $[CO_2]$ ($R^2 > 0.97$). For the control samples, the $\delta^{13}C$ values were allowed to plateau for ~1 hr before the values were recorded.

We used a two-source isotope mixing model (Post 2002) to calculate the f_L values representing the proportion of C and N derived from the ^{13}C-CO_2 pulse and ^{15}N source for all soil, plant, and microbial pools.

$$f_L = \frac{{}^{H}AP_S - {}^{H}AP_C}{{}^{H}AP_L - {}^{H}AP_C}$$

Wherein f_L is the fraction of C or N in the enriched pool derived from label (pulse of enriched CO_2 or enriched N amendments), ^{H}APs is the atom% C or N of the enriched sample, $^{H}AP_C$ is the enrichment level of the corresponding control (natural abundance) fraction (in atom%), and $^{H}AP_L$ is the enrichment level of the amendment (98 atom% ^{13}C-CO_2) or 15N (10 atom % urea, 7.5 atom % cover crop).

The f_L values were then applied to the total pool sizes to estimate the total amount of label-derived C and N in each pool as follows:

$$m_L = m_S \times f_L$$

Wherein m_L is the mass of C or N in the pool that is derived from the label and m_S is the mass of C or N in the sample.

2.2.5. Statistical Analysis

Each response variable was fitted to a linear mixed model with genotype, N treatment and the genotype x N treatment interaction as fixed effects, block as a random effect, and days after transplanting (until labeling/destructive harvest) as a covariate. The label-derived soil respiration data were divided by the label-derived C amount in roots and microbial pools before further analysis. Variables were log-transformed as needed to meet the assumptions of ANOVA (homogeneity of variance and normality of residuals). Pairwise least-square means comparison was conducted using Tukey's adjustment. For all statistical analysis, $p < 0.05$ was considered significant and $p < 0.1$ as marginally significant. One dead plant (teosinte, organic N) was excluded from all statistical analyses (n = 19), and another (modern maize, synthetic N) was excluded only from label-derived CN analyses (n = 18) due to an issue with pulse-labeling. All statistical analyses and data visualization were performed on R software version 4.0.2 (R Core Team, 2020),with the R packages "ggplot2" (Wickham, 2016), "lmerTest" (Kuznetsova *et al*., 2017), "lme4" (Bates *et al*., 2015), and "emmeans" (Lenth, 2020).

2.3. Results

2.3.1. Plant growth

Genotype and N sources had large significant effects on plant growth (Table 2.1). The total biomass of modern maize was, on average, double that of teosinte (Table 2.1). Plants of

either genotype grown with synthetic N (urea) produced greater shoot and root biomass and roughly twice as much total biomass as those grown with organic N (Table 2.1). Compared to teosinte, modern maize produced greater shoot biomass but not root biomass (Table 2.1). We observed a genotype x N treatment interaction in biomass root:shoot (R:S) ratio showing that modern maize maintained a stable R:S ratio under both N sources, while teosinte increased its R:S ratio by roughly 50% when grown with organic N (Fig. 2.2a).

Table 2.1. Total dry biomass and tissue (roots and shoots) N concentration (values shown in mean ± SE) of maize plants (M = modern maize, T = teosinte) grown within mesocosms in a greenhouse under two N treatments (S = Synthetic N, O = Organic N). The bottom three rows denote the p-values associated with genotype (G), N treatment (N) and the interaction (G x N). Significant effects ($p < 0.05$) are italicized.

		Plants						
		Shoots		Roots		**Plant Total**		
		Biomass (g)	%N	Biomass (g)	%N	**Biomass (g)**	**%N**	**Biomass N (mg)**
M	S	21.00 ± 1.08	1.55 ± 0.11	6.66 ± 0.43	0.73 ± 0.03	27.66 ± 1.33	1.34 ± 0.08	370.8 ± 25.4
	O	8.66 ± 0.83	1.12 ± 0.05	2.77 ± 0.27	0.76 ± 0.04	11.43 ± 1.05	1.03 ± 0.04	117.5 ± 11.3
T	S	11.44 ± 2.59	2.69 ± 0.50	4.76 ± 1.24	1.17 ± 0.15	16.19 ± 3.70	2.24 ± 0.40	306.9 ± 23.6
	O	4.51 ± 0.84	2.01 ± 0.53	2.76 ± 0.46	1.02 ± 0.08	7.27 ± 1.17	1.61 ± 0.16	112.9 ± 8.8
G		*<0.001*	*<0.001*	0.15	*<0.001*	*0.001*	*0.001*	*0.034*
N		*<0.001*	0.051	*<0.001*	0.861	*<0.001*	*0.040*	*<0.001*
G x N		0.134	0.671	0.216	0.396	0.131	0.989	0.237

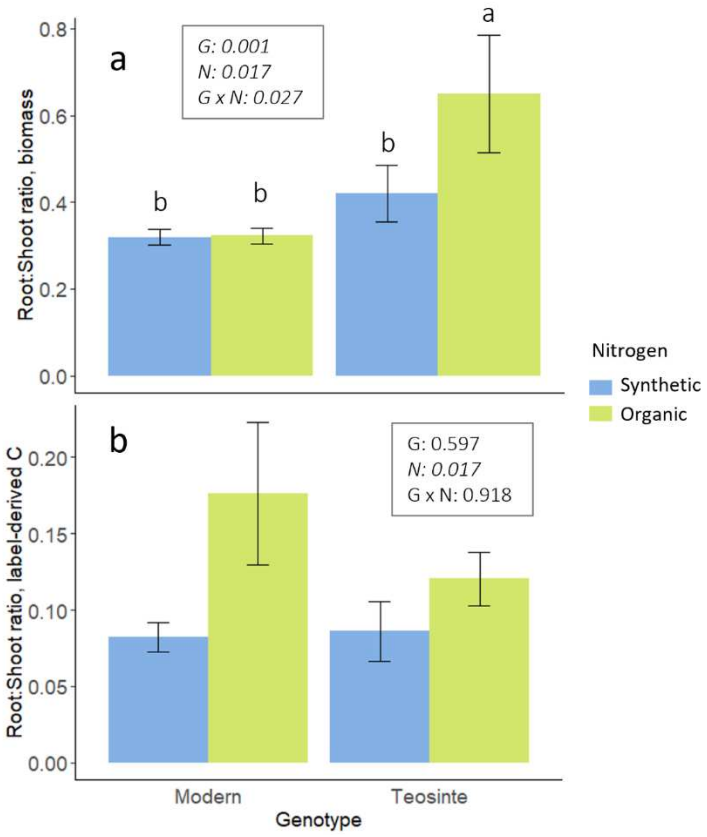

Figure. 2.2 R:S ratio, for **(a)** total C and **(b)** label-derived C. The boxes in the panels indicate the p values associated with genotype (G), N treatment (N), and the interaction (G x N). Significant effects ($p < 0.05$) are italicized. Letters in **(a)** denote significant difference at 0.05 level (Tukey's post-hoc test).

2.3.2. Soil C, DOC, and MBC

Soil C concentration ranged from 8.8 to 11.6 mg C g dry soil $^{-1}$ (Table 2.2). Total soil C concentrations were 13.6% greater in the organic N treatment than in the synthetic N treatment (Table 2.2). Similarly, dissolved organic C (DOC) was on average 62% higher in the organic N treatments than in synthetic N treatment (Table 2.2). We found no genotype effects on total soil C or DOC concentrations (Table 2.2). Microbial biomass C (MBC) did not differ with N treatments or genotypes (Table 2.2).

Table 2.2. C and N concentration in each soil pool (soil total, dissolved, and microbial biomass) as well as total soil C:N ratio under two maize genotypes (M = modern maize, T = teosinte) grown with two N treatments (S = Synthetic N, O = Organic N). Values shown in mean ± SE. The bottom three rows denote the p-values associated with genotype (G), N treatment (N) and the interaction (G x N). Significant effects ($p < 0.05$) are italicized.

		Soil Pools						
		C			N			
		Total soil (mg C g dry soil $^{-1}$)	DOC (µg C g dry soil $^{-1}$)	MBC (µg C g dry soil $^{-1}$)	Total soil (mg N g dry soil $^{-1}$)	TDN (µg N g dry soil $^{-1}$)	MBN (µg N g dry soil $^{-1}$)	Total soil C:N
M	S	9.35 ± 0.28	14.90 ± 0.69	78.61 ± 3.45	1.03 ± 0.03	2.85 ± 0.26	6.05 ± 0.16	9.10 ± 0.05
	O	10.94 ± 0.21	24.87 ± 0.68	95.59 ± 4.49	1.19 ± 0.02	4.28 ± 0.16	7.72 ± 0.36	9.20 ± 0.06
T	S	9.39 ± 0.18	15.15 ± 0.49	78.13 ± 1.54	1.03 ± 0.01	3.95 ± 0.65	6.91 ± 0.23	9.14 ± 0.08
	O	10.29 ± 0.28	23.79 ± 0.79	77.32 ± 14.18	1.13 ± 0.02	4.98 ± 0.38	6.71 ± 0.81	9.09 ± 0.06
G		0.111	0.579	0.220	0.076	*0.011*	0.967	0.497
N		*<0.001*	*<0.001*	0.248	*<0.001*	*0.001*	0.065	0.848
G x N		0.087	0.412	0.261	0.107	0.725	0.075	0.129

2.3.3. Recovery and distribution of ^{13}C

The amount of label-derived C found in the plant biomass ranged from 8.06 to 19.19 mg C per mesocosm (Table 2.3). We observed no genotype effects on label-derived C recovered in shoots, roots, or total plant biomass (Table 2.3). For both genotypes, plants grown with synthetic N contained more label-derived C in their shoots (Table 2.3).

N treatment significantly affected the distribution of label-derived C between shoot and roots. Plants grown with organic N had more label-derived C in the roots compared to those grown with synthetic N (91 % and 37% greater for modern maize and teosinte, respectively; Fig. 2.2b). However, there was no genotype x N treatment interaction for R:S ratio of label-derived C (Fig. 2.2b).

Table 2.3. Amount and recovery of label-derived C in plant and soil pools in two maize genotypes (M = modern maize, T = teosinte) grown with two N treatments (S = Synthetic N, O = Organic N; values shown in mean ± SE). The bottom three rows denote the p-values associated with genotype (G), N treatment (N) and the interaction (G x N) and significant effects ($p < 0.05$) are italicized.

		Label-derived C (mg C)					
		Plant					
		Shoots	Roots	Plant total	Soil	Total Recovered	Recovery rate (%)
M	S	13.52 ± 1.43	1.13 ± 0.24	14.66 ± 1.64	1.86 ± 0.42	16.52 ± 1.80	56.81 ± 6.19
	O	10.82 ± 1.13	1.90 ± 0.61	12.72 ± 1.44	2.26 ± 0.48	14.98 ± 1.69	51.50 ± 5.83
T	S	13.05 ± 1.81	0.99 ± 0.10	14.04 ± 1.74	1.79 ± 0.34	15.83 ± 1.96	54.45 ± 6.73
	O	9.93 ± 0.67	1.18 ± 0.15	11.11 ± 0.67	1.79 ± 0.29	12.90 ± 0.69	44.35 ± 2.39
G		0.543	0.370	0.422	0.509	0.391	
N		*0.031*	0.123	0.086	0.731	0.346	
G x N		0.635	0.777	0.573	0.605	0.688	

Label-derived C was detected in the DOC and the MBC pools (3.05 ± 0.45 ug C and 171.44 ± 26.27 ug C, respectively, per mesocosm). The amount of label-derived DOC was ~2.5 times higher in the organic N treatment for both plant genotypes (Fig. 2.3a). Similarly, there was a marginally significant effect of N treatment on label-derived C in MBC ($p = 0.088$), which was on average ~2 times higher for the organic N treatment (Fig. 2.3b). Label-derived DOC and label-derived MBC were positively correlated (Fig. 2.3c). Despite the observed differences in DOC and MBC, we found no N treatment effects on label-derived total C in soil (Table 2.3). There were no consistent genotype effects on label-derived DOC, MBC (Figs. 2.3a, b) and total soil C (Table 2.3). On average, 50 % of the C provided in the ^{13}C-CO_2 pulse-labelling event was recovered in the plant and soil pools, with no significant differences in recovery between genotypes or N treatments (Table 2.3).

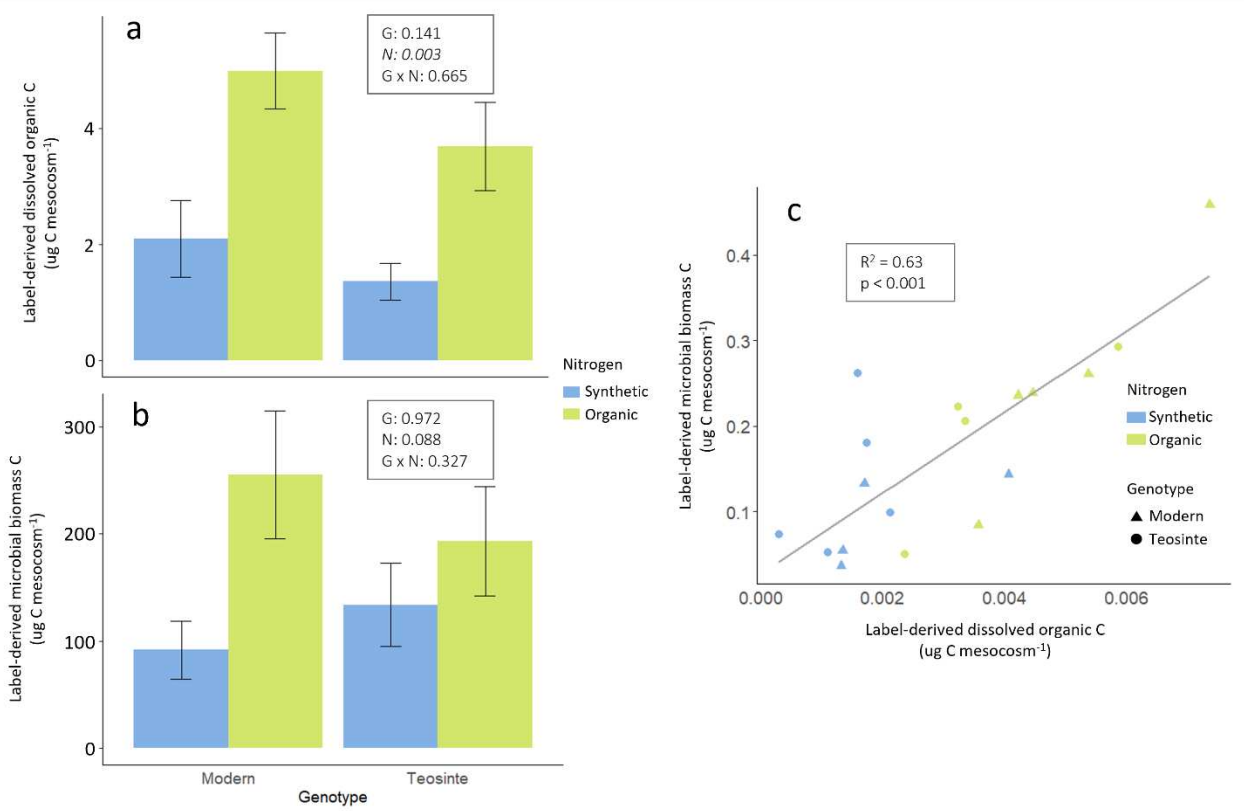

Figure. 2.3 The amount of label-derived C in **(a)** dissolved organic C pool and **(b)** microbial biomass C pool (values shown in mean ± SE) as well as **(c)** their correlation. The boxes in **(a)** and **(b)** denote the p-values associated with genotype (G), N treatment (N) and the interaction (G x N). Significant effects ($p < 0.05$) are italicized. The box in **(c)** denotes the R2 value and associated p value for the correlation. **(a)** There was a significant N treatment effect on the amount of label-derived C for the DOC pool (O > S, Tukey's post hoc test). **(c)** Label derived DOC and MBC were positively correlated.

2.3.4. Soil respiration

The soil respiration rates ranged between 2.11 and 10.19 mg CO_2 min^{-1} m^{-2}. Label-derived CO_2 respiration rate normalized by label-derived root biomass C (i.e., label-derived soil respiration rate per mg of label-derived root C) was approximately 3-fold higher in teosinte but no N treatment effect was observed (Fig. 2.4).

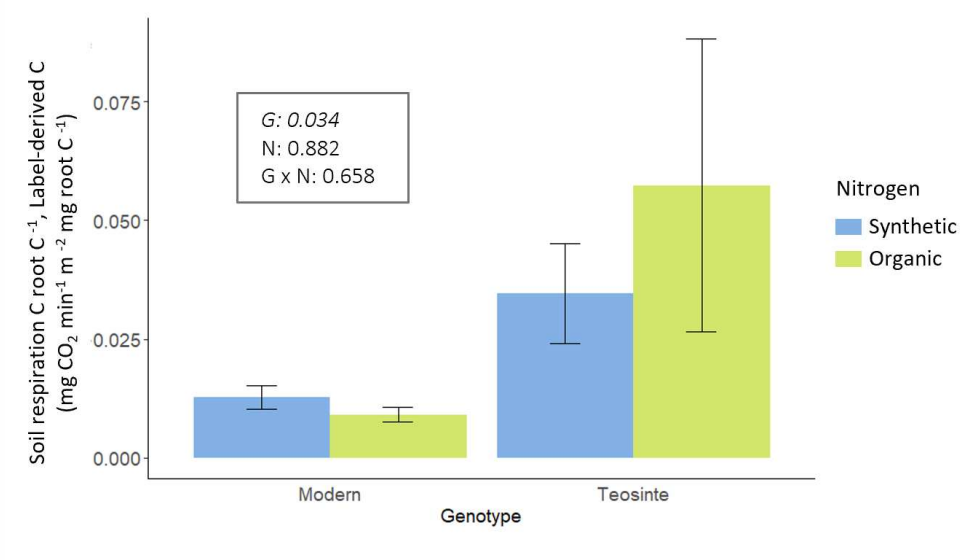

Figure. 2.4 Soil respiration rate to root ratios for label-derived C (values shown in mean ± SE). The box denotes the p-values associated with genotype (G), N treatment (N) and the interaction (G x N). Significant effects ($p < 0.05$) are italicized.

2.3.5. Plant biomass N, Soil N, TDN, and MBN

Teosinte had a greater total plant N concentration compared to modern maize, with a 79% higher shoot N concentration and a 47% higher root N concentration (Table 2.1). Total soil N concentration ranged between 0.92 and 1.25 mg N g dry soil $^{-1}$ and was 13.1% greater in the organic N treatment (Table 2.2). There were no genotype or N treatment effects on soil C:N ratio (Table 2.2). Both genotype and N treatment effects were observed in the TDN pool, wherein TDN was 34.9% higher in the organic N treatment and 23.7% higher under teosinte (Table 2.2). No genotype or N treatment effects were found in MBN (Table 2.2).

2.3.6. Recovery and distribution of ^{15}N

There was a significant genotype x N treatment interaction in label-derived N within plant biomass (Table 2.4). In the organic N treatment, the two genotypes did not differ and took

up similarly low amounts of label-derived N (Table 2.4). However, in the synthetic N treatment, modern maize took up much greater label-derived N than teosinte did (Table 2.4).

Table 2.4. Amount and proportion of label-derived N (% ldN) vs. total N in different plant and soil pools as well as overall recovery of the labeled N in two maize genotypes (M = modern maize, T = teosinte) grown with two N treatments (S = Synthetic N, O = Organic N; values shown in mean ± SE). The bottom three rows denote the p-values associated with genotype (G), N treatment (N) and the interaction (G x N). Significant effects ($p < 0.05$) are italicized.

		Label-derived N									
		Plant		Soil							
				TDN		MBN		**Total soil**		**Total Recovered (mg N)**	**Recovery rate (%)**
		mg N	% ldN	mg N	% ldN	mg N	% ldN	mg N	% ldN		
M	S	220.93 ± 16.35 *a*	57.70 ± 1.48	0.86 ± 0.16	7.05 ± 0.74	1.51 ± 0.16	5.86 ± 0.59	42.19 ± 3.66	0.97 ± 0.06	**263.12 ± 13.68**	**79.73 ± 4.14**
	O	39.12 ± 4.30 *c*	33.12 ± 0.83	2.93 ± 0.14	15.60 ± 0.52	6.71 ± 0.36	19.80 ± 0.38	282.33 ± 8.57	5.42 ± 0.23	**321.45 ± 11.88**	**97.41 ± 3.60**
T	S	164.27 ± 12.53 *b*	53.54 ± 1.39	1.18 ± 0.21	7.01 ± 0.57	4.03 ± 1.60	13.38 ± 5.04	47.44 ± 9.38	1.07 ± 0.21	**211.72 ± 17.12**	**64.15 ± 5.19**
	O	37.12 ± 1.83 *c*	33.15 ± 1.17	3.37 ± 0.17	15.35 ± 0.59	6.24 ± 1.28	20.20 ± 2.29	273.82 ± 5.20	5.46 ± 0.09	**310.94 ± 6.54**	**94.23 ± 1.98**
G		*0.014*	0.148	*0.048*	0.657	0.293	0.180	0.803	0.731	*0.015*	
N		*<0.001*	*<0.001*	*<0.001*	*<0.001*	*0.003*	*0.004*	*<0.001*	*<0.001*	*<0.001*	
G x N		*0.049*	0.074	0.569	0.639	0.271	0.402	0.354	0.805	0.078	

Label-derived TDN and MBN were higher in the organic N treatment regardless of genotype (Table 2.4). We also observed a genotype effect, wherein the soil under teosinte had a slightly (7.3%) greater amount of label-derived TDN than that under modern maize. Label-derived total soil N was nearly six times greater in the organic N treatment than in the synthetic N treatments (Table 2.4).

The proportion of label-derived N in plant and soil pools only differed by N treatment (Table 2.4). Plants in the synthetic N treatment had a higher proportion of N coming from label compared to those in organic N environment (Table 2.4). The inverse was true for soil pools (soil, TDN, and MBN), where the proportion of label-derived N was greater in the organic N treatment (Table 2.4).

Recovery rates for the label-derived N in all plant and soil pools showed both N treatment and genotype effects (Table2. 4). Recovery rate was 35.1% higher in organic N treatment than in the synthetic N treatment and 15.5% higher in modern maize than for teosinte (Table 2.4). A genotype x N treatment interaction was marginally significant ($p = 0.078$; Table 2.4), indicating that recovery of synthetic N was especially lower in teosinte. We did not observe any leaching from the mesocosms throughout the experiment.

2.4. Discussion

2.4.1. Plant C allocation and its implication on N uptake

We hypothesized that C allocation for teosinte would be more responsive to the type of N amendment compared to its modern maize counterpart. More specifically, we expected that teosinte would allocate a greater amount of C belowground (via root exudation, root growth, etc.) compared to modern maize, especially when soil is amended with organic N that requires microbial processing to become available to plants. In support of this idea, we found that teosinte, but not modern maize, had greater biomass R:S ratio in the organic N treatment than the synthetic N treatment (Fig. 2.2a). This result suggests that modern maize may have lost its ability to modify C allocation and growth pattern in response to organic N resources. Since greater C allocation towards the belowground structures (i.e., root system) can enhance N uptake (Chapman *et al.*, 2012), the loss of plasticity by modern maize could lead to reduced uptake of organic N. However, we found both genotypes to take up similar amounts of cover crop N (Table 2.4). A genotype difference was only present in the synthetic N treatment, wherein modern maize was significantly better at utilizing urea-derived N than teosinte (Table 2.4). Our results suggest that despite

its loss of plasticity for biomass allocation belowground, modern maize has largely retained its ability to take up organic N and that domestication and modern breeding have improved modern maize's ability to take up synthetic N.

Interestingly, allocation of label-derived C, representing recently assimilated photosynthates, differed from that observed for total plant biomass. We found that both modern maize and teosinte allocated greater amounts of their recent photosynthate belowground in the organic N treatment (Fig. 2.2a). Both R:S ratio of label-derived C and amount of label-derived DOC were greater in the organic N treatment regardless of genotype (Figs. 2.2b, 3a). We suspect that this label-derived DOC was likely a mixture of root exudates and rapidly processed recent rhizodeposits, both of which represent short-term C allocation from plant to soil (An *et al*., 2015). The label-derived MBC pool was positively correlated with label-derived DOC (Fig. 2.3c), suggesting rapid assimilation of rhizodeposits into the microbial pools. We suspect that the above effects are due to N type (organic vs synthetic) rather than N stress, even though organic N treatment led to lower N uptake (Table 2.1). In support of this idea, we observed greater N availability (amount of TDN; Table 2.2) in the organic N treatment and we note that neither genotype showed any obvious signs of N stress aboveground (i.e., leaf yellowing; data not shown). Furthermore, others have shown that at least some varieties of modern maize can increase their root:shoot ratio in response to N stress (Gaudin *et al*., 2011), which was not the case for our modern maize grown with organic N (Fig. 2.2a).

Allocation of labile C belowground by both genotypes may explain why both genotypes were able to take up similar amounts of organic N. Greater rhizodeposition has been linked

to enhanced organic N uptake via increased N mineralization (Meier *et al*., 2017). In an experiment involving winter wheat, Kelly *et al*. (2022b) found that label-derived DOC and MBC were associated with greater N cycling enzyme activity and uptake of cover crop-derived N. Similarly, de Graaf *et al*. (2009) found that rhizodeposition by both wild and cultivated wheat genotypes can lead to greater soil N mineralization. It should also be noted that greater N availability can be induced by root exudates interacting with the mineral associated organic matter N (MAOM N; Jilling *et al*., 2018), with minimal microbial involvement. While we do not have more direct measurements of N-related soil processes to better elucidate the mechanisms, we did observe greater total and label-derived TDN in the soil amended with organic N (Table 2.4), supporting the idea that greater rhizodeposition may be improving plant access to organic N. Though teosinte did not exhibit any advantages in organic N uptake, we did observe a slightly greater amount of TDN (both total and label-derived) under teosinte for both N treatments (Table 2.2, 2.4). While this may support our initial hypothesis that teosinte can induce greater N availability in the soil, it may simply be evidence of slower uptake of available N by teosinte (Table 2.2, 2.4). The combined results suggest that both modern maize and teosinte can modify their recent photosynthate C allocation patterns and take up similar amounts of organic N. This finding went against our hypothesis that modern maize would be less efficient at acquiring organic N due to breeding under high synthetic N conditions (Doebley, 2004). One possible explanation may be that the agricultural soil used in our experiment was lower in soil organic N content than the soil that teosinte evolved in. In degraded agricultural soils, residue N often replenishes the MAOM pool first instead of being taken up by the plants the

same year the residue is applied (Daly *et al.*, 2021; Crews *et al.*, 2022). Therefore, the cover crop residue N in our study may also have entered the MAOM N pool instead of being taken up by plants. In support of this, we recovered most of the labeled cover crop N in the soil N pool, though we cannot ascertain how much of this N was in the MAOM fraction (Table 2.4). As soil organic N increases, mineral surfaces become more saturated with organic molecules, and more organic N remains plant-available (Daly *et al.*, 2021). It is possible that teosinte's advantage of having evolved in the wild would also become more apparent once enough soil organic N has accumulated. In a past study, teosinte's biomass increased more dramatically, compared to modern maize, when both were grown in soil with a legacy of organic management (Schmidt *et al.*, 2020). It is possible that the organically managed soil accrued enough soil organic N, making more organic N available to plants, which in turn led to greater N uptake by teosinte.

Another explanation involves differential endophytic microbial community in teosinte and modern maize. It has been suggested that endophytic microbes may support growth of teosinte under low N conditions (Dumigan *et al.*, 2021). A past study found that those microbial strains extracted from teosinte roots promoted growth in other grass species under low N stress (Dumigan *et al.*, 2021). The authors also suggested that such endophytes can be vertically transferred via the seeds (Dumigan *et al.*, 2021). Such interaction was likely prevented in our study since we used agricultural soil that teosinte has not grown in previously and sterilized the exterior of the seeds prior to planting to avoid complications with disease. This may have led to teosinte being unable to recruit beneficial

microbes that it coevolved with, hence the lack of low N tolerance seen in other studies (Dumigan *et al.*, 2021).

Lastly, we suspect that despite a shift to synthetic N inputs, soil organic N has remained an important N source for maize. For example, Yan *et al.*(2015) found that fertilizer N uptake efficiencies tend to be relatively low (<50%) despite high N requirements, indicating that crops take up a considerable portion of their N from soil organic N pools even in heavily fertilized soils. This may explain why modern maize retained its ability to take up organic N even as its synthetic N uptake improved over its domestication and breeding.

2.4.2. Soil respiration

Soils with teosinte had higher label-derived soil respiration than soils under modern maize, independent of N treatment (Fig. 2.4a). Previously, Pausch *et al.* (2013) demonstrated that label-derived respiration is dominated by root respiration (RR) with a minor contribution from rhizomicrobial respiration (i.e., heterotrophs mineralizing rhizodeposits) for the first 20 hours following pulse labeling. Since we monitored soil respiration for only 3 hours after labeling, most of the label-derived respiration was likely RR. Furthermore, microbial respiration was likely mostly respiration of root exudates and not of other rhizodeposits (e.g., sloughed off root border cells, root hairs) since structural elements in rhizodeposits likely take a few days or more to be cycled and respired (Kuzyakov, 2006).

Past research suggests that RR is positively correlated with root N concentration across many plant species (Reich *et al.*, 2008; Wang *et al.*, 2021). Since teosinte had consistently higher root N concentration than modern maize (Table 2.1), this is in line with greater respiration we observed. Additionally, root growth, maintenance, and ion (such as NO_3^-,

NH_4^+) uptake activities all contribute to RR (Johnson, 1990; Eissenstat, 1997). However, teosinte did not grow a greater root system, nor did it take up greater amount of N (Table 2.1). Therefore, the recent photosynthate allocated belowground by teosinte does not seem to directly influence plant N uptake and growth.

2.4.3. Conclusions

To avoid deleterious environmental effects, agroecosystems are moving away from high synthetic N inputs towards more organic N-based systems. It is important that crops are adapted to these changes to maintain productivity while avoiding further N losses. Our findings indicate that modern maize may have lost some C allocation plasticity in response to organic N sources, while retaining its ability to use various sources of N. These findings, at least with regards to the genotypes and N environments studied here, suggest that modern maize may be just as well-suited for this transition as teosinte balsas, even after millennia of domestication and breeding. However, it must be noted that *Zea mays* subsp. *parviglumis* is but one genotype among many teosinte lines, and that we also compared it to only one of many available modern maize hybrids. Thus, we exercise caution when extrapolating our results to genotypes we are yet to explore. On the other hand, this simply means that there is much agroecological potential to be explored in wild relatives of maize and landraces. Undiscovered among the constellation of genetic diversity may be traits that may undergird our future agroecosystems.

CHAPTER 3: FINE ROOT PRODUCTION AND SPECIFIC EXUDATION RATE ARE ENHANCED IN A NOVEL PERENNIAL CEREAL HYBRID COMPARED TO ITS ANNUAL AND PERENNIAL PARENTS.

3.1. Introduction

Perennial agriculture is a potential alternative to the current industrial agriculture paradigm (Crews *et al*., 2016). Perennial crops could reduce energy input and improve soil health via reduced tillage, increased water and nutrient use efficiency, and carbon (C) sequestration (Crews *et al*., 2016; van der Pol *et al*., 2022). Researchers have greatly advanced crop breeding efforts in recent decades to create novel perennial cereal crops and associated cropping systems to populate this potential perennial agriculture landscape (DeHaan *et al*., 2018). *De novo* domestication and wide hybridization represent two main crop development approaches. Kernza is a product of *de novo* domestication of intermediate wheatgrass (IWG; *Thinopyrum intermedium*, DeHaan *et al*., 2018). Intermediate wheatgrass was introduced to North America as a forage grass and has survived as a wild cold-season perennial grass (DeHaan *et al*., 2018). Domestication efforts have resulted in dramatic increases in yield, which led to Kernza becoming the first commercially available perennial cereal (Bajgain *et al*., 2020). Perennial wheat is a product of wide hybridization between Kernza and annual durum wheat (*Triticum turgidum* subsp. *durum*, Hayes *et al*., 2018). It seeks to combine the perenniality of Kernza with the greater yield of annual wheat (Hayes *et al*., 2018).

Though perenniality is the focus of these breeding programs, it is far from the only trait that IWG offers. Wild plants such as IWG have been theorized and demonstrated to possess beneficial traits that may have been inadvertently lost in modern crops (Renzi *et al.*, 2022). Of particular importance among these traits are those that govern plant rhizosphere communities (Pérez-Jaramillo *et al.*, 2016). Plants are known to assemble distinct microbial communities in their rhizosphere by modulating root exudation (Zhalnina *et al.*, 2018) and other rhizodeposits. Rhizosphere microbial communities can then confer specific benefits that support nutrient acquisition and pathogen resistance (Dumigan *et al.*, 2021; Abdullaeva *et al.*, 2024). Past studies have demonstrated that domestication focused on aboveground characteristics (e.g., yield, plant height) can affect every level of this plant-microbe interaction over time (Pérez-Jaramillo *et al.*, 2016). For example, Iannucci *et al.* (2017) compared modern durum wheat and its wild crop relatives and found that their root exudate chemical profiles differed significantly. Various studies comparing microbial communities of modern crops with their wild crop relatives have yielded similar results in rice (Chang *et al.*, 2021), maize (Brisson *et al.*, 2019), and sunflowers (Leff *et al.*, 2017). Lastly, those microbial communities associated with wild crop relatives of maize (Dumigan *et al.*, 2021) and wheat (Abdullaeva *et al.*, 2024) have shown abilities to confer nitrogen (N) stress tolerance and fungal pathogen resistance, respectively.

Kernza, though not a wild crop relative, may still possess beneficial rhizosphere traits, especially given its more recent domestication history (DeHaan *et al.*, 2018). If so, perennial wheat, being a hybrid between Kernza and annual durum, may have also inherited such traits. Indeed, wide hybridization has been used before specifically to bring

in rhizosphere traits from one species to another. For example, Cui *et al.* (2022) found that the hybrid between annual wheat and tall wheatgrass (*Thinopyrum elongatum*) had distinct microbial communities compared to its annual parent. This shift in microbial community also led to greater salinity stress tolerance in the hybrid (Cui *et al.*, 2022). However, results of wide hybridization are difficult to predict. For example, in one study, a rice hybrid had greater fungal pathogen resistance compared to its two parents, an example of heterosis (hybrid vigor; Zhang *et al.*, 2023). In contrast, another study showed that some wheat hybrid combinations led to autoimmune response leading to cell death (hybrid necrosis; Mizuno *et al.*, 2010). Though it plays a crucial role in crop performance, relatively little is known about rhizosphere interactions in Kernza, specifically root exudate quantity and composition, as well as the rhizosphere microbial communities of Kernza and whether/how they are passed down to perennial wheat.

Based on these knowledge gaps, we aimed to characterize the root architecture, exudation rate, and exudate composition of annual durum wheat, perennial wheat, and Kernza as well as their influence on the rhizosphere microbial community. We hypothesized that (1) relative belowground investment (root biomass and exudation rate) are the greatest in Kernza, followed by perennial wheat and then by annual wheat since the latter has been bred to maximize aboveground growth, (2) exudate chemical composition and microbial community composition differ the most between the annual and perennial parents, with the perennial hybrid being intermediate between the two, given the heritability of rhizosphere characteristics. Identifying belowground traits in perennial cereal that support beneficial rhizosphere interactions can help inform plant breeding efforts interactions.

3.2. Methods and Materials

3.2.1. Experimental design and set-up

This experiment was carried out at the Plant Growth Facility at Colorado State University (CSU; Fort Collins CO). The temperature within the facility averaged 19.4 -23.9 °C (night-day) with a standard day length of 16 h achieved via supplemental lights.

Soil was acquired from CSU's Agriculture Research, Demonstration and Education Center (40°39'09.4"N 104°59'48.1"W, elevation: 1,552 m) and is classified as a Fort Collins loam (fine-loamy, mixed, superactive, mesic Aridic Haplustalfs; Soil Survey Staff, 2019). The soil was collected to a depth of 20 cm and air-dried before being ground to pass through a 2 mm sieve. Soil was mixed with silica sand (Granusil® 4075, Covia Corp, Independence OH) in a 1:1 ratio by volume to facilitate infiltration and drainage. The sand used in the soil mix was tested for microbial DNA to ensure no contamination with this material (data not shown).

Three species/genotypes grown for this experiment: 1) Kernza® (intermediate wheatgrass, *Thinopyrum intermedium*), 2) annual durum wheat (*Triticum turgidum* subsp. *durum*), and 3) perennial wheat (*Th. intermedium* x *T. turgidum* subsp. *durum*). Lines 1 and 3 were developed and provided by the Land Institute (Salina, KS). Each plant genotype was replicated three times within each of the five blocks for a total of 15 replicates per genotype. Each block was planted and processed one week apart due to the time-consuming nature of exudate collection process (see below).

Seeds were germinated on a damp paper towel for a week before being transplanted to 1 L pots filled with the soil-sand mixture (~ 1 kg). The plants were watered three times a week (to roughly 80% of field capacity) during the 8-week growth period. No fertilizer was added to the pots.

3.2.2. Root exudate collection

We used a root exudate collection method based on Williams *et al.* (2021). This method allows for plant-soil interaction during early stages of plant growth and limits contamination of exudate samples via dissolved organic matter. After 8 weeks, plants were uprooted from their pots and most of the loose soil was carefully brushed off with gloved hands and a clean paintbrush. The rest of the soil still clinging to the roots was then removed with a softer brush and collected as rhizosphere soil. Rhizosphere soil samples were frozen at -20 °C until subsequent analysis. The roots were then carefully and thoroughly cleaned with DI water. Afterwards, the plants were placed in an aerated soil solution in individual bottles for 3 days to recover from potential root damage during the washing step. The soil solution was made by adding 800 g of air-dried field soil into 11 L of DI water, letting it settle for at least 12 hours, and filtering it through a 0.2 mm sieve to remove any plant detritus.

At the end of the 3-day recovery period, the plants were removed from the bottles and the roots were rinsed again with DI water and then with milliQ water. The plants were then placed carefully into a 250-mL glass media bottle filled with 100 mL of milliQ water so that all roots were submerged. At this stage, we introduced two negative control samples to each block, which were simply glass bottles filled with milliQ water without any plants in

them. These negative controls, along with those containing actual plant samples, were then gently shaken on an orbital shaker for 2 hrs at 60 rpm under a grow light (Sun Blaze® T5HO-44, Sunlight Supply® Inc, Vancouver WA).

After 2 hours, the plants were removed from the bottles and processed. The shoots were cut, placed in a paper bag, and dried at 55 °C. The roots were stored in 10% ethanol solution until further processing. The resulting exudate samples were first filtered with 0.22 µm syringe filters to remove microbial cells and root debris. The filtered samples were divided into three subsamples; one subsample was reserved for total C and N analysis (see *Exudate Analysis* below). The other two subsamples for LC-MS/MS were freeze-dried, resuspended with HPLC grade water to combine them, then freeze-dried again. The freeze-dried subsamples for LC-MS/MS were stored at -20 °C until further processing.

3.2.3. Root scanning

Root scanning was used to provide insight on root architecture and the relative distribution roots among different diameter classes. Roots were first dyed with 1% Neutral Red dye solution, rinsed with DI to eliminate excess dye, and arranged on a transparent scanner tray filled with shallow water to avoid overlaps. The roots were then scanned using ScanMaker 9800XL (Microtek International Inc., Santa Fe Springs, CA) at 600 dpi. A light box (Picker International Inc, Charlotte NC) was used against the roots to create a sharper image. The root images were processed using RhizoVision v2.0.3 (Seethepalli and York, 2020) and with the algorithm described by Seethepalli *et al.* (2021). Scanned roots were categorized into five root size classes: 0-250 µm, 250-500 µm, 0.5-1 mm, and > 1 mm to yield roughly equal volume in each of the first three diameter classes. After being scanned, the total root

biomass of each plant was dried at 55 °C for 72 hours and weighed. Total root length and root surface area were divided by total root biomass to calculate specific root length (SRL) and specific root area (SRA), respectively.

3.2.4. Exudate analysis

Total C and N analysis of the exudate subsamples was performed on TOC-L TNM-L (Shimadzu Corp, Kyoto, Japan) and converted to exudation rate by dividing with total incubation time (2 hrs). Specific exudation rate was calculated by dividing the exudation rate by the root mass.

Untargeted metabolomics analysis of the exudate samples took place at the Analytic Resources Core at CSU (Fort Collins, CO; RRID: SCR_021758). The freeze-dried root exudate pellets were resuspended in 375 µL of methanol solution (methanol:water, 1:8, v:v) and transferred to autosampler vials equipped with 200 µL inserts. We also pooled 20 µL of each sample to create pooled quality control samples. These quality control samples were run every 12 samples to ensure inter-sample consistency and to detect retention time (RT) drift over a run. Lastly, an internal standard mix of acetyl carnitine (*m/z* 214) and resperine (*m/z* 609) was added to each sample.

Chromatographic separation was performed on Acquity UPLC H-Class® (Waters Corp, Milford MA) equipped with Acquity UPLC T3 Column® (1.8 µM, 1.0 x 100 mm; Waters Corp, Milford MA) as described by Boot *et al*. (2022). A gradient of mobile phase A (water, 0.1% formic acid) and mobile phase B (acetonitrile, 0.1% formic acid) was used in the following sequence: 0-1 min, 100% mobile phase A; 1-12 min 0-95% mobile phase B; 12-15 min,

95% mobile phase B; 15-15.05 min 5-100% mobile phase A; and 15.05-20 min, 100% mobile phase A. Throughout, the column and sample temperature were kept constant at 50 °C and 5 °C, respectively.

Column eluent was then introduced to a Bruker maXis Plus® ultra-high resolution quadrupole time of flight (QTOF) mass spectrometer equipped with an electrospray ionization (ESI) source (Bruker Corp, Billerica MA). The ESI source was run both in positive and negative modes to maximize data acquisition. For both ionization modes, the ions were scanned at a rate of 4 Hz through 50-1300 m/z range. Other parameters for the mass spectrometry were as follows: capillary voltage 4500 V, nebulizer pressure 3.0 bar, drying gas 8.0 l/min, drying temp 220 C. Data dependent MS/MS spectra were collected with 3 precursors per cycle with active exclusion after three spectra and release after 0.3 min. Source and acquisition parameters were identical for negative ion mode with the exception of the capillary voltage which was set at 3000 V.

Data were calibrated in Compass HyStar (Bruker) prior to converting to .mzML format as centroided and peak-picked data files using msconvert in ProteoWizard with 32-bit binary encoding and MS levels 1-2.

3.2.5. Root exudate data processing

mzML data files were processed with MZmine 3 (Schmid *et al.*, 2023). LC and MS1 data were used to filter out noise and identify peaks representing chemical “features” present in the sample. Detailed MZmine parameterizations are available in the supplemental information.

The resulting feature table along with MS2 data corresponding to each feature were imported to SIRIUS (Dührkop *et al.*, 2019) for feature identification using default parameters.

In addition to MZMine 3's built in dereplication step, we manually dereplicated some features using RT and *m/z* ranges. We further filtered the list of features by first discarding those features that were missing from more than 80% of the samples. Afterwards, we used Maaslin2 R package (Mallick *et al.*, 2021) to separate the plant-originated features from contaminants and internal standards. We categorized a feature as an exudate feature if its abundance was higher ($\alpha = 0.05$) in samples than in negative controls, with the blocking variable as the random effect in the model. We did not control for multiple comparison at this stage as it was not a formal hypothesis testing but rather a data filtering step.

3.2.6. DNA extraction and sequencing

Soil DNA was extracted using Zymo Quick-DNA Fecal/Soil Microbe Miniprep Kit (Zymo Research Corporation, Irvine CA) according to the manufacturer instructions. Extracted DNA was quantified on Qubit 2.0 fluorometer using Qubit dsDNA HS Assay Kit (ThermoFisher Scientific Inc., Waltham MA). Primer sets 515F/806R and ITS1f/ITS2 from Earth Microbiome Project (Thompson *et al.*, 2017) were used to construct amplicon libraries for 16S rRNA and ITS region, respectively. Sequencing was performed at Microbial Community Sequencing Lab (University of Colorado Boulder, Boulder CO) on Illumina MiSeq® platform (Illumina Inc., San Diego CA) using 251 base pair (bp) paired-end reads, which generated averages of 31,972 and 68,871 reads per sample for 16S and ITS, respectively. Resulting reads were demultiplexed using QIIME2 (Bolyen *et al.*, 2019).

Demultiplexed reads were then denoised using DADA2 (Callahan *et al*., 2016) trimming all reads to 0-250 bp. Bacterial and archaeal taxonomy was assigned to 16S ASV sequences using the naïve Bayes sklearn classifier trained with the GTDB-Tk species representative genomes (release 207). Fungal ITS ASV sequence taxonomy was assigned using the naïve Bayes sklearn classifier trained with sequences from the UNITE database (version 9). Lastly, we filtered out those reads belonging to chloroplast and mitochondria.

3.2.7. Statistical analysis

Univariate statistical tests were performed using analysis of variance (ANOVA) with crop genotype as the main effect and block as a random effect. All variables and residuals were examined to ensure that assumptions of ANOVA were met, and log transformed as needed. All statistical analyses were performed in R (R Core Team, 2020). R packages *lme4* (Bates *et al*., 2015) and *lmerTest* (Kuznetsova *et al*., 2017) packages were used for mixed effect model construction and applying ANOVA, respectively. Pairwise comparisons between genotypes were performed using the *emmeans* (Lenth, 2020) package, applying Tukey adjustment for multiple comparisons.

The microbial communities and root exudate metabolites were described with nonmetric multidimensional scaling (NMDS) using Bray-Curtis dissimilarity index (*vegan* package; Oksanen *et al*., 2022). Two dimensional NMDS was used to describe both the 16S and ITS dataset, as well as the positive and negative ionization metabolites (stress = 0.186, 0.120, 0.160, 0.106 respectively). To elucidate crop genotype effect on microbial communities and the exudate metabolome, we performed permutational multivariate analysis of variance (PERMANOVA; maximum permutation = 999) with crop genotype as the sole main

effect and block as a random effect. MaAsLin2 package (Mallick *et al*., 2021) was used to elucidate genotype effect on individual ASVs and metabolites, with genotype as the fixed effect and block as the random effect.

The interactions between root architecture, root exudate composition, and 16S/ITS profiles were investigated using distance-based redundance analysis (dbRDA; *vegan* package, Oksanen *et al*., 2022). For root architecture's interaction with metabolites and microbial communities, proportions of root volume in the first three diameter classes as well as SRL were modeled as independent data matrices. For root exudates' interaction with microbial communities, we chose the top 25 positive ionization metabolites based on their relative enrichment in samples vs negative control as mentioned in subsection *root exudate data processing*. Only 16 negative ionization metabolites were deemed to have originated from plants, so no further filtering was necessary. Each ionization mode was modeled separately as an independent data matrix and each amplicon data matrix was modeled as response data matrix. In total, we performed six independent dbRDA. When we found a significant model effect, we applied the same model but with marginal tests, which allowed us to test the effect of each variable within independent data matrix independently.

One replicate of annual wheat was excluded from all data analysis due to plant mortality. Another replicate of annual wheat was excluded from 16S analysis due to poor sequencing results. Raw LC-MS/MS data from two annual wheat plants and one Kernza plant (positive ionization mode), as well as one perennial wheat (negative ionization mode;) were excluded from subsequent data processing for poor data quality. For multiple co-inertia analysis, we only chose those samples with valid 16S, ITS, negative and positive ionization

metabolomics profiles and excluded one additional Kernza plant for being an outlier (n = 38). For all analyses, $p < 0.05$ was considered significant. The *p*-values were adjusted for multiple comparisons using false discovery rate (fdr; Benjamini and Hochberg, 1995).

R packages within *tidyverse* (Wickham *et al.*, 2019) were also used for data manipulation and visualization. Open source graphics software Inkscape (the Inkscape Project, 2023) was used for arranging graphs and creating graphics.

3.3. Results

3.3.1. Plant growth and root characteristics

Total biomass for annual wheat was 48% and 38% greater than perennial wheat and Kernza, respectively (Table 3.1). Shoot biomass followed a similar pattern, while for root biomass annual wheat was only higher than perennial wheat, but not Kernza (Table 3.1). At the same time, Kernza demonstrated the highest R:S ratio, which was 37 % greater than annual wheat, while the R:S ratio of perennial wheat was intermediate and not different from the other two genotypes (Table 3.1).

Table 3.1. Biomass of shoots, roots, and whole plant for all three genotypes (annual wheat, perennial wheat, Kernza) and their root:shoot ratio following 8 weeks of growth in greenhouse conditions. Values shown are the mean ± standard error. The *p*-values associated with genotype effects are presented at the bottom, with significant values ($p < 0.05$) in italics. Lower-case letters in each coumn denote significant ($p < 0.05$) pairwise differences between genotypes (Tukey's post-hoc).

	Biomass (mg)			Root :Shoot
	Shoots	Roots	Total	
Annual wheat	499.1 ± 26.4 a	260.0 ± 15.4 a	759.1 ± 39.8 a	0.52 ± 0.02 b
Perennial wheat	312.2 ± 18.8 b	200.4 ± 20.0 b	512.6 ± 35.4 b	0.64 ± 0.05 ab
Kernza	321.9 ± 21.6 b	227.5 ± 23.3 ab	549.3 ± 40.0 b	0.71 ± 0.06 a

p-value	*<0.001*	*0.038*	*<0.001*	*0.039*

All three genotypes had significantly different root volume across the four root diameter classes (< 250 µm, 250-500 µm, 0.5-1 mm, > 1mm; Fig. 3.1). In absolute amount (root volume in cm^3), annual wheat had the highest volume of roots within the 250- 500 µm diameter class compared to the other two genotypes (Fig. 3.1). In contrast, Kernza had the highest root volume in the > 1 mm diameter class, more than three times greater than that of annual wheat (Fig. 3.1).

We also calculated root volume in each diameter class as a proportion of the total root volume to understand relative investment in different kinds of roots (Fig. 3.1). Perennial wheat had the highest proportion of roots in the < 250 µm size class and was significantly greater than Kernza (Fig 3.1). In the next class (250-500 µm), proportion of roots was the highest for annual wheat, followed by perennial wheat, and then by Kernza (Fig. 3.1). Kernza had a highest proportion of coarse roots (0.5-1.0 mm; > 1.0 mm) compared to the other two genotypes (Fig. 3.1).

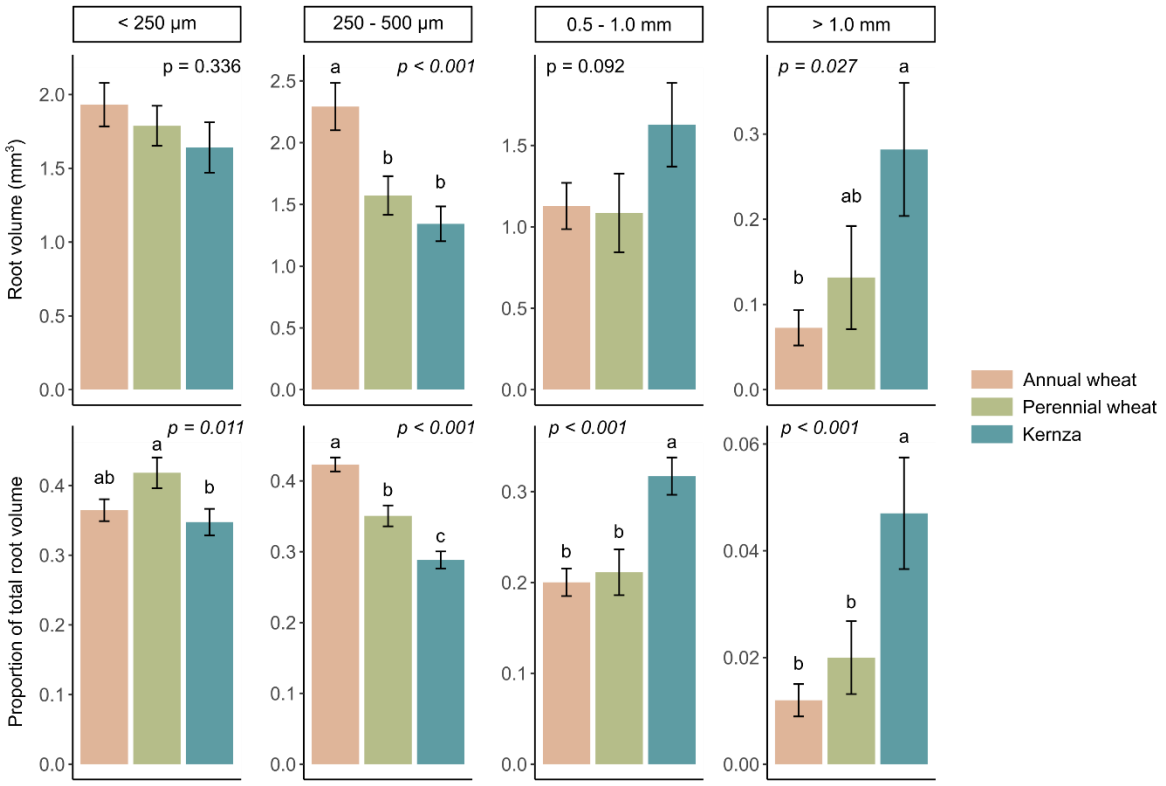

Figure 3.1. Mean distribution of root volume across four diameter categories (error bars represent the standard error) for three genotypes (annual wheat, perennial wheat, Kernza) following 8 weeks of growth in greenhouse conditions. Top row shows root volume in absolute value (mm^3), while the bottom row shows root volume as a proportion of the total for each genotype. Significance of the genotype effect are denoted within each panel and significant values ($p < 0.05$) are italicized. Lower-case letters above the bars in each panel denotes significant ($p < 0.05$) pairwise difference between the genotypes (Tukey's post-hoc).

Despite differences in root volume, genotype did not have a significant effect on total root length, surface area, total volume, or SRL (Table 3.2). However, perennial wheat had 16% greater SRA than Kernza (Table 3.2).

Table 3.2. Root total length, surface area, volume, specific root length (SRL), and specific root area (SRA) for all three genotypes (annual wheat, perennial wheat, Kernza) following 8 weeks of growth in greenhouse conditions. Values shown are the mean ± standard error. The *p*-values associated with genotype effects are presented at the bottom, with significant values ($p < 0.05$) in italics. Lower-case letters in each coumn denote significant ($p < 0.05$) pairwise differences between genotypes (Tukey's post-hoc).

	Total length (m)	Surface area (cm^2)	Volume (cm^3)	Specific root length ($mm\ mg^{-1}$)	Specific root area ($cm^2\ mg^{-1}$)
Annual wheat	43.8 ± 3.5	443.5 ± 34.6	5.42 ± 0.46	57.8 ± 3.2	1.69 ± 0.06 ab
Perennial wheat	33.4 ± 2.5	363.9 ± 30.2	4.58 ± 0.53	66.4 ± 4.6	1.86 ± 0.08 a
Kernza	37.6 ± 4.0	369.6 ± 39.1	4.89 ± 0.59	67.5 ± 4.9	1.61 ± 0.05 b
p-value	0.079	0.160	0.421	0.265	*0.019*

3.3.2. Root exudate rate

Exudation rate ranged from 53.7 to 149.1 μg C hr^{-1} $plant^{-1}$ and varied significantly between genotypes. Annual wheat exuded 25% more C per hour compared to Kernza, with perennial wheat being intermediate (Fig 3.2a). When exudation rate was normalized by root weight (specific exudation rate), we found that perennial wheat exuded greatest amount of C per unit root biomass, followed by annual wheat and Kernza (Fig. 3.2b). Exudation rate was highly correlated with all four root parameters (total length, surface area, volume, and biomass), but most closely with surface area ($R^2 = 0.44$, $p < 0.001$; Fig. S3.1).

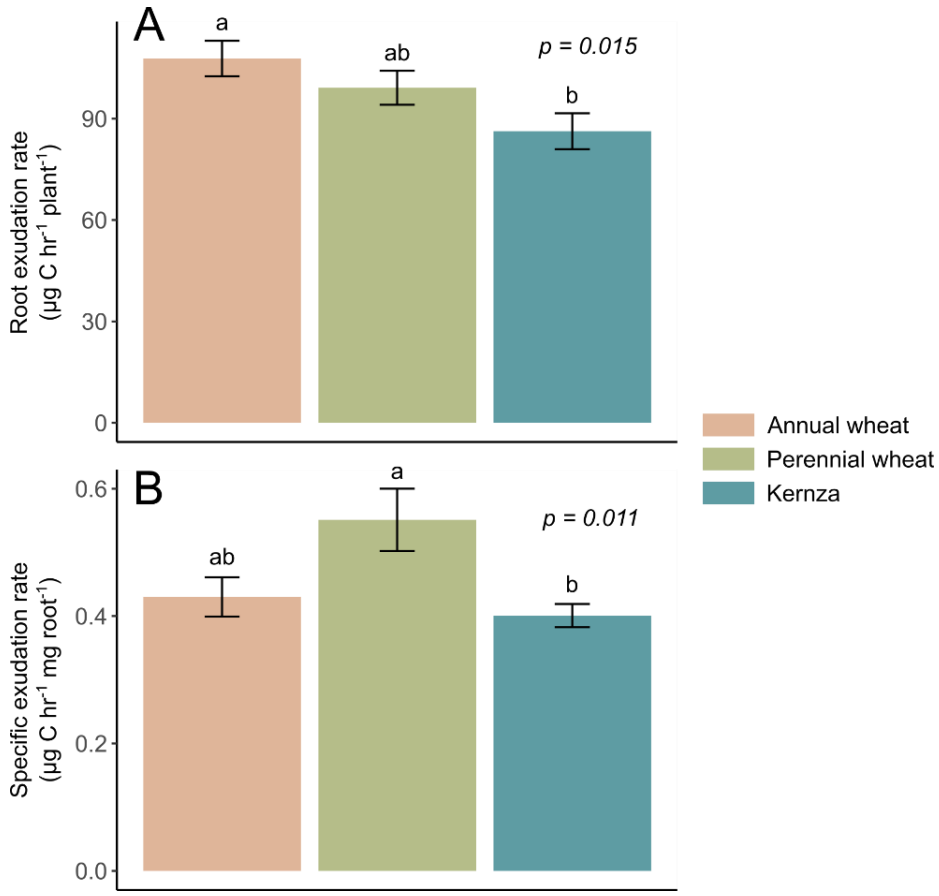

Figure 3.2. (A) Mean root exudation rate and (B) specific exudation rate for all three genotypes (annual wheat, perennial wheat, Kernza; error bars represent the standard error) following 8 weeks of growth in greenhouse conditions. The *p*-values for the genotype effect are denoted within each panel and significant values ($p < 0.05$) are italicized. Lower-case letters above the bars in denote significant ($p < 0.05$) pairwise difference between the genotypes (Tukey's post-hoc).

3.3.3. Integrated analysis of root exudate and microbial community profiles

We identified 318 and 118 unique chemical features from the LC-MS/MS in positive and negative ionization modes, respectively (Table S3.1). Of these features, 57 positive ionization and 16 negative ionization features were significantly enriched in exudate samples vs controls (Table S3.1). Among these 73 total features, 19 positive ionization and 9 negative ionization features had associated MS2 spectra and hence corresponding

chemical formula annotation (Table S3.1). SIRIUS provided compound identity annotation for five features from each ionization mode (Table S3.1).

Additionally, we obtained 10,668 and 3,566 ASVs via 16S and ITS sequencing, respectively. Of these ASVs, 6,286 and 2,427 were taxonomically identified beyond the family level. Among the identified ASVs, the genus *Nitrosocosmicus* was the most abundant archaeal genus with 32,213 reads from 7 ASVs and *Gp6-AA40* was the most abundant bacterial genus with 10,947 reads from 46 ASVs. For the fungal genus, *Solicoccozyma* was the most abundant (87,774 reads, 144 ASVs).

PERMANOVA on each of the four individual -omics data (positive- and negative-ionization exudates, 16S and ITS sequences) did not reveal any significant genotype effects (Figs S3.2a, d; S3a, d).

Lastly, we investigated the relationship between root architecture, root exudates, and microbial community via dbRDA. Root architecture showed significant association with both positive and negative ionization metabolites (Figs 3.3a, b). Specifically, proportion of roots in diameter class 2 (250-500 μm) was correlated with positive ionization metabolites and those in class 1 and 3 (< 250um and 0.5-1.0 mm) were related with negative ionization metabolites (Figs 3.3a, b). In turn, the negative ionization exudate metabolites were significantly associated with 16S profile regardless of plant genotype (Fig 3.3c). Among these 16 metabolites, we found that compound neg.C42 (*unidentified; m/z = 250.13*) specifically associated with the 16S profile (Fig 3.3c). Among the five ASVs that responded most sensitively to negative ionization exudates were two bacterial ASVs belonging to

phylum *Cyanobacteria*, and three archaeal ASVs belonging to phylum *Thermoproteota* (Fig 3.3c). Other pairings (root architecture on either 16S or ITS, negative ionization exudates on ITS, positive ionization exudates on 16S and ITS) did not show any significant relationships ($p > 0.05$, dbRDA, data not shown).

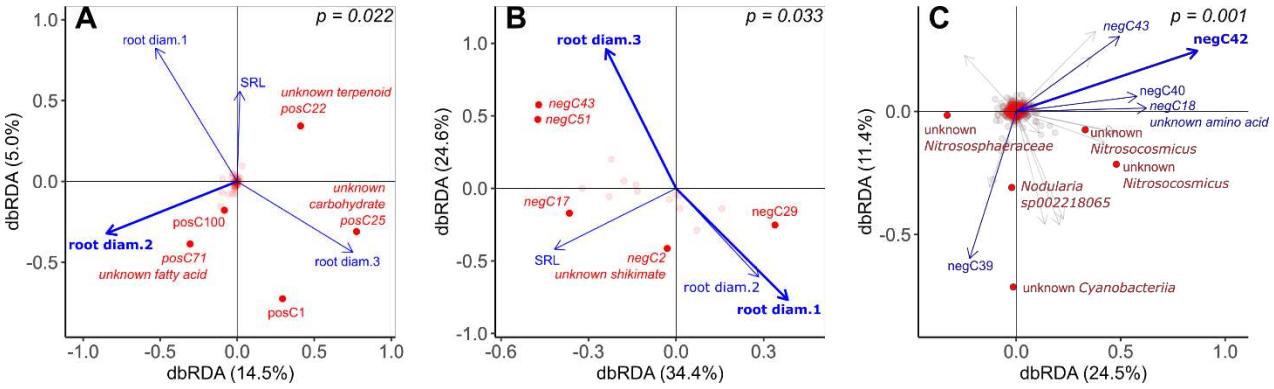

Figure 3.3. Interactions between root architecture and (A) positive ionization exudates, (B) negative ionization exudates, and (C) between negative ionization exudates and 16S profiles via distance-based redundancy analysis (dbRDA). Root architecture data were obtained via root scanning, exudates via LC-MS/MS, and 16S via rhizosphere soil DNA amplicon sequencing. Analyses were performed on Bray-Curtis dissimilarity matrices. The blue arrows and the red dots indicate the independent variable matrix and the response matrix, respectively. Significance of the whole model is noted in the upper right corner of each panel. Marginal tests were performed for each model and those individual variables significant at $p < 0.05$ level were highlighted with bold lines and bold fonts. Only those response variables that are the farthest from (0, 0) point in each panel were labeled (n = 5). In panel (C), five independent variables were chosen in the same manner. If exudates were annotated in any manner in Table S3.1 they were highlighted in italics. When available, compound notation for exudate was given along the compound number. (root diam.1; proportion of root volume with diameter < 250 µm, SRL; specific root length, posC- and negC-; positive and negative ionization exudate compounds, respectively)

3.3.4. Analysis of individual metabolites/ASVs, diversity indices, and fungal trophic modes

Differential abundance analysis of individual metabolites/ASVs via pairwise MaAsLin2 showed that one positive ionization feature (pos.C149; unidentified) was more abundant in perennial wheat than in Kernza (Fig S3.4). Similarly, one negative ionization feature (neg.G.C5.C7; 2-[(3-Carboxyanilino)carbonyl]-5-nitrobenzoic acid) was more abundant in

annual wheat than in Kernza (Fig S3.4). We did not find any individual ASVs that varied significantly in abundance between genotypes.

We also analyzed alpha diversity of all four -omics datasets. We found that Kernza's negative ionization exudate profile was less diverse than that of annual wheat and perennial wheat, in both richness and evenness (Shannon's index; ANOVA; Fig S3.2e, f). We found no evidence of genotype effect on alpha diversity of positive ionization exudate profile (Fig S3.2b, c) or 16S/ITS community profiles (Fig S3.3b, c, e, f).

Using FUNGuildR, we found trophic mode information for 2569 fungal ASVs out of total of 3,566 ASVs. Among these, 1,285 ASVs' trophic mode assignments were ranked as "Probable" or "Highly probable". Saprotrophs were the largest group with 466 ASVs, followed by pathotrophs at 188 ASVs and symbiotrophs at 67 ASVs. The rest had two or more fungal trophic mode assignments. We found that both perennial varieties had greater relative abundance of pathotrophic fungi in its rhizosphere than annual wheat (Fig 3.4). We also calculated symbiotroph to pathotroph ratio, which was the highest in annual wheat, intermediate in perennial wheat, and the lowest in Kernza (Fig 3.4).

3.4. Discussion

3.4.1. Genotype effect on root architecture and exudation rate

We hypothesized that Kernza, a perennial variety that has been domesticated only recently, would invest belowground most heavily out of the three genotypes. On the other hand, we expected annual wheat, optimized for high grain yield, would prioritize aboveground growth

at the expense of the belowground investment. Lastly, we hypothesized that perennial wheat, being the hybrid of the two, would show intermediate belowground investment.

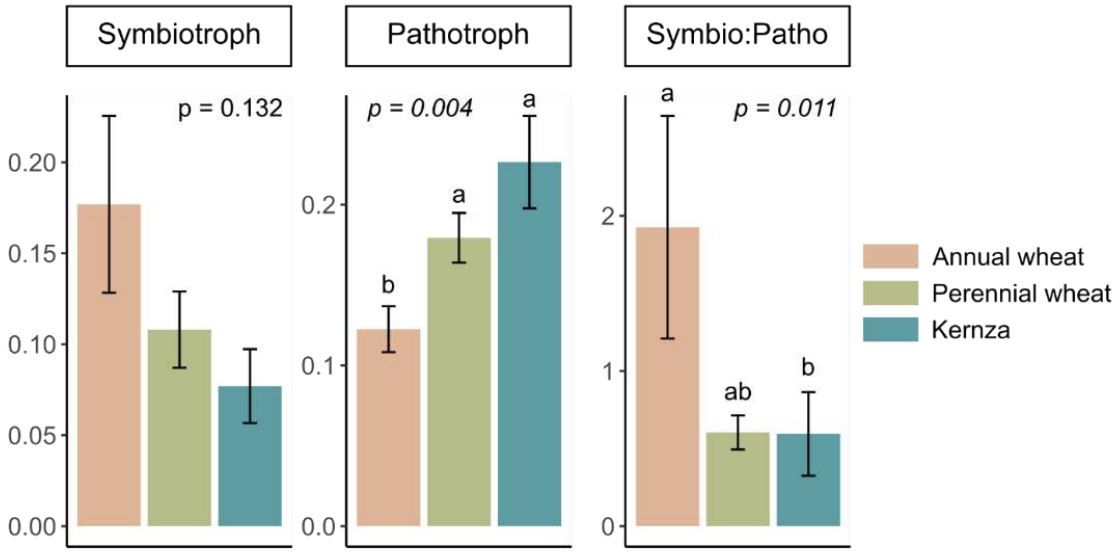

Figure 3.4. Relative abundances of fungal ASVs classified as symbiotrophs and pathotrophs (among those with positive identification via FUNGuildR; Nguyen *et al.*, 2016; Furneaux and Song, 2021) as well as the ratio between symbiotrophs and pathotrophs extracted from the rhizosphere of three genotypes (annual wheat, perennial wheat, Kernza) growing for 8 weeks under greenhouse conditions. Values represent the mean, and error bars are the standard error. The *p*-values for the genotype effect are denoted within each panel and significant values ($p < 0.05$) are italicized. Lower-case letters above the bars denote significant ($p < 0.05$) pairwise difference between the genotypes (Tukey's post-hoc).

We used R:S ratio as one of primary indicators of relative belowground investment. As we hypothesized, the R:S ratio of the three genotypes was the highest in Kernza, intermediate in perennial wheat, and lowest in annual wheat (Table 3.1). This result is in line with a past study that found that an annual wheat hybrid had intermediate R:S ratio compared to its parents (Wang *et al.*, 2006).

Another indicator of relative belowground investment was specific exudation rate. Surprisingly, perennial wheat exceeded both Kernza and annual wheat in specific

exudation rate despite being the hybrid (Fig 3.2b). We suspect that this unexpected result is driven by root investment allocation pattern across different diameter classes. Each genotype had at least one diameter class into which they invested more heavily than the other two genotypes. For instance, proportion of very fine (< 250 μm) roots was higher in perennial wheat than either of its parent lines (Fig 3.1). This likely contributed to perennial wheat's high specific root area, which was also higher than those of Kernza and annual wheat (Table 3.2). Root surface area was strongly correlated with root exudation rate (Fig S3.1). In summary, perennial wheat preferentially grew very fine (< 250 μm) roots, which increased SRA and contributed to a greater specific exudation rate (Figs 3.1, 3.2b, Table 3.2).

Hybrids investing more heavily belowground compared to their parents have been reported in some past studies. For example, Chairi *et al.* (2016) studied maize inbred lines and the hybrids in and out of water stress and found that most root measurements (e.g., root weight density, specific root length) were greater in the hybrids regardless of the water stress. Similarly, Cavani and Mimmo (2007) found that a hybrid maize line increased total organic C in soil compared to either of its parental lines (Cavani and Mimmo, 2007). The authors concluded that the increase in soil C was driven by greater rhizodeposition by the hybrids, which is echoed by the findings in our study (Cavani and Mimmo, 2007). These phenomena are likely instances of "heterosis", or hybrid vigor (Baldauf and Hochholdinger, 2023). The above literature explored absolute differences in belowground investment unlike our result, which used relative measures. However, our findings could also be yet another example of belowground heterosis. If perennial wheat had a greater proportion of

thicker roots like either of its parents, it would have had smaller total root surface area and thus lower exudation rate. Both of those traits (surface area and exudation rate) are linked to greater soil nutrient uptake (Raghothama and Karthikeyan, 2005; Meier *et al.*, 2017). Therefore, by investing more heavily into very fine roots, which in turn increases surface area and exudation rate, perennial wheat may be maximizing its nutrient uptake potential with its limited biomass resources.

3.4.2. Root exudate and microbial community composition

We hypothesized that Kernza and annual wheat would have the two most distinct root exudate and microbial community profiles, and that perennial wheat would fall somewhere in between the two extremes. Despite our expectations, analysis of individual -omics dataset via PERMANOVA revealed no genotype effects and thus did not support our hypothesis (Figs S3.2, S3.3).

This lack of a genotype effect was surprising given the past studies that have found distinct exudate profiles/ microbial communities under more closely related plants. For instance, Iannucci *et al.* (2017) studied modern durum wheat and its wild relatives and found that their root exudate chemical compositions differed. Similarly, Leff *et al.* (2017) showed that sunflower and its wild relatives fostered slightly different fungal communities. Therefore, we expected greater separation between Kernza and annual wheat given that they are two distinct species with varying degrees of domestication. Furthermore, some studies have specifically focused on crop hybrids and shown that their rhizosphere environments were distinct from those of their parental lines. One study examined organic acid abundance in root exudates of two maize hybrids and found the levels to be distinct from those of the

parental lines (Cavani and Mimmo, 2007). Other studies have specifically investigated hybridization of annual wheat lines and *Thinopyrum elongatum*, a perennial wheatgrass species related to Kernza (Cui *et al*., 2022; Yang *et al*., 2022). Those studies have found that the microbial communities of the hybrids were always distinct from those of the annual parents (Cui *et al*., 2022; Yang *et al*., 2022).

However, genotype effect on rhizosphere environment is not always consistent. Kelly *et al*. (2022) found that rhizosphere community composition did not differ among twelve distinct winter wheat varieties. They speculated that the difference in microbial community may become more evident if they had grown additional landraces and compared domestication groups (e.g. landraces vs. modern wheat) instead of comparing individual genotypes (Kelly *et al*., 2022a).

Another explanation for the lack of a genotype effect is the plant age. In a parallel field experiment, we found that Kernza and perennial wheat shared a similar 16S profile that was distinct from that of annual wheat (Hwang *et al*., *in prep*). These plants were harvested at maturity rather than at 8 weeks. It is possible that over time, the genotype effect would become more evident. Indeed, both exudate profiles and microbial communities have been shown to change throughout plant growth stages (Aulakh *et al*., 2004; Sugiyama *et al*., 2014). We must note, however, that when Cui *et al*. (2022) and Yang *et al*. (2022) studied an annual wheat hybrid with *Th. elongatum*, they observed genotype effects on 16S profiles as early as at 3-leaf stage. Therefore, in certain cases, genotype effects manifest even at early stages, which we did not observe in our study.

3.4.3. Root exudate identities and diversity

We successfully identified one metabolite (G.C5.C7) in the exudate samples belonging to anthranilic acid family (2-[(3-Carboxyanilino)carbonyl]-5-nitrobenzoic acid). Though overall exudate profiles did not differ between genotypes, G.C5.C7 was found in greater abundance in annual wheat exudate samples than in Kernza exudate samples (Fig S3.4). In the past, anthranilic acid has been found in the leaves of *Isatis indigotica* (Cao *et al*., 2020). Cao *et al* (2020) observed that its concentration decreased with decreasing N amendment inputs and concluded that low levels of anthranilic acid could be a sign of N limitation within plants. While this conclusion would suggest that Kernza may be experiencing N limitation, we did not observe any other signs of N stress.

Low rate of identification for metabolites is not uncommon for untargeted metabolomics approach (Patti *et al*., 2012). Compared to targeted metabolomics, untargeted metabolomics tend to generate more comprehensive profiles that can include unknown and novel compounds involved in the ecological process of interest (Patti *et al*., 2012). This broad approach could also explain why we have found metabolites belonging to groups such as fatty acids, terpenoids, and alkaloids that are seldom found in other root exudate studies (Table S3.1; Williams *et al*., 2022; McLaughlin *et al*., 2023).

3.4.4. Fungal trophic modes

While the ITS profiles did not differ between genotypes (Fig S3.3d), we organized ASVs into discrete fungal trophic modes via FUNGuildR and found evidence of a genotype effect (Fig 3.4). Annual wheat had the lowest proportion of pathotrophs among those ASVs with positive trophic mode assignment (Fig 3.4). Kernza had the highest proportion, while

perennial wheat showed intermediate values (Fig 3.4). Similarly, the symbiotroph-to-pathotroph ratio was the highest in annual wheat and the lowest in Kernza (Fig 3.4).

On one hand, this highlights heritability of rhizosphere fungal assembly in wide hybridizations. Hybridization has been used to confer fungal disease resistance from a parent onto the hybrid (Scholze *et al*., 2010; Zhang *et al*., 2023), and our result provides further evidence that such a transfer can happen. It seems that in our case, annual wheat conferred some fungal disease resistance to perennial wheat (Fig 3.4). On the other hand, it is surprising that it was annual wheat, not Kernza, that possessed such an ability. The life history of annual wheat as an intensively managed cereal crop wherein use of fungicide is common and provides a good context for a species to lose the ability to repel pathogenic fungi. The opposite can be said about Kernza, which has survived in the wild far more recently than annual wheat has (DeHaan *et al*., 2018). Indeed, greater resistance to fungal diseases has been reported in wild relatives of maize, rice, cotton, and soybeans (reviewed by Mammadov *et al*., 2018). However, the opposite trend, wherein domesticated crops develop rather than lose pathogen resistance, has also been documented. For instance, Leff *et al*. (2017) found lower relative abundance of known fungal pathogens in domesticated sunflowers compared to its wild relatives. Furthermore, one study has shown that modern wheat harbor fewer pathogenic fungi in its rhizosphere than its wild relatives (Spor *et al*., 2020). The latter study is especially applicable since it also looked at annual durum wheat. We suspect that millennia of artificial selection within a specific timeframe – following initial domestication but prior to wide adoption of fungicide use – may have led to accumulation of pathogen resistance in annual durum wheat.

Alternatively, plant age could have played a role here again. In our parallel field experiment, we found that symbiotroph-to-pathotroph ratio was higher in Kernza than in perennial wheat at maturity (Hwang *et al.*, *in prep*). It is possible that the fungal communities under these genotypes would change as plants mature.

3.4.5. Interactions between root architecture, exudates, and microbial community

Despite the general lack of genotype effect on the rhizosphere environment, we found that root architecture was correlated with both positive and negative ionization exudate profiles (Figs 3.3a, b), and the negative ionization exudate profile, in turn, was correlated with rhizosphere 16S profile (Fig 3.3c). Therefore, across all three genotypes, root architecture may have influenced the 16S profiles via distinct exudate profiles. Other studies have highlighted linkages between root architecture and microbial community. Pérez-Jaramillo *et al.* (2017) studied variation in common bean rhizosphere microbial composition and found that 11% of the total variation could be explained by root morphological traits. Similarly, Zai *et al.* (2021) demonstrated that wheat/maize roots of different diameter classes harbored distinct microbial communities. In the latter study, the authors speculated that root diameter had a strong effect via differences in turnover rate and root exudation. Indeed, in a recent review by Galindo-Castañeda *et al.* (2024), the authors suggested that different rates and composition of root exudate may mediate root architecture effect on rhizosphere microbial assembly. Our results appear to corroborate speculation by Zai *et al.* (2021) and Castañeda *et al.* (2024); We found that root architecture did not directly affect microbial community composition but was correlated with both positive and negative ionization exudate profiles (Figs 3.3a, b). Negative

ionization exudate profile, in turn, was correlated with rhizosphere 16S profile (Fig 3.3c). Therefore, across all three genotypes, root architecture may have influenced the 16S profiles via distinct exudate profiles.

3.4.6. Conclusion

Kernza and perennial wheat present an opportunity to introduce to modern agriculture not only perenniality, but also a suite of potentially beneficial rhizosphere traits. In this study, we found that via hybridization, perennial wheat achieved greater specific exudation rate compared to both of its parents. This finding has agroecological implications since greater exudation could lead to greater nutrient availability in the rhizosphere and associated plant uptake. While we did not find evidence of a genotype effect, we did demonstrate important relationships between root architecture, exudate composition, and microbial community assembly. We believe that these relationships can inform future efforts to modify crop microbiome, either through breeding or microbial inoculants.

Future studies will have to focus on the development of these exudates and microbial profiles over time as plants age. The genotype effects may become more pronounced over time and easier to detect. Other tests of rhizosphere function (such as pathogen exposure, arbuscular mycorrhizal fungi symbiosis, nutrient cycling, etc.) could help determine how much genotype affects rhizosphere function rather than structure. Regardless, the present study suggests that, within Kernza and perennial wheat, there are indeed interesting heterotic interactions as well as some level of rhizosphere trait interaction that merit further investigation. This study is therefore an important first step in integrating these traits

into breeding pipelines to create high-yielding perennial that can leverage beneficial rhizosphere interactions.

CHAPTER 4: PERENNIALIZATION AND INTERCROPPING EFFECTS ON WHEAT RHIZOSPHERE COMMUNITIES

4.1. Introduction

Perennial agriculture has been suggested as an alternative agriculture paradigm that can reduce the negative environmental impacts often associated with modern industrial agriculture (Crews *et al*., 2018). Growing perennial grains requires less energy input for planting and tillage and reduces soil disturbance, leading to conserved energy and improved soil health (Crews *et al*., 2016). The larger root systems of perennial crops also provide opportunities to increase water and nutrient uptake efficiencies (Mårtensson *et al*., 2022) and build soil organic matter (SOM; van der Pol *et al*., 2022). There is considerable interest in pairing perennial grains with legumes in cereal-legume biculture (or intercropping), as a means to reduce nitrogen (N) fertilizer inputs to the system (Crews *et al*., 2016; Reilly *et al*., 2022). The two main pillars of perennial agriculture research are therefore, 1) developing novel perennial cereal crops and 2) evaluating them in the context of cereal-legume bicultures.

Wild perennial plants are often used as sources of new perennial crop development via *de novo* domestication (Van Tassel *et al*., 2017; DeHaan *et al*., 2018). Breeders target promising wild perennials and apply artificial selection to increase their yield while maintaining their perenniality (Van Tassel *et al*., 2022). Kernza® is a grain from the domestication of intermediate wheatgrass (IWG; *Thinopyrum intermedium*) is one of such crop species (DeHaan *et al*., 2018). Once a wild perennial cool season grass, Kernza's yield

has and continues to be improved through breeding efforts involving traditional and newer molecular techniques such as genomic selection, and it along with rice have become the first perennial cereal grains available to the public (DeHaan *et al*., 2023). Another perennial grain development approach involves wide hybridization, where the perenniality of the chosen wild plants is introduced to modern crops by hybridizing them (Hayes *et al*., 2018). Perennial wheat, a cross between IWG and annual durum wheat (*Triticum turgidum* subsp. *durum*) is one example of this method (Cox *et al*., 2010; Hayes *et al*., 2018).

Perenniality is not the only trait that the wild plant species can provide via *de novo* domestication. They can also act as sources of many other ecologically beneficial traits, some of which have direct impact on cereal-legume biculture integration. For example, wild relatives of modern crops have been shown to possess greater physiological plasticity compared to their modern counterparts (Renzi *et al*., 2022). This is because domestication often acts as an evolutionary bottleneck that favors robustness (consistency) in trait expression (Renzi *et al*., 2022). In examining seven common crops and their wild relatives, Matesanz and Milla (2018) demonstrated that the wild relatives modulated their physiology to greater extent under nutrient and water limitation than their domesticated counterparts. Such plasticity is not limited to yield and aboveground traits. Wild relatives of barley, for example, demonstrated a greater plasticity in its root architecture in response to nutrient limitation than either the modern or landrace varieties (Grossman and Rice, 2012). Similarly, Junaidi *et al*. (2018) found progenitor of wheat (*Aegilops tauschii*) to have more plastic responses in belowground allocation than modern spring wheat varieties, when exposed to different nutrient sources (compost vs fertilizer). It has been suggested that

plasticity in root growth could help the wild varieties adapt readily to uneven distribution of nutrients in the soil (Grossman and Rice, 2012).

Physiological plasticity in root growth and belowground C allocation can help plants adapt to biculture conditions as it can allow for greater degree of niche partitioning (Bourke *et al*., 2021). For example, in maize-soybean biculture, soybean modified its root architecture to reduce its competition against maize specifically for water resources, thus enhancing the water uptake efficiency of the biculture vs. monoculture stands (Zhang *et al*., 2022). Similarly, in a wheat-maize biculture, wheat modified its root architecture to a greater extent in response to N availability than maize and saw greater benefit within the biculture system (Liu *et al*., 2015).

One of the primary benefits of cereal-legume biculture is the legume-to-cereal N transfer (Crews *et al*., 2022). This process depends not only on plant physiology but also on rhizosphere microbial community, via microbial depolymerization and mineralization of legume rhizodeposits (Høgh-Jensen, 2006). This mechanism therefore depends on an active microbial community that can break down N-containing organic molecules (Lai *et al*., 2022). Another mechanism is via common mycorrhizal networks (CMN; He *et al*., 2003) that connect cereal and legume roots, allowing for direct transfer of N via fungal hyphae. Therefore, the ideal candidate cereal would possess the ability to recognize the presence of neighboring legumes and modulate its microbial community assembly to facilitate both processes. In line with the above-mentioned findings for belowground allocation, wild plant species seem to possess a greater degree of plasticity in regulating rhizosphere assembly as well. In a recent study by Jacquiod *et al* (2022), the authors grew modern and ancient

wheat with or without chemical inputs (N fertilizer, fungi- and herbicides) and found that 16S diversity was greatly reduced in the ancient varieties' rhizosphere with chemical inputs. In contrast, the 16S profiles of the modern varieties remained unchanged (Jacquiod *et al.*, 2022). While this study was conducted with ancient crop relatives rather than the wild ones, we could assume the same trend would extend to wild varieties if those were compared to the modern varieties.

Kernza, being a recent domesticate, might also be expected to possess greater plasticity in microbial community assembly compared to modern cereal grain crops (DeHaan *et al.*, 2018). This would imply Kernza could adjust its rhizosphere microbial community when grown next to legumes, presumably to take greater advantage of the potential N source. Furthermore, microbial characteristics have been shown to be heritable in wide hybridization (Yang *et al.*, 2022). This implies that microbial community plasticity present in one parent could also be passed down to the hybrid. Therefore, if Kernza indeed possessed plasticity in regulating rhizosphere assembly, perennial wheat may have partially inherited such trait. Despite its importance in cereal-legume biculture, however, plasticity of rhizosphere microbial community assembly of the recently developed perennial cereals remains poorly understood.

To address the knowledge gaps outlined above, we established a field trial to characterize the rhizosphere microbial community of each of the three cereal crops (annual wheat, perennial wheat, and Kernza) as well as the response of intercropping these cereals with alfalfa (*Medicago sativa*), a deep-rooted perennial legume. We hypothesized that: 1) rhizosphere microbial community composition of annual wheat and Kernza will be most

dissimilar from each other with perennial wheat (the hybrid) being intermediate, and 2) all microbial communities will shift in biculture, but the greatest change will occur in Kernza and the smallest change in annual wheat since the former could have retained adaptive capabilities slowly bred out in the latter. Understanding how the rhizosphere microbial community of cereals changes when planted with legumes can help us better design perennial cropping systems and inform breeding efforts for future generations of crops that are better adapted to ecologically intensive agroecosystems.

4.2. Methods

4.2.1. Experimental Design

This study took place at the Colorado State University (CSU) Agriculture Research Demonstration and Education Center (ARDEC) near Fort Collins, CO (40°39'09.4"N 104°59'48.1"W, elevation: 1,552 m). This area has 0-3 % slope, receives an average of 270 mm of precipitation, with average maximum temperature of 30 °C in July and average minimum temperature of -10 °C in December (Colorado Agricultural Meteorological Network and USDA ARS, 2024). The soils at this site are classified as Fort Collins loam (fine-loamy, mixed, superactive, mesic Aridic Haplustalfs; Soil Survey Staff, 2019).

Cereal varieties evaluated consist of annual durum wheat (*Triticum turgidum* subsp. *durum*), perennial wheat (*Triticum turgidum* subsp. *durum x Thinopyrum intermedium*), and Kernza (*Thinopyrum intermedium*). All seeds were provided by the Land Institute (Salina, KS). Each of these cereals was planted in monoculture or in biculture with alfalfa (*Medicago sativa*). Each plot was 1.8 m wide and 6.1 m long, with nine rows (19-cm spacing between rows) within each plot. In biculture plots, we planted the cereal and alfalfa in

alternating rows, with five cereal rows and four alfalfa rows. The trial was established as a randomized complete block design, with each of the five replicate blocks containing all six factorial combinations of genotypes and cropping systems (mono- and biculture) as well as an alfalfa monoculture plot.

We planted the plots on Sept 14th in 2020 and again on October 8th in 2021 (annual and perennial wheat only) at the depths of 6-12 mm for Kernza and 25-40 mm for perennial wheat and annual wheat. Plots were irrigated by sprinkler for the first few weeks after seeding to facilitate establishment.

4.2.2. Biomass sampling and calculations

Biomass harvest took place on June 24th, 2021, and July 20th, 2022. We cut a 1.2 m wide 6.1 m long strip from the center of each plot to avoid edge effects. Biomass was cut ~5 cm from the ground and weighed fresh in the field. Two representative subsamples (~ 1 kg fresh biomass) were taken from this biomass sample and one of the subsamples was weighed before and after oven-drying at 60°C to determine water content of the harvested biomass. The other subsample was divided into cereal grain, alfalfa, and weeds before being dried to calculate dry mass composition of each plot. We calculated full plot equivalent yield for cereal in biculture plots by multiplying the yield by a factor of 1.8 (since only five of the nine rows contained cereal).

Relative competitive intensity (RCI) is a measurement of competition in a species mixture and is insensitive to differences in absolute productivity (Grace, 1995). RCI was calculated

for both cereals and alfalfa in biculture treatment using the following formula, derived from Grace (1995):

$$RCI = \frac{Y_{mono} - \left(Y_{bi} \times {d_{bi}}^{-1}\right)}{Y_{mono}}$$

Where Y_{mono} is the yield of the plant in monoculture in kg ha^{-1}, Y_{bi} is the yield of the plant in biculture, and d_{bi} is the planting density in biculture (5/9 for cereal, 4/9 for alfalfa). Positive RCI indicates that the plant species is experiencing competitive pressure.

Land equivalent ratio (LER) is a measurement of yield advantage in species mixture/ intercropping and corresponds to the relative monoculture land area required to achieve the same yield as the mixture (Mead and Willey, 1980). LER > 1 indicates that mixture/intercropping advantage is present (Mead and Willey, 1980). LER was calculated for each genotype in biculture treatment using the following formula from Osiru and Willey (1972):

$$LER = \frac{Yc_{bi}}{Yc_{mono}} + \frac{Ya_{bi}}{Ya_{mono}}$$

Where Yc_{bi} and Yc_{mono} are cereal yield in biculture and monoculture, respectively, and Ya_{bi} and Ya_{mono} are corresponding alfalfa yields. LER was calculated for each block x year combination for all three genotypes, using one alfalfa monoculture from each block as Ya_{mono} for each of the three cereals.

4.2.3. Rhizosphere sampling

Rhizosphere sampling took place on June 17th, 2021, and July 16th, 2022, prior to biomass harvest. From each plot, we randomly chose three cereal plants with no weeds in the immediately adjacent area (i.e., 20 cm radius). The cereal plants were carefully excavated from the soil to a depth of 15 cm using a shovel, with roots intact. The roots were shaken to remove loose adhering soil. The remaining soil on the roots was then carefully brushed off and collected as rhizosphere soil samples. The rhizosphere soil samples were frozen at -20°C until further analysis.

4.2.4. DNA extraction and analysis

Soil DNA was extracted using Zymo Quick-DNA Fecal/Soil Microbe Miniprep Kit (Zymo Research Corporation, Irvine CA) according to the manufacturer instructions. Qubit 2.0 fluorometer and Qubit dsDNA HS Assay Kit (ThermoFisher Scientific Inc., Waltham MA) was used to quantify the extracted DNA. Primer sets 515F/806R and ITS1f/ITS2 from Earth Microbiome Project (Thompson *et al*., 2017) were used to construct amplicon libraries for 16S rRNA and ITS region, respectively. Microbial Community Sequencing Lab (University of Colorado Boulder, Boulder CO) performed library sequencing on Illumina MiSeq® platform (Illumina Inc., San Diego CA) using 251 base pair (bp) paired-end reads, which generated averages of 24,735 and 42,974 reads per sample for 16S and ITS, respectively. Resulting reads were demultiplexed using QIIME2 (Bolyen *et al*., 2019) and then denoised using DADA2 (Callahan *et al*., 2016) trimming all reads to 0 – 250 bp. Bacterial and archaeal taxonomy was assigned to 16S ASV sequences using the naïve Bayes sklearn classifier trained with the GTDB-Tk species representative genomes (release 207). Fungal ITS ASV

sequence taxonomy was assigned using the naïve Bayes sklearn classifier trained with sequences from the UNITE database (version 9). Lastly, we filtered out those reads belonging to chloroplast and mitochondria. All data were rarefied to 10k reads per sample.

Additionally for ITS data, we assigned functional guild and trophic mode to each ASV using the FUNGuild database (Nguyen *et al*., 2016) and *FUNGuildR* package (Furneaux and Song, 2021). Per developer recommendation, we only retained those designations with confidence ranking "probable" or "highly probable." We further filtered out ASVs with more than one guild/trophic mode assignments to avoid overinterpreting the data (Nelson *et al*., 2024).

4.2.5. Statistical analysis

All statistical analyses were performed in RStudio (RStudio Team, 2020).

We analyzed biomass yield, relative abundance of fungal guilds, and microbial diversity indices (Shannon's and Chao1), with repeated measures analysis of variance (ANOVA). Model construction was done with *lme4* (Bates *et al*., 2015) package and statistical tests was performed with *lmerTest* (Kuznetsova *et al*., 2017) package. Crop genotype, cropping system, and year were modeled as fixed effects, while blocks and plots were modeled as random effects. The model also included all two and three-way interactions between the fixed effects. We used log or square root transformation to ensure that the assumptions of ANOVA were met. When appropriate, we performed pairwise comparisons of significant factors using *emmeans* (Lenth, 2020) package. We used Tukey adjustment for multiple

comparisons. Two-tail t-tests were used to determine if RCI or LER significantly differed from a set value (0 for RCI, and 1 for LER).

Multivariate statistics were performed with *vegan* R package (Oksanen *et al*., 2022). Microbial community data were described with nonmetric multidimensional scaling (NMDS) using Bray-Curtis Dissimilarity Index. Two-dimensional NMDS was used for the 16S data (k = 2, stress = 0.10) and three-dimensional NMDS was used for the ITS data (k = 3, stress = 0.16). Permutational analysis of variance (PERMANOVA; 999 permutations) was performed via adonis2 package to analyze treatment effect on microbial communities. Model construction was the same as ANOVA. When performing PERMANOVA, we opted for marginal tests to disregard the order in which the main effects were entered. Since marginal tests in *adonis2* function tests the significance of the highest order interaction, we systematically tested for significant effects in a stepwise fashion; the one three-way interaction (plant genotype x cropping system x year) was first tested; if not significant, we tested the three two-way interactions; if none were significant, we tested for the main effects without interaction terms. When we found significant two-way interactions, we performed pairwise comparison of one factor levels stratified by levels of another factor and vice versa. When we found a significant main effect, we performed simple pairwise comparison using a subset of the data containing only two levels of the factor at a time. The *p*-values generated in any pairwise comparisons were adjusted using the Benjamini-Hochberg method (Benjamini and Hochberg, 1995).

When we found a factor or an interaction of factors that influenced the microbial community via PERMANOVA, we also investigated its effect on individual ASVs using

Maaslin2 package (Mallick *et al*., 2021). For these analyses, we filtered out those ASVs present in fewer than 25% of the samples. Similarly to PERMANOVA, in case of interaction between factors, we investigated the effect of one factor separately for each level of the other factor.

We considered all *p*-values lower than 0.05 to be significant and those between 0.075 and 0.05 to be marginally significant. R packages in *tidyverse* (Wickham *et al*., 2019) were used for basic data manipulation and Inkscape (The Inkscape Project, 2023) was used for graph processing.

4.3. Results

4.3.1. Biomass yield

Whole plot biomass yield (cereal + alfalfa + weeds) in a season ranged from 950 kg ha^{-1} to 13,731 kg ha^{-1} across both years. Kernza plots produced markedly greater overall plant biomass than the other two genotypes regardless of cropping system or year (Table 4.1). For Kernza, the monoculture plots produced greater biomass than biculture plots (Table 4.1). For the other two genotypes, the inverse was true and the biculture plots outproduced the monoculture plots (Table 4.1). Monoculture plots decreased in biomass production in the second year across the genotypes, whereas biculture plots produced a consistent amount of biomass in both years (Table 4.1).

Table 4.1. Biomass production of annual wheat, perennial wheat, and Kernza in both monoculture and biculture (with alfalfa) cropping systems over a two-year period near Fort Collins, CO. Data shown in mean ± standard error. All cereal biomass numbers in biculture treatments are converted to full plot equivalent figures (see *biomass sampling and calculations* under the *methods* section). Pre-conversion values are given in parentheses. In the last row of each year is the mean alfalfa yield for each year that was used to calculate

RCI and LER (Table 4.2). All values given in parentheses were excluded from the statistical tests whose results are reported in the bottom section. The bottom section lists *p*-values associated with each response variable obtained via mixed effect linear model (G = crop genotype, S = cropping system, Y = sampling year), with significant values (< 0.05) denoted in bold.

Year	Crop genotype	Cropping system	Dry biomass (kg ha^{-1})			
			Whole plot	Cereal*	Alfalfa†	Weed
2021	Annual wheat	Mono	3,868 ± 507	2,588 ± 503	-	1060 ± 155
		Bi	6,807 ± 453	3,533 ± 766 *(1,963 ± 426)*	4,457 ± 216	387 ± 178
	Perennial wheat	Mono	3,725 ± 289	2,127 ± 365	-	1502 ± 198
		Bi	6,078 ± 522	875 ± 333 *(486 ± 185)*	4,506 ± 345	1086 ± 576
	Kernza	Mono	12,377 ± 679	12,350 ± 676	-	11 ± 7
		Bi	7,594 ± 192	9,014 ± 455 *(5,008 ± 253)*	2,284 ± 252	301 ± 137
	Alfalfa		-	-	*(5,154 ± 125)*	-
2022	Annual wheat	Mono	1,453 ± 228	36 ± 22	-	1300 ± 250
		Bi	5,915 ± 172	42 ± 18 *(23 ± 10)*	5,122 ± 417	825 ± 202
	Perennial wheat	Mono	2,065 ± 305	863 ± 281	-	1133 ± 395
		Bi	6,820 ± 248	706 ± 257 *(392 ± 143)*	5,944 ± 401	484 ± 310
	Kernza	Mono	11,376 ± 668	11,299 ± 707	-	78 ± 59
		Bi	8,645 ± 1,015	12,404 ± 2,333 *(6,891 ± 1,296)*	1,912 ± 533	88 ± 80
	Alfalfa		-	-	*(4,164 ± 198)*	-
		G	**<0.001**	**<0.001**	**<0.001**	**<0.001**
		S	**<0.001**	0.171	-	0.074
		Y	**<0.001**	**<0.001**	**0.016**	0.415
		G:S	**<0.001**	0.133	-	**0.029**
		G:Y	**0.003**	**<0.001**	**0.013**	**0.049**
		S:Y	**<0.001**	0.061	-	0.451
		G:S:Y	0.348	0.107	-	0.246
		trans‡	*sqrt*	*sqrt*	*none*	*sqrt*

* = biculture figures converted to full plot equivalent, pre-conversion values in the parentheses

† = excludes volunteer alfalfa in monoculture treatments

‡= type of transformation performed to ensure that we meet ANOVA's conditions (sqrt = square root transformation).

When we analyzed cereal biomass separately, Kernza still outproduced the other two genotypes (Table 4.1). The inverse was true for alfalfa, where alfalfa in the annual wheat plots and perennial wheat plots produced roughly 2.4 and 2.6 times more biomass than produced in the Kernza plots (averaged over both years; Table 4.1). This difference was greater in 2022 than in 2021 (Table 4.1). When we adjusted biculture cereal yield for number of rows, cereal biomass was slightly greater in monoculture than in biculture, only in 2021 (Table 4.1).

Weed biomass was greater for annual and perennial wheat compared to Kernza, especially in the monoculture treatments and in 2022 (Table 4.1). Monocultures tended to have greater amount of weed biomass compared to biculture, in annual and perennial wheat specifically (Table 4.1). We did not observe any year-by-year changes in weed biomass except for in perennial wheat, where we found a small decline in weed biomass in 2022 (Table 4.1).

Table 4.2. Relative Competitive Intensity (RCI) and Land Equivalent Ratio (LER) of each cereal genotype (annual wheat, perennial wheat, and Kernza) in both sampling years (2021-2022). Data shown in mean ± standard error. RCI is further divided into cereal and alfalfa, calculated based on their corresponding monoculture yield. Those values that significantly deviate from 0 (for RCI) and 1 (for LER) at 0.05 level are highlighted in bold. Positive RCI indicates presence of competition.

Year	Genotype	RCI		LER
		Cereal	Alfalfa	
2021	Annual wheat	-0.40 ± 0.47	**-0.89 ± 0.16**	1.62 ± 0.26
	Perennial wheat	**0.53 ± 0.18**	**-0.98 ± 0.18**	1.14 ± 0.08
	Kernza	**0.26 ± 0.05**	-0.01 ± 0.12	**0.86 ± 0.05**

	Annual wheat	-2.38 ± 1.32	**-1.74 ± 0.22**	3.09 ± 0.80
2022	Perennial wheat	-0.84 ± 1.26	**-2.26 ± 0.24**	2.47 ± 0.71
	Kernza	-0.10 ± 0.15	-0.01 ± 0.19	1.06 ± 0.10

Only perennial wheat and Kernza had significant positive RCI values in 2021 (Table 4.2). Alfalfa RCI value, on the other hand, was significantly negative for annual and perennial wheat for both years (Table 4.2). Only Kernza in 2021 had LER significantly lower than 1 (Table 4.2).

4.3.2. Microbial Community Composition and Diversity

Sequencing data resulted in 12,406 bacterial ASVs, 84 archaeal ASVs, and 4,815 fungal ASVs. Out of the 12,490 total 16S ASVs, we were able to identify 7,788 down to the genus level, with a total number of 547 unique bacterial/archaeal genera. We successfully identified 3,335 fungal ASVs to 57 genera.

Alpha diversity of rhizosphere prokaryote community (16S) was not affected by either cereal genotype or cropping system but was affected by an interaction of the two (Table 4.3). Perennial wheat rhizosphere bacterial/archaeal community was more diverse in monoculture than in biculture (Shannon's index), while the Kernza rhizosphere was marginally more diverse in biculture (Chao1; $p = 0.060$, Tukey's post-hoc test; Table 4.3). Rhizosphere fungal communities were not influenced by genotype or cropping system but were more diverse (Shannon's index and Chao1 index) in 2022 than in 2021 (Table 4.3).

Table 4.3. ASV evenness (Shannon's) and richness (Chao1) of both 16S and ITS extracted from rhizosphere of all three genotypes (annual wheat, perennial wheat, Kernza) in two cropping systems (monoculture and biculture) across two years (2021-2022). Data shown in mean ± standard error. The bottom section lists p values associated with each response

variable obtained via mixed effect linear model (G = crop genotype, S = cropping system, Y = sampling year). Those significant at 0.05 level are highlighted in bold. The final row denotes the type of transformation performed to ensure that we meet ANOVA's conditions (sqrt = square root transformation).

			Diversity			
			16S		ITS	
Year	Crop genotype	Cropping system	Shannon's	Chao1	Shannon's	Chao1
2021	Annual wheat	Mono	6.14 ± 0.06	921.9 ± 70.9	3.47 ± 0.11	123.6 ± 13.0
		Bi	6.14 ± 0.04	935.5 ± 43.3	3.38 ± 0.14	124.5 ± 15.7
	Perennial wheat	Mono	6.15 ± 0.03	957.3 ± 47.8	3.32 ± 0.07	113.2 ± 10.0
		Bi	6.01 ± 0.07	836.0 ± 64.6	3.49 ± 0.12	116.6 ± 14.1
	Kernza	Mono	6.00 ± 0.08	779.6 ± 41.9	3.31 ± 0.10	84.2 ± 8.3
		Bi	6.06 ± 0.07	853.7 ± 75.1	3.39 ± 0.15	117.2 ± 32.3
2022	Annual wheat	Mono	5.91 ± 0.04	768.2 ± 47.6	3.67 ± 0.09	143.1 ± 14.8
		Bi	6.05 ± 0.04	915.3 ± 28.7	3.63 ± 0.24	147.1 ± 30.3
	Perennial wheat	Mono	6.04 ± 0.04	866.7 ± 74.9	3.51 ± 0.10	111.0 ± 10.6
		Bi	5.91 ± 0.06	783.6 ± 42.3	3.49 ± 0.22	135.5 ± 13.8
	Kernza	Mono	5.98 ± 0.11	825.7 ± 84.1	3.64 ± 0.17	140.1 ± 26.9
		Bi	6.17 ± 0.12	1012.3 ± 106.1	3.52 ± 0.08	146.6 ± 10.0
		G	0.830	0.869	0.645	0.435
		S	0.616	0.351	0.888	0.252
		Y	0.084	0.625	**0.014**	**0.014**
		G:S	**0.037**	**0.044**	0.637	0.815
		G:Y	0.150	0.099	0.742	0.354
		S:Y	0.278	0.224	0.591	0.879
		G:S:Y	0.788	0.862	0.810	0.621
		trans	*none*	*none*	*none*	*none*

Based on our PERMANOVA results, we found evidence of significant genotype and cropping system effects, as well as a significant interaction between these factors in the 16S profiles (Fig 4.1). Specifically, perennial wheat and Kernza (the latter only marginally; p = 0.060) had distinct 16S profiles from annual wheat only in the monoculture system (Fig 4.1). We also found a significant year effect in the 16S profile, but it did not interact with the other two main factors (Fig 4.1). The ITS profiles, on the other hand, showed a significant cropping

system by year interaction (Fig 4.2), such that only the monocultures changed between the two years and monoculture differed from biculture, only in 2022 (Fig 4.2). Crop genotype did not affect the ITS profiles (Fig 4.2).

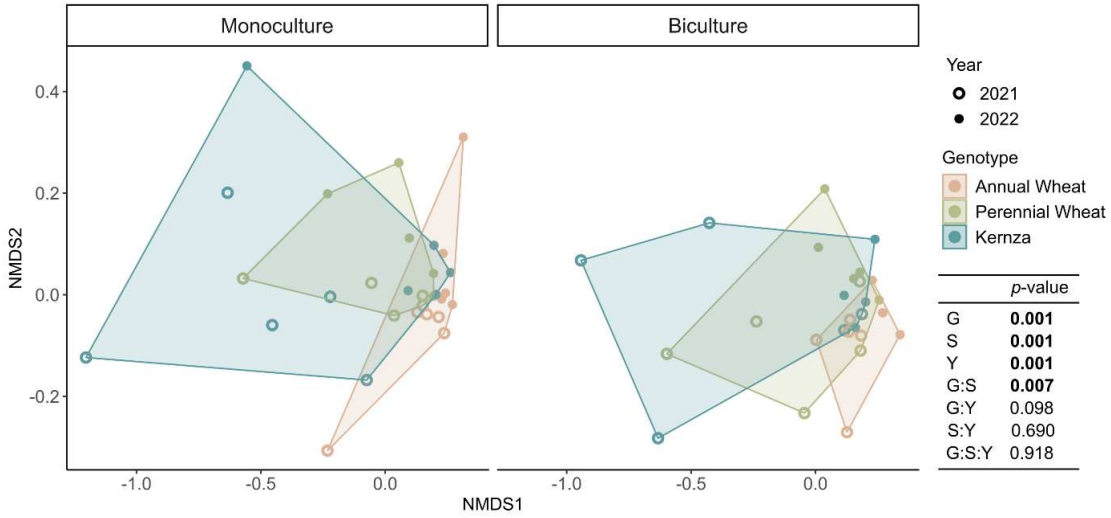

Figure 4.1. Ordination plot (NMDS) showing prokaryote (16S) community composition in rhizospheres of three crop genotypes (annual wheat, perennial wheat, Kernza) in two different cropping systems (monoculture, biculture) over two years (2021-2022). The distances were calculated using the Bray-Curtis Dissimilarity Index. The colored outlines encompass crop genotypes for both 2021 and 2022, as there was no significant interaction between sampling and the other two factors. Instead, sampling year is simply noted with empty (2021) and filled (2022) dots. The table in the bottom right corner indicates p-values for all interactions and main effects obtained with PERMANOVA (G = crop genotype, S = cropping system, Y = sampling year). Those values significant at 0.05 level are highlighted in bold.

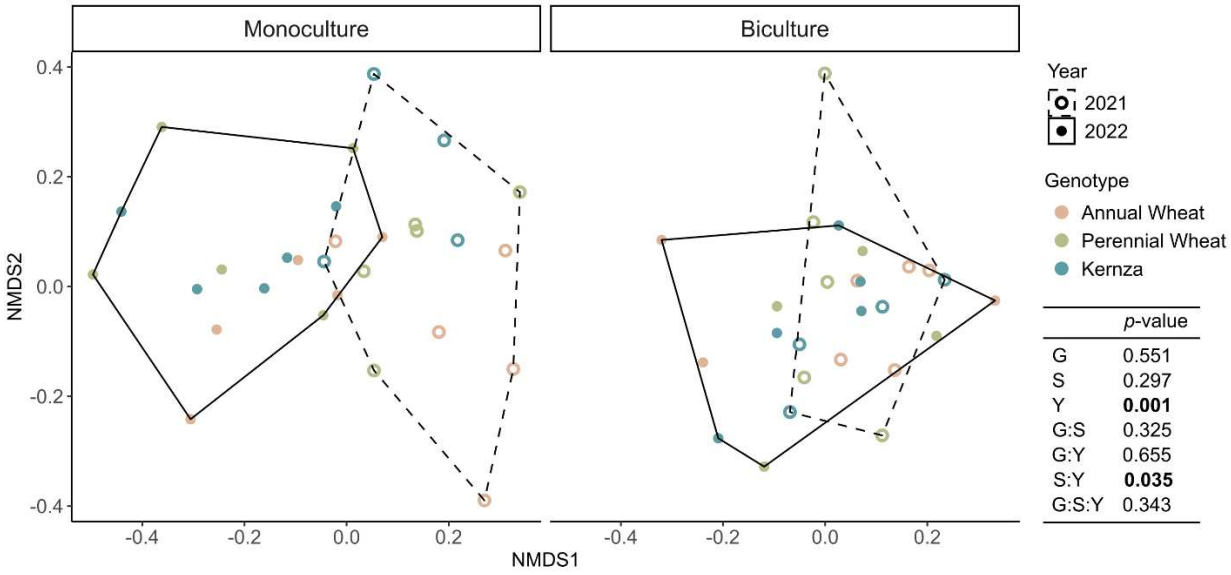

Figure 4.2. Ordination plot (NMDS) showing changes in rhizosphere fungal community composition of three crop genotypes (annual wheat, perennial wheat, Kernza) in two different cropping systems (monoculture, biculture) over two years (2021-2022). Distances were calculated using Bray-Curtis Dissimilarity Index. Outlines encompass all genotypes within each year x cropping system combination. The table in the bottom right corner indicates p-values for all interactions and main effects obtained with PERMANOVA (G = crop genotype, S = cropping system, Y = sampling year). Those values significant at 0.05 level are highlighted in bold.

4.3.3. Fungal Trophic Mode

Out of 4,815 fungal ASVs, we were able to assign 917 ASVs (19% of the total) to specific trophic modes and functional guilds using the FUNGuildR package. Among the identified ASVs, 48 ASVs (1% of total) were symbiotrophs, 184 ASVs (4% of total) were pathotrophs, and the rest were saprotrophs.

We investigated the abundance of symbiotroph and pathotroph as proportions of all ASVs that have been given proper trophic mode assignments. The proportion of symbiotrophs was higher in monoculture vs. biculture, and lower in 2022 than in 2021 (Fig 4.3; Table 4.4) but was not affected by crop genotype. The proportion of pathotrophs in perennial wheat

was nearly 3 times greater than that in Kernza, with annual wheat being intermediate (Fig 4.3; Table 4.4). Overall, pathotrophs were more abundant in 2021 than in 2022, especially for monocultures (Table 4.4).

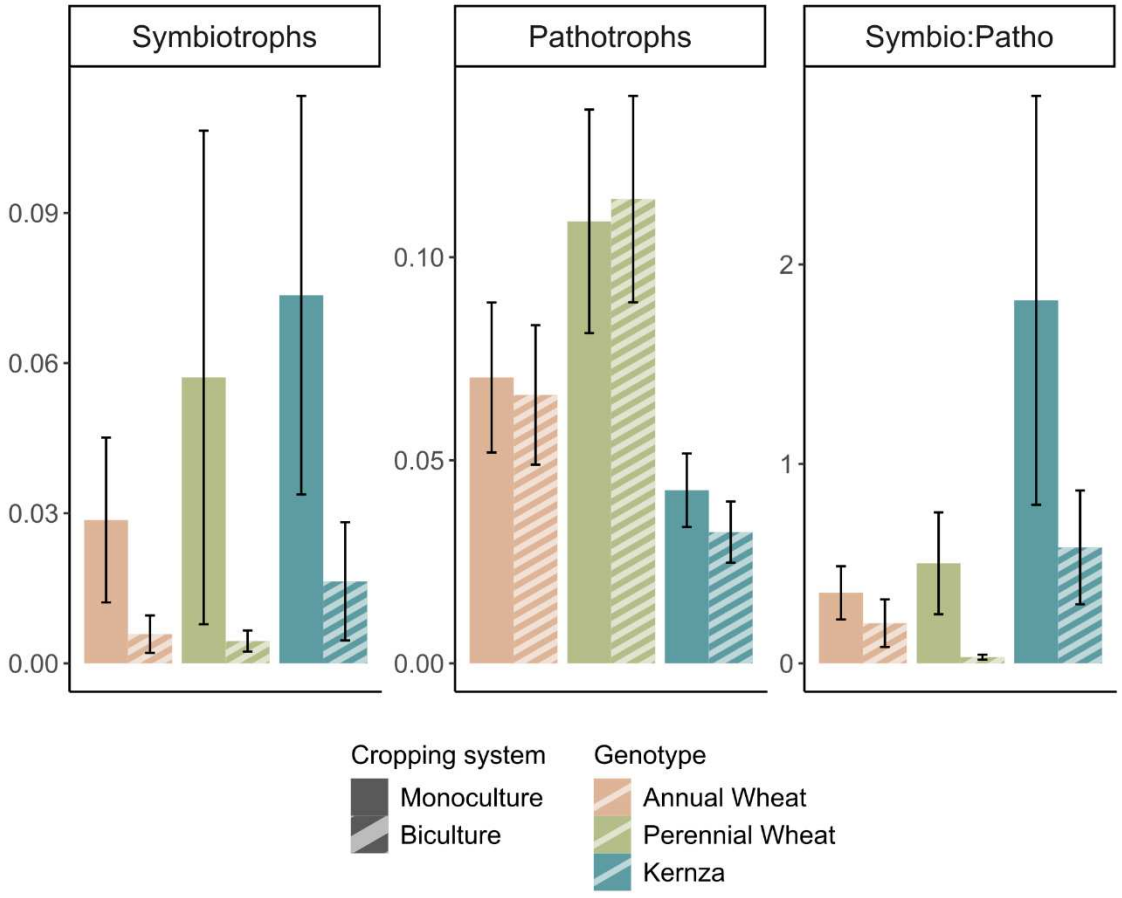

Figure 4.3. Relative abundance of symbiotrophic fungi and pathotrophic fungi as well as their ratio in rhizosphere of three genotypes (annual wheat, perennial wheat, Kernza) in two cropping systems (monoculture and biculture; data shown as mean ± standard error). ITS amplicon library was prepared from the extracted soil DNA and fungal trophic mode was assigned by FUNguildR (Furneaux and Song, 2021). Figure represents data averaged over both sampling years and the unabridged data can be found in Table 4.4.

Table 4.4. Relative abundance of symbiotrophs and pathotrophs based on total amount of ASVs given proper trophic mode assignment via FUNGuildR (Furneaux and Song, 2021), as well as the ratio between symbiotrophs and pathotrophs. DNA was extracted from rhizosphere of all three genotypes (annual wheat, perennial wheat, Kernza) in two cropping systems (monoculture and biculture) across two years (2021-2022). Data shown in mean ±

standard error. The bottom section lists *p*-values associated with each response variable obtained via mixed effect linear model (G = crop genotype, S = cropping system, Y = sampling year). Those significant at 0.05 level are highlighted in bold. The final row denotes the type of transformation performed to ensure that we meet ANOVA's conditions (sqrt = square root transformation).

			Fungal Trophic Modes		
Year	Crop genotype	Cropping system	Symbiotroph	Pathotroph	Symbio-patho ratio
2021	Annual wheat	Mono	0.053 ± 0.030	0.104 ± 0.027	0.449 ± 0.221
		Bi	0.006 ± 0.006	0.072 ± 0.022	0.121 ± 0.121
	Perennial wheat	Mono	0.103 ± 0.099	0.184 ± 0.021	0.516 ± 0.493
		Bi	0.006 ± 0.003	0.110 ± 0.038	0.044 ± 0.019
	Kernza	Mono	0.133 ± 0.084	0.051 ± 0.014	3.308 ± 2.178
		Bi	0.033 ± 0.026	0.040 ± 0.010	0.788 ± 0.571
2022	Annual wheat	Mono	0.004 ± 0.002	0.036 ± 0.014	0.235 ± 0.129
		Bi	0.006 ± 0.003	0.056 ± 0.033	0.335 ± 0.264
	Perennial wheat	Mono	0.011 ± 0.006	0.034 ± 0.013	0.487 ± 0.223
		Bi	0.002 ± 0.002	0.120 ± 0.037	0.014 ± 0.013
	Kernza	Mono	0.026 ± 0.014	0.036 ± 0.012	0.630 ± 0.373
		Bi	0.003 ± 0.002	0.026 ± 0.011	0.416 ± 0.286
		G	0.255	**0.003**	**0.021**
		S	**0.032**	0.945	**0.040**
		Y	**0.023**	**0.003**	0.311
		G:S	0.912	0.720	0.804
		G:Y	0.522	0.494	0.108
		S:Y	0.244	**0.020**	0.550
		G:S:Y	0.800	0.086	0.486
		trans	sqrt	sqrt	sqrt

We also calculated the symbiotroph-to-pathotroph ratio (S:P) and found that it was affected by both crop genotype and cropping system (Fig 4.3; Table 4.4). Kernza had a higher S:P ratio compared to perennial wheat, but not annual wheat (Fig 4.3; Table 4.4). Regardless of crop genotype, monocultures tended to demonstrate higher S:P ratios than bicultures (Fig 4.3; Table 4.4).

4.3.4. Individual ASV Differential Abundance

On the individual ASV level, we found one bacterial ASV, belonging to the phylum *Chloroflexota*, that was 69% more abundant in biculture than in monoculture for annual wheat only (Fig S4.1).

Individual fungal ASVs, much like overall ITS profile, responded only to a cropping system-year interaction (Fig S4.1). We found one ASV was more abundant in biculture only in 2021 (Fig S4.1). We also found one ASV that had higher abundance in monoculture and three that were more abundant in biculture, only in 2022 (Fig S4.1). One ASV was more abundant in biculture both years (Fig S4.1).

Likewise, we found three ASVs that increased and one that decreased in 2022, only in monoculture (Fig S4.1). One ASV increased in 2022, only for monoculture (Fig S4.1). Two ASVs increased in abundance in 2022 in both cropping systems (Fig S4.1).

4.4. Discussion

4.4.1. Biomass production

Cereal biomass production and its response to biculture treatment was influenced by both crop genotype and sampling year. When grown with alfalfa, annual wheat produced equivalent amount of biomass in both cropping systems (when corrected for planting density), suggesting a lack of competitive pressure from alfalfa (Tables 1, 2). On the other hand, both perennial varieties experienced competitive pressure in year 1, as indicated by the positive RCI values (Tables 1, 2). Interestingly, competitive pressure with alfalfa was no longer present for Kernza in year 2 (Table 4.2).

These discrepancies between the annual and the perennial cereals as well as Kernza's change in competitive pressure over time may be due to long-term changes in soil N status. In year 1, the field may have had sudden availability of inorganic N caused by tillage and subsequent microbial mineralization (Jackson *et al*., 2003). Such conditions would have been more beneficial to annual wheat that can take advantage of the inorganic N with rapid early growth (Gioia *et al*., 2015). But as cereal-legume plots mature, facilitative relationship may have developed between the alfalfa and cereals. Rhizodeposition by legumes could "replenish" soil organic N pool and cause more N to be available to neighboring plants (Daly *et al*., 2021). Additionally, direct N transfer from legumes to cereals can take place via direct root contact (He *et al*., 2003; Thilakarathna *et al*., 2016). Kernza was the only cereal that did not get resown in year 2. Therefore, Kernza likely had accrued greater root system by year 2 which led to greater root contact with neighboring legumes. Thus, the lack of competitive pressure observed in year 2 Kernza cereal yield may be due to changing soil organic N status as well as increased root contact.

Past studies have shown that not only can Kernza and alfalfa move away from a competitive relationship as they mature, but they can also form facilitative relationships over time. Reilly *et al*. (2022) found that relationship of Kernza grain and alfalfa biomass yield is competitive in year 1, neutral in year 2, and facilitative in year 3. Similarly, Crews *et al*. (2022) found that Kernza-alfalfa biculture takes time (3~5 years) to outproduce monocultures. Though our experiment only ran for two years, these past studies suggest that the same forces that eventually allows for facilitative relationship between Kernza and legumes may have been in effect in our study as well.

Unfortunately, perennial wheat did not survive well past its first-year harvest and had to be reseeded along with annual wheat for year 2. Furthermore, both annual and perennial wheat showed poor establishment in year 2, which was coupled with high weed pressure (Table 4.1). This made it difficult to compare Kernza's performance with that of other varieties. Therefore, we must take caution when interpreting the biomass data, especially for annual and perennial wheat, in year 2. Nevertheless, we believe that the above interpretation of Kernza biomass trend *per se* is still valid since Kernza's survival and establishment were satisfactory throughout the study.

We suspect that had annual wheat been established properly, it would have started experiencing competitive pressure from alfalfa as the dominant N form shifted from inorganic to organic. It is more difficult to predict what perennial wheat's year 2 performance would have looked like. In 2021, its biomass was lower in biculture than in monoculture, mirroring the cropping system effect in Kernza (Table 4.1). Therefore, in 2022, we might have seen a neutral response to cropping systems in perennial wheat, as we did in Kernza (Table 4.1).

4.4.2. Genotype effect on microbial community

We hypothesized that all three genotypes would harbor distinct microbial communities with perennial wheat being intermediate. In partial support for this hypothesis, we found that the perennial varieties (both Kernza and perennial wheat) had distinct 16S profiles to that of annual wheat (PERMANOVA; Fig 4.1). As hypothesized, perennial wheat also clustered between Kernza and annual wheat in the ordination plot, though it was not significantly different from Kernza (PERMANOVA; Fig 4.1). This result demonstrates that

perennial wheat's bacterial/archaeal community assembly skewed more towards Kernza than annual wheat despite being a hybrid of the two. In a similar study by Cui *et al*. (2022), the authors compared a wheat variety JN177 with SR4, an annual hybrid between JN177 and tall wheatgrass (*Thinopyrum elongatum*), a perennial. Here, much like in our study, Cui *et al*. (2022) found that the annual parent and the hybrid harbored two distinct prokaryotic communities. Together, these results suggest that rhizosphere 16S profiles of hybrids may resemble one parent and not the other, despite inheriting genetic materials from both parents. Additionally, this trend seen in 16S profiles was likely a true genotype effect rather than management (i.e. reseeding), weed biomass, or stand age effect. Both perennial and annual wheat had to be reseeded the second year and had significant weed biomass (Table 4.1), yet perennial wheat's 16S profile resembled that of Kernza, not annual wheat.

Unlike the prokaryotes, the overall fungal community did not show any evidence of a genotype effect. Instead, the genotype effect was observed in relative abundance of pathotrophic fungi. Pathotrophic fungi's relative abundance was the lowest in Kernza and highest in perennial wheat (Table 4.4, Fig 4.3). On one hand, it is surprising that perennial wheat, the hybrid, exceeded both of its parents in relative abundance of pathotrophic fungi. Often, crop hybrids are explored for heterosis, or 'hybrid vigor', in their traits, including fungal pathogen resistance (Scholze *et al*., 2010). For instance, Zhang *et al* (2023) has shown that a rice hybrid exceeded its parent lines in terms of its fungal pathogen resistance. In certain cases, however, it has been reported that hybridization can lead to accumulation of susceptibility genes, especially when the progeny is selected based on grain yield (Huang *et al*., 2015; Calvo-Baltanás *et al*., 2021). Increased pathotrophic fungi

relative abundance seen in perennial wheat rhizosphere, therefore, could be the result of a similar process.

Kernza's low relative abundance of pathotrophic fungi highlights its potential ability to suppress fungal disease. Such ability can be especially beneficial given Kernza's perenniality. Crop rotations are often used to prevent pathogen build up, and one of the vulnerabilities of perennial agroecosystems is inability to rotate crops when problems arise (Peralta *et al.*, 2018). However, we must reiterate that this is not a direct measurement of pathogen resistance, but rather relative abundance of known pathotrophs. Future studies could more directly investigate pathogen resistance in these genotypes and confirm whether the fungal membership leads to observable shifts in fungal function.

4.4.3. Intercropping effect on microbial community

We also hypothesized that a shift in microbial community in response to biculture treatment would be the greatest in Kernza and the smallest in annual wheat. In contrast to our hypothesis, incorporating legumes into cereal production led to convergence, rather than divergence, of cereal 16S profiles. As discussed in the above section, the rhizosphere prokaryote communities of Kernza and perennial wheat separated from annual wheat when in monoculture (Fig 4.1). However, this genotype effect was no longer significant in biculture (Fig 4.1).

One of the potential explanations involves competitive pressure. Past studies have reported interspecific competition-induced shifts in rhizosphere microbial communities. For example, Cavalieri *et al* (2020), found that the less competitive species (*Trifolium*

repens) in a species mixture shifted in its rhizosphere 16S profile. The resulting 16S profile was distinct and did not resemble that of the neighboring, more competitive, species (*Centaurea cyanus*). The authors found that the shift in *T. repens*' 16S profile was driven mostly by a decrease in *Rhizobium* abundance (Cavalieri *et al*., 2020). Cavalieri *et al*. (2020) speculated that interspecific competition drove *T. repens* to recruit taxa that are not as efficient at fixing N as *Rhizobium*, but can confer other benefits to withstand the competitive pressure.

Our RCI data shows that Kernza and perennial wheat experienced competitive pressure from alfalfa in biculture in year 1 while annual wheat did not (Table 4.2). Therefore, it is possible that the competitive pressure from alfalfa caused the 16S profiles of the perennials to shift, driven by perennial varieties recruiting other beneficial microbial taxa.

The other explanation involves "microbial spillover", in which microbial community of one plant simply colonizes the adjacent plant, often through close root contact (Ulbrich *et al*., 2022). Given the row-spacing and alfalfa's large root size, the legume roots likely came in contact with the cereal roots. Microbial spillover from alfalfa could explain why all three genotypes converged in 16S profiles vs in monoculture. Without the 16S profile of the alfalfa rhizosphere, however, it is difficult to confirm whether this mechanism was in effect. We must note that microbial spillover is a distinct ecological process, not simply sample contamination artifact. We took much care to excavate the cereals and collect only the soil adhering to the cereal roots. Therefore, we are confident that if microbes from alfalfa were present in cereal rhizosphere, the transfer happened prior to sampling via microbial spillover rather than via post-sampling cross contamination.

Even without sample cross-contamination, however, considerable amount of weed biomass could have affected cereal 16S profiles via either mechanism explored above (competition-induced shift and microbial spillover). Weed biomass was greater in perennial and annual wheat monocultures and could have exerted competitive pressure on the cereals as alfalfa did (Table 4.1). Similarly, close contact with weed roots could have led to microbial spillover from weed rhizosphere to cereal rhizosphere. Therefore, we must exercise caution in interpreting data including perennial and annual wheat, especially in monocultures.

Composition of the fungal community, unlike the prokaryotes, was only affected by cropping system and sampling year. In year 1, monoculture and biculture ITS profiles were not significantly different from each other (Fig 4.2). In year 2, monoculture's ITS profile shifted from the previous year while biculture ITS remained unchanged, leading to a significant difference between the two (Fig 4.2). This result implies that presence of legumes stabilized the fungal communities under cereals. Stand age or weediness likely did not affect the fungal community since all three genotypes shifted in the same manner in year 2 despite only two of them being reseeded and having greater weed biomass.

Differentiating effect of having conspecific neighbor that we observe in our ITS data has been reported in the past literature. For instance, Morris *et al* (2013) studied arbuscular mycorrhizal fungi (AMF) assemblages under *Plantago lanceolata* and found that denser monocultural environment led to greater differentiation in AMF profile. In contrast, the presence of other neighboring plant species had little influence on the focal plant AMF composition (Morris *et al*., 2013). They argued that, with more conspecific neighbors, the

focal plant was able to more efficiently recruit AMFs suited for single plant species (Morris *et al.*, 2013). On the other hand, in species mixtures, recruitment may be disrupted by other plant roots fostering and recruiting different fungi (Morris *et al.*, 2013). This may explain why only the monocultures developed distinct fungal communities in year 2 (Fig 4.2). Accumulated effect of specialized fungal recruitment by cereal monoculture could have simply carried over to the second year. This would have then helped further differentiate monoculture fungal community from the biculture, regardless of the poor establishment by annual and perennial wheat.

Furthermore, we observed greater relative abundance of symbiotrophic fungi in monocultures (Table 4.4, Fig 4.3), which may be due to more effective recruitment by cereals in monoculture vs in biculture. However, we must also note that relative abundance of symbiotrophic fungi decreased significantly in year 2 (Table 4.4, Fig 4.3). In other words, the shift in monoculture fungal community was not accompanied by continued accumulation of symbiotrophs nor did it help with establishment the following year.

4.4.4. Conclusion

Development of perennial cereal grains along with the spatial integration of legumes present opportunities to promote soil health and reduce fertilizer inputs. The essential pieces of this puzzle are the belowground characteristics of perennial cereals, and specifically how they adapt to cereal-legume biculture context. We found that Kernza, a domesticated perennial wheatgrass, has some promising belowground traits. Kernza had a lower relative abundance of pathotrophic fungi in its rhizosphere and overcame alfalfa's

competitive pressure by year 2. Perennial wheat, on the other hand, had some negative traits such as the highest pathotrophic fungal abundance in its rhizosphere. However, it also shared a similar rhizosphere 16S profile as Kernza in monoculture, demonstrating some belowground trait heritability. Our results also demonstrate the need for continued breeding efforts for greater survival and yield in perennial wheat. Broadly, we highlight the importance of evaluating both above- and belowground traits in and out of cereal-legume biculture systems. Future work may focus on quantifying N fluxes within the system including soil N status and legume-cereal N transfer. Different management decisions within cereal-legume biculture (legume species identity, seasonal cutting of legumes, row spacing, etc.) must also be considered in future research endeavors. Understanding belowground mechanism (plant-microbe interactions, topic explored in this paper) behind function of interest (increasing biologically fixed N in the cereals) and how to modulate this function (management techniques) will help us design cereal-legume biculture system that maximizes its potential benefits.

CHAPTER 5: INTERCROPPING IMPACTS ON RHIZOSPHERE COMMUNITIES AND ^{15}N TRANSFER ACROSS ANNUAL AND PERENNIAL CEREALS

5.1. Introduction

Perennial polyculture has been suggested as an ecologically sound alternative to the industrial paradigm pervasive in today's global agriculture (Crews *et al.*, 2016). Perennial systems have the potential to provide a suite of ecosystem services related to soil organic matter formation, nutrient retention, and weed suppression, in part, by mimicking temporal and spatial growth patterns that are common in natural systems (Glover *et al.*, 2010; Crews *et al.*, 2016; de Oliveira *et al.*, 2018). Spatial integration of legumes and grasses within agroecosystems can also reduce reliance on external nitrogen (N) inputs and lead to tighter nutrient cycling that can help avoid deleterious losses of N to the environment (Crews *et al.*, 2016).

Over the past few decades there have been significant advances in developing perennial cereal grains. Kernza, the first commercially available perennial cereal grain, was created by domesticating intermediate wheatgrass (*Thinopyrum intermedium;* DeHaan *et al.*, 2018). Perennial wheat was later developed by hybridizing Kernza with annual durum wheat (*Triticum durum*), with the goal of bringing together the perenniality of Kernza and yield of the annual wheat (Hayes *et al.*, 2018).

Despite the great promise of perennial polycultures, integrating perennial cereals into a legume-cereal biculture faces some challenges. For example, Crews *et al.* (2022) examined on an alfalfa-Kernza biculture, and found that legumes were not able to provide enough N

to support Kernza demand during the first 3 years after establishment, thus resulting in sub-optimal yield of Kernza. Rather than supporting Kernza N uptake, excess N from alfalfa instead appeared to be replenishing the soil organic N pool (Crews *et al*., 2022). Thus, there appears to be an adaptation period following intercrop establishment, wherein cereal's N requirement goes unmet. Improved understanding of perennial grain N uptake processes can help to address this challenge.

Short-term legume N transfer to adjacent cereals can occur via three main pathways (Høgh-Jensen, 2006): 1) direct transfer via root-to-root contact (i.e. release of N rich material by legume followed immediately by direct uptake of the material by nearby cereal roots), 2) direct transfer via common mycorrhizal networks (CMNs), and 3) mineralization and uptake of legume rhizodeposits. Direct transfer via close root contact can be improved with a larger, more extensive root systems that increase overlap of cereal and legume roots. Direct transfer via CMNs can be improved with better arbuscular mycorrhizal fungi (AMF) recruitment via signal molecules (flavonoids, strigolactones, etc.) in root exudates (He *et al*., 2003; Abdel-Lateif *et al*., 2012; Tian *et al*., 2021). Lastly, mineralization of legume rhizodeposits can be improved via increased belowground allocation (i.e. root exudates and other rhizodeposits), which can provide microbes with energy to synthesize N-cycling enzymes and enhance N availability (Meier *et al*., 2017).

Kernza, being a perennial, often has a much larger root system compared to annual wheat (DeHaan *et al*., 2018). This may increase root-to-root contact with neighboring legume and lead to greater N transfer. Additionally, Kernza has a much shorter domestication and breeding history compared to annual wheat (DeHaan *et al*., 2018). We suspect that with

Kernza evolving in more diverse and low-N environments compared to wheat, it has relied more on organic N supplies such as legume-derived N and other organic N pools. Therefore, Kernza may retain an improved ability to acquire N from legumes through CMN or legume rhizodeposits. Wheat, unlike Kernza, has been extensively bred in high input, monoculture conditions for centuries (Iannucci *et al*., 2017). In a previous greenhouse experiment we observed that annual durum wheat grows much faster compared to Kernza or perennial wheat in the first 8 weeks after germination (Hwang *et al*., in prep). This suggests that wheat is better able to compete for N compared to the perennial cereals at least the first few weeks after establishment. However, perennial cereals may invest more heavily in processes that lead to greater N acquisition from legume sources in the longer term. Understanding the short-term N acquisition strategies of annual wheat and Kernza, and how those traits are passed down to the hybrid could help us provide optimal environment for the success perennial cereals. However, little is known about the N dynamics of perennial wheat or Kernza, especially when grown in polyculture with legumes.

To address the knowledge gaps above, we conducted a greenhouse study in which we grew Kernza, perennial wheat, and annual wheat with or without alfalfa. We used a ^{15}N leaf feeding method to track the movement of N from alfalfa into neighboring cereals and examined rhizosphere communities to understand the impact of intercropping on root associated organisms. We hypothesized that: 1) annual wheat would have the highest biomass overall, but Kernza would display the greatest increase in biomass when grown in biculture vs in monoculture, 2) Kernza would have the highest proportion of legume derived

N in its biomass followed by perennial wheat, and that 3) Kernza would have the highest rate of infection from AMF, especially in biculture. Quantifying and elucidating the factors that govern N transfer between legumes and cereals would greatly inform the development of more effective polyculture systems.

5.2. Methods

5.2.1. Experimental Design

The experiment was conducted in Plant Growth Facility at Colorado State University, Fort Collins, CO. The soil used in the experiment was collected from Colorado State University's Agriculture Research Demonstration Education Center (ARDEC; 40°39'09.4"N 104°59'48.1"W, elevation: 1,552 m). The soils at this site are classified as Fort Collins loam (fine-loamy, mixed, superactive, mesic Aridic Haplustalfs; Soil Survey Staff, 2019). The soil was first air-dried and passed through a 2-mm sieve and then well-mixed to homogenize it. The 2-mm sieved soil was mixed with silica sand (1:1 ratio by volume; Granusil® 4075, Covia Corp, Independence OH) to facilitate better water infiltration and drainage.

The cereals used in the experiment were: 1) Kernza (intermediate wheatgrass; *Thinopyrum intermedium*), 2) durum wheat (*Triticum turgidum* subsp. *durum*), 3) and perennial wheat (*Th. intermedium* x *T. turgidum* subsp. *durum*), and alfalfa (*Medicago sativa*) was the legume of choice. The Land Institute (Salina, KS) developed the cereal lines 1 and 3, and supplied all seeds used in this experiment.

Each of the three cereal genotypes was planted either in monoculture or biculture with alfalfa. We also included one treatment of alfalfa monoculture. Each of the seven

treatment combinations was replicated in five blocks in a randomized complete block design (n = 35).

Seeds of each species were germinated on damp paper towel for a week before transplanting into 1 gal pots (radius = 7 cm, height = 25 cm) filled with the soil-sand mixture (~ 3kg dry weight). Two germinated seeds were planted in each pot, such that two seedlings of the same species were planted in monoculture treatments, and one cereal and one alfalfa seeding were planted in the biculture pots. The plants were watered three times a week for the duration of the experiment. No fertilizer was added to the pots.

5.2.2. ^{15}N leaf labeling

The ^{15}N leaf-feeding method used in this study was adapted from Høgh-Jensen and Schjoerring (2000) and Rasmussen *et al*. (2019). While many different approaches for N transfer estimation exist, the^{15}N leaf-feeding method is advantageous because it allows greater separation of isotopic signature between the N donor and recipient and minimizes the damage to the legume plants (Chalk *et al*., 2014). Briefly, 17 weeks after transplanting, two healthy leaves from each alfalfa plant in the biculture treatments were carefully placed in 2-mL tubes containing 1 mL of isotopically enriched urea-$^{15}N_2$ solution (0.5%; w/v, 98 atom%). Leaves were secured to the tube with parafilm, which also prevented losses of the urea solution due to volatilization. The 2-mL tubes were held in place with supports to prevent them from weighing down or damaging the alfalfa stems. Extra care was taken to ensure no urea solution spilled or came in contact with the soil or grass leaves.

5.2.3. Plant and soil sampling

Eight days after the beginning of ^{15}N leaf labeling and 18 weeks after transplanting, all units were destructively harvested. For monoculture treatments, one plant out of the two in the pot was randomly selected as the plant of interest. We chose this method instead of taking a mean value from both plants to avoid artificially lowering the variability. Aboveground biomass was cut at the soil surface and oven-dried at 55 °C. Alfalfa leaves that had been selected for leaf labeling were cut and stored separately to avoid surface contamination. Afterwards, the root system was excavated carefully with gloved hands and a small paintbrush to minimize root damage. After all large soil aggregates (> 10 mm) were broken apart from the roots, the rest of the still adhering to the roots was considered rhizosphere soil and was collected by brushing it off the roots with small paintbrush. These rhizosphere soil samples were stored at -20 °C until further processing.

Roots were then carefully washed using DI water and gloved hands. A few (>3) representative subsamples (<1 g in total fresh weight) of the roots were taken and preserved in 70% ethanol until being prepared for AMF scoring. The remaining roots were frozen until further processing.

All biomass samples were oven-dried at 55 °C for 72 hours, weighed, and ground to fine powder (<1 mm) before being analyzed for total CN content as well as ^{15}N enrichment level.

Rhizosphere soil samples were subsampled (~0.5 g) for DNA extraction and stored at –80 °C until extraction (see 5.2.5 DNA extraction method details below). The remaining soil samples were temporarily thawed and passed through a 2 mm sieve. Afterwards, they were

subsampled again for microbial biomass extraction (2 x 10 g fresh weight; see below) and gravimetric water content (~10 g fresh weight). Gravimetric water content was calculated by weighing the soil subsample before and after oven-drying at 105 °C. The resulting dried soil samples were also ground with a mortar and pestle to fine powder and analyzed for CN content and ^{15}N enrichment level.

5.2.4. Microbial biomass and soil carbon and nitrogen extraction

Microbial biomass extraction protocol was adapted from Weintraub *et al*. (2007). Each soil sample was subsampled twice – one to be chloroform fumigated and one to remain unfumigated. Fumigated samples received 4 mL of ethanol free chloroform. Both fumigated and unfumigated samples were then sealed and incubated at room temperature for 24 hours. After incubation period, fumigated samples were then vented to allow chloroform to evaporate. We then added 50 mL of 0.05 M K_2SO_4 solution to all samples. They were then shaken for 1 hr at 140 rpm and filtered (Whatman #1 filter). The resulting solution was divided into two aliquots for each sample. One aliquot was lyophilized and analyzed for ^{15}N enrichment at UC Davis Stable Isotope Facility (SIF; Davis, CA). The other aliquot was analyzed for dissolved organic C (DOC) and total dissolved N (TDN) was taken directly from the unfumigated samples. Microbial biomass C (MBC) and N (MBN) were calculated by subtracting fumigated from unfumigated DOC and TDN. We also included two no-soil controls per 10 true samples throughout the extraction process in order to rule-out potential contamination.

5.2.5. DNA extraction

Soil DNA was extracted using Zymo Quick-DNA Fecal/Soil Microbe Miniprep Kit (Zymo Research Corporation, Irvine CA) according to the manufacturer instructions. Extracted DNA was quantified on Qubit 2.0 fluorometer using Qubit dsDNA HS Assay Kit (ThermoFisher Scientific Inc., Waltham MA). Primer sets 515F/806R from Earth Microbiome Project (Thompson *et al.*, 2017) were used to construct amplicon libraries for 16S rRNA region. Sequencing was performed at Microbial Community Sequencing Lab (University of Colorado Boulder, Boulder CO) on Illumina MiSeq® platform (Illumina Inc., San Diego CA) using 251 base pair (bp) paired-end reads, which generated averages of 36,843 reads per sample. Resulting reads were demultiplexed using QIIME2 (Bolyen *et al.*, 2019). Demultiplexed reads were then denoised using DADA2 (Callahan *et al.*, 2016) trimming all reads to 5 – 220 bp. Bacterial and archaeal taxonomy was assigned to 16S ASV sequences using the naïve Bayes sklearn classifier trained with the full-length SILVA database (silva138.99). Lastly, we filtered out those reads belonging to chloroplast and mitochondria.

5.2.6. AMF quantification

Each sampled plant root was subsampled and scored for AMF colonization using the intersection method (McGonigle *et al.*, 1990). Briefly, roots were first stained using Trypan Blue and prepared on a glass slide. Using a microscope, a predetermined path was taken through the root sample, intersecting the root sample 20 times via the path. At each intersection, the presence of hyphae was noted. If arbuscules, or spores were present, they were noted separately. In a few cases, AMF parts could not be identified due to poor

staining. We only used those root samples with at least 15 usable intersects, and the rest (n = 6) were discarded.

5.2.7. Isotope analysis and calculation

All isotopic analyses were performed at UC Davis SIF, using Elementar vario MICRO cube elemental analyzer (Elementar Analysensysteme GmbH, Langenselbold, Germany) interfaced to a Sercon Europa 20-20 isotope ratio mass spectrometer (Sercon Ltd., Cheshire, United Kingdom).

We used a two-source mixing model to calculate the proportion of N in a given pool derived from the legume (Post, 2002).

$$f_{(\leftarrow leg)} = \frac{AP_{bi} - AP_{mono}}{AP_{leg} - AP_{mono}}$$

Where $f_{(\leftarrow leg)}$ is proportion of N within the cereal associated pool derived from legume, AP_{bi} is ^{15}N enrichment level (in atom %) of the cereal-associated pool (plant biomass, microbial biomass, dissolved, and soil) in biculture, AP_{mono} is ^{15}N that in monoculture, and AP_{leg} is the ^{15}N enrichment level of legume shoots, all expressed in atom%. The notation was derived from Chalk *et al*. (2014). Many methods exist that estimate legume N transfer. Much of the discrepancy stems from our inability to measure ^{15}N signature of the N that is transferred from legume to cereal. Here, legume shoot was used as one of the end members in the mixing model because it was most highly enriched. For further discussion of the legume N transfer calculation, refer to Chalk *et al*. (2014).

Absolute amount of N derived from legume was calculated with the following formula:

$$N_{(\leftarrow leg)} = N_{bi} \times f_{(\leftarrow leg)}$$

Where $N_{(\leftarrow leg)}$ is the amount of N in each cereal associated pool derived from legume, N_{bi} is the amount N in the cereal-associated pool in biculture, and $f_{(\leftarrow leg)}$ is proportion of N within the cereal-associated pool derived from legume as calculated above. For pools that were only calculated as concentrations (e.g. MBN; ug N g $soil^{-1}$), concentration, not absolute amount, of N derived from legume was calculated instead.

Three experimental units were calculated to have more ^{15}N in their combined biomass (cereal and alfalfa) than provided via leaf-labeling (< 4.7 mg ^{15}N) and were excluded from analysis. In addition, some specific pools had proportion of legume-derived N greater than 100% and were excluded from analysis (n = 2 for root and total biomass, and n = 3 for TDN and MBN)

5.2.8. Statistical Analysis

Univariate analyses were performed with ANOVA. All variables and model residuals were inspected to ensure the assumptions for ANOVA were met and were log-transformed as necessary. In a few cases wherein neither log- nor square root- transformation was adequate, Kruskal-Wallace test was performed instead. For all univariate analyses, cereals and alfalfa were analyzed separately. For cereals, genotype and cropping system were modeled as fixed effects. Those analyses involving legume derived N in cereals only had genotype as the fixed effect. Legumes were analyzed twice, once to compare alfalfa grown next to any cereals against alfalfa grown in monoculture, and again to compare within biculture alfalfa for the effect of neighboring cereal genotype. Cropping system and cereal

genotype were modeled as sole fixed effects in the models, respectively. In all models, block was used as a random effect. R packages lme4, lmerTest, emmeans were used for mixed effects model construction, mixed effects ANOVA, and post-hoc pairwise-comparison with Tukey adjustment, respectively.

The 16 profiles were graphically represented via nonmetric multidimensional scaling (NMDS) using Bray-Curtis dissimilarity index. Statistical analyses of these relationships were achieved by performing permutational multivariate analysis of variance (PERMANOVA).

5.3. Results

5.3.1. Biomass and N concentrations

At harvest, total (shoot + root) biomass of cereals ranged from 2.27 g to 11.84 g per plant (Table 5.1). Cereal biomass was significantly affected by the cropping system (Table 5.1), such that cereal shoot, root, and total mass were greater in biculture than in monoculture (Table 5.1). However, there was no evidence of a genotype effect or an interaction with cropping system on cereal biomass (Table 5.1). We also calculated root:shoot ratio of cereal biomass which ranged from 0.34 to 0.93 but was not affected by genotype or cropping system (Table 5.1). Similarly, there were no differences in N concentrations of shoots, roots, and total biomass between genotypes or cropping systems (Table 5.1).

Alfalfa biomass ranged from 1.18 g to 17.36 g per plant but did not display significant cropping systems or genotype effects (Table S5.1). Similarly, the root:shoot ratio and N concentrations for alfalfa did not vary between cropping system or genotype (Table S5.1).

5.3.2. Soil C and N pools

We investigated microbial and dissolved C and N fractions in the soil, under both cereals and alfalfa. We found a significant cropping system effect on cereal rhizosphere DOC (Fig 5.1a), such that cereals in biculture had ~2.8 times greater level of DOC in its rhizosphere compared to those in monoculture (Fig 5.1a). However, a significant interaction with genotype suggests that this effect was more pronounced for annual wheat and Kernza, than for perennial wheat. Significant genotype x cropping system interaction was also found for MBC of the cereal rhizosphere (Fig 5.1b), where the perennial varieties in both cropping systems and annual wheat in monoculture all had similar levels of MBC in their rhizosphere (Fig 5.1b). Annual wheat in biculture, however, showed significantly lower MBC (Fig 5.1b).

In addition, we observed a significant cropping system effect on TDN in cereal rhizosphere (Fig 5.1c) such that TDN was 17% higher in monocultures than in bicultures across all genotypes (Tukey's post-hoc; Fig 5.1c). We did not observe either genotype or cropping system effect in MBN (Fig 5.1d), but total soil N was higher in monocultures vs. bicultures (Fig 5.1e)

Table 5.1. Biomass and N concentrations of three cereals (annual wheat, perennial wheat, Kernza) and root:shoot ratio (R:S) in monoculture and in biculture with alfalfa. Dry mass and N concentration are given for shoots, roots, and total biomass of a single cereal plant in each treatment. Data shown in mean ± standard error. The bottom section lists p-values associated with each response variable obtained via mixed effect linear model, with significant values (< 0.05) denoted in italics. G = genotype effect, S = cropping system effect, G x S = genotype x cropping system interaction. The last row indicates what transformation, if any, was taken place to meet the assumptions for ANOVA.

		Biomass						
		Shoots		Roots		Total		
Crop genotype	Cropping system	g plant $^{-1}$	%N	g plant $^{-1}$	%N	g plant $^{-1}$	%N	R:S
Annual wheat	Mono	2.39 ± 0.29	1.35 ± 0.09	1.57 ± 0.24	0.72 ± 0.11	3.95 ± 0.52	1.18 ± 0.04	0.65 ± 0.03
	Bi	3.61 ± 0.31	1.17 ± 0.07	2.3 ± 0.33	1.17 ± 0.41	5.91 ± 0.62	1.2 ± 0.15	0.63 ± 0.05
Perennial wheat	Mono	3.02 ± 0.39	1.17 ± 0.08	1.84 ± 0.31	0.85 ± 0.07	4.86 ± 0.64	1.04 ± 0.07	0.61 ± 0.08
	Bi	4.34 ± 0.68	1.37 ± 0.12	2.11 ± 0.4	1.05 ± 0.33	6.45 ± 1.03	1.28 ± 0.18	0.49 ± 0.05
Kernza	Mono	2.53 ± 0.72	1.19 ± 0.13	1.71 ± 0.54	0.94 ± 0.11	4.25 ± 1.24	1.09 ± 0.09	0.65 ± 0.08
	Bi	4.56 ± 0.84	1.08 ± 0.16	2.69 ± 0.53	1.67 ± 0.47	7.25 ± 1.33	1.32 ± 0.24	0.59 ± 0.06
	G	0.475	0.423	0.764	0.334	0.644	0.973	0.244
	S	*0.004*	0.774	*0.050*	0.315	*0.010*	0.360	0.169
	G x S	0.754	0.204	0.654	0.777	0.741	0.767	0.730
	trans	none	none	none	log	none	log	log

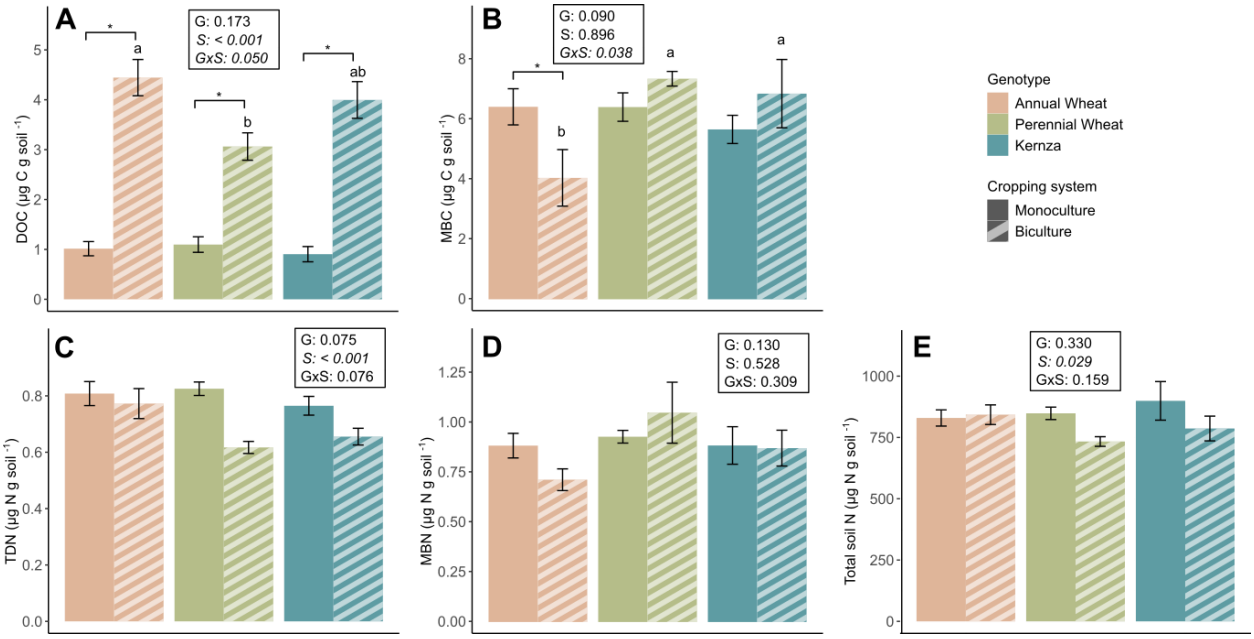

Figure 5.1. Labile CN pools (a-d) and total soil N concentration (e) found in cereal (annual wheat, perennial wheat, and Kernza) rhizosphere in monoculture and in biculture. Data shown in mean ± standard error. DOC = dissolved organic C, MBC = microbial biomass C, TDN = total dissolved N, MBN = microbial biomass N. Small boxes within each panel denote p-values associated with each response variable obtained via mixed effect linear model, with significant values (< 0.05) denoted in italics. G = genotype effect, S = cropping system effect, G x S = genotype x cropping system interaction. In case of significant G x S interaction, lower-case letters were used above the bars denote to significant ($p < 0.05$) pairwise difference between the genotypes within one cropping system (Tukey's post-hoc). Cropping system effect within one genotype was noted with a bottom facing bracket and a * sign (Tukey's post-hoc).

We also analyzed the same labile C and N pools in the alfalfa rhizosphere (Fig 5.2, Table S5.2) and found that both DOC and MBC (the latter only marginally) were higher in biculture than in monoculture (Fig 5.2), but no differences were observed for TDN and MBN (Table S5.2). We note cereal genotype had no significant effects on the measured C and N pools in the alfalfa rhizosphere (Fig 5.2, Table S5.2). No genotype or cropping system effects were found in the legume rhizosphere total soil N (Table S5.2).

5.3.3. N transfer

Alfalfa plants labeled with ^{15}N urea showed various degrees of ^{15}N enrichment, their enrichment levels in the shoots ranging from 0.04 atom% to 0.24 atom%. We calculated both proportion and absolute amount/concentration of N derived from legume in both cereal biomass (shoots, roots, total) and soil rhizosphere pools (TDN, MBN, total). The estimated percentage of legume-derived N varied widely across all six pools, ranging between 0.01 % and 88 %.

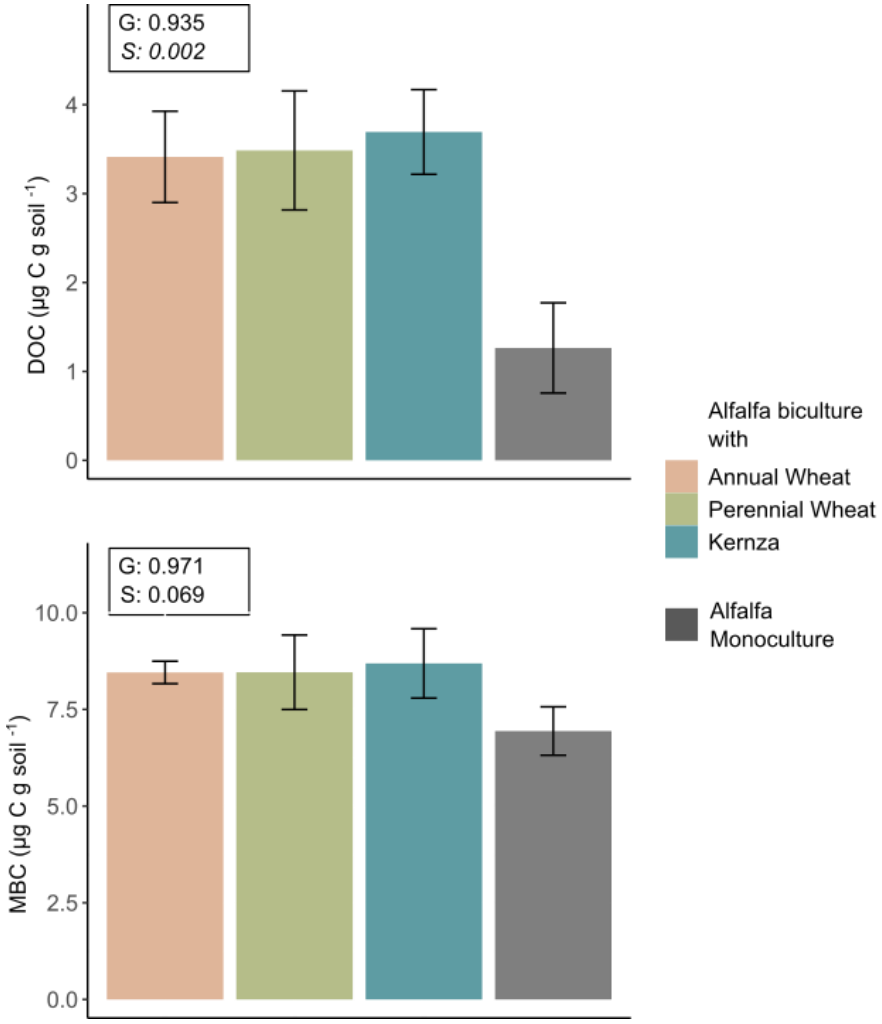

Figure 5.2. Labile C pools found in alfalfa rhizosphere in monoculture and in biculture with three cereals (annual wheat, perennial wheat, and Kernza). Data shown in mean ± standard

error. DOC = dissolved organic C, MBC = microbial biomass C. Small boxes within each panel denote p-values associated with each response variable obtained via mixed effect linear model, with significant values (< 0.05) denoted in italics. G = genotype effect, S = cropping system effect. Note that genotype effect tests only those alfalfa in biculture and cropping system effect compares all biculture alfalfa against the monoculture alfalfa.

We did not find genotype or cropping system effects in either proportion or absolute amount of legume derived N. We note that, while not significant, Kernza had the highest average amount of legume-derived N in the total plan biomass, with an average of 25% of its N coming from alfalfa, compared to just 8 % for perennial wheat and 2% for annual wheat (Table 5.2).

5.3.4. 16S sequencing and AMF quantification

We obtained 7,832 ASVs from 16S sequencing of cereal and alfalfa rhizosphere soils. The resulting 16S profiles were used to compare cereal in monoculture, cereal in biculture, and alfalfa in biculture against each other via PERMANOVA (Fig 5.3). The analysis revealed that all three groups above differed significantly from each other (Fig 5.3). Additionally, we saw evidence of significant genotype effect and the subsequent pairwise PERMANOVA showed that 16S profile of annual wheat rhizosphere was significantly different from those of the two perennials (Fig 5.3).

We also analyzed rhizospheres of legumes separately, comparing across cropping system and across genotypes of the neighboring cereals but did not find a significant difference in either comparison (Fig S5.1). Diversity indices (ASV richness, Shannon's index) were calculated from the 16S profiles, but did not reveal differences for any of the factors listed above (Table S5.3).

Lastly, we quantified AMF infection rate by counting the number of roots with visible hyphal infection. We found a genotype effect on cereal AMF infection rate such that perennial wheat had the highest hyphal presence and Kernza had the lowest (Table 5.3). There was no effect of cropping system on AMF infection rate.

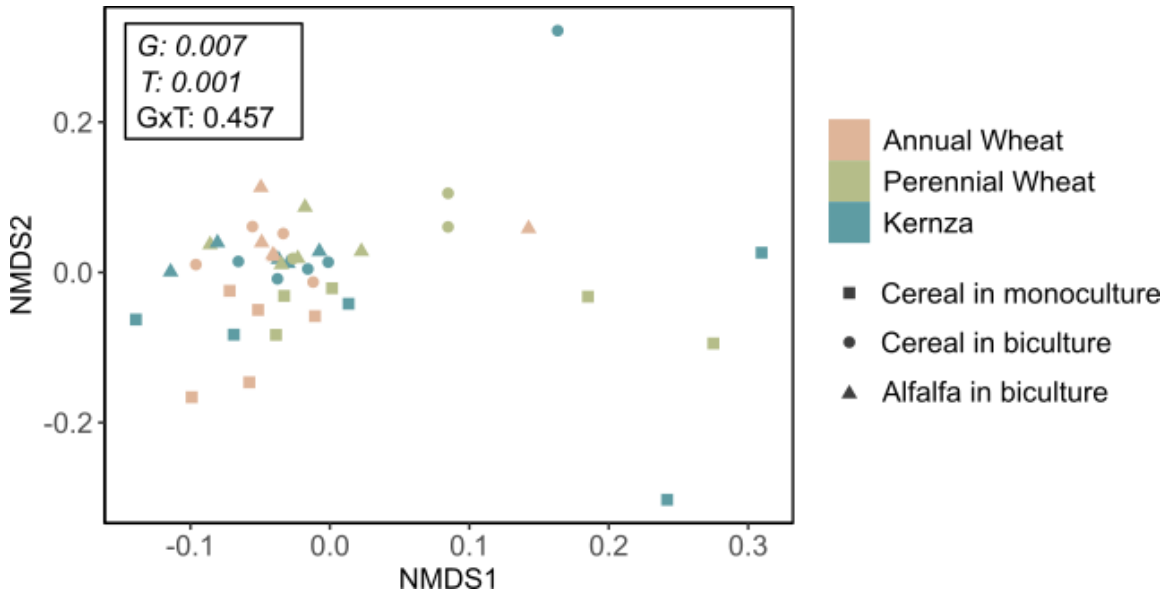

Figure 5.3. Ordination plot (NMDS) showing prokaryote (16S) community composition in rhizospheres of three crop genotypes (annual wheat, perennial wheat, Kernza) in two different cropping systems (monoculture, square; biculture, circle) as well as those belonging to neighboring alfalfas (triangles). The distances were calculated using the Bray-Curtis Dissimilarity Index. The small box inside the panel indicates p-values for all interactions and main effects obtained with PERMANOVA. G = crop genotype, T = crop type (cereal in monoculture, cereal in biculture, and alfalfa in biculture). Those values significant at 0.05 level are highlighted in italics.

Table 5.2. Percentages and absolute amount of legume derived N in cereal biomass and rhizosphere. Legume-derived N was calculated for cereals (AW = annual wheat, PW = perennial wheat, K = Kernza) in biculture treatment using the ^{15}N enrichment of each pool in respect to their neighboring legumes and cereals in monoculture. Data shown in mean ± standard error. The bottom section lists p-values associated with genotype (G) effect obtained via mixed effect linear model, with significant values (< 0.05) denoted in italics. The last row indicates what transformation, if any, was applied to meet the assumptions for ANOVA. Where appropriate, non-parametric test was performed instead and was noted as "KW" (Kruskal-Wallace).

	N derived from alfalfa					
	Biomass					
	Shoot		Root		Total	
Genotype	%	mg plant $^{-1}$	%	mg plant $^{-1}$	%	mg plant $^{-1}$
Annual wheat	1.98 ± 0.89	0.89 ± 0.41	4.36 ± 1.52	0.37 ± 0.18	2.07 ± 1.26	1.16 ± 0.75
Perennial wheat	3.95 ± 1.94	2.82 ± 1.49	13.18 ± 9.44	2.72 ± 2.06	5.88 ± 3.41	5.41 ± 3.37
Kernza	0.62 ± 0.51	0.24 ± 0.19	40.25 ± 22.47	28.53 ± 16.18	25.17 ± 14.42	28.76 ± 16.29
G	0.252	0.150	0.592	0.153	0.285	0.168
trans/ analysis	none	none	log	log	log	log
	Soil					
	TDN		MBN		Total	
Genotype	%	ng N g soil $^{-1}$	%	ng N g soil $^{-1}$	%	ug N g soil $^{-1}$
Annual wheat	7.55 ± 2.59	54.8 ± 14.5	14.5 ± 5.76	94.2 ± 39.3	1.8 ± 0.54	15.75 ± 5.17
Perennial wheat	8.34 ± 2.60	54.9 ± 20.6	2.94 ± 0.30	41.1 ± 6.7	9.67 ± 6.34	74.29 ± 51.10
Kernza	2.62 ± 0.92	18.0 ± 6.8	23.77 ± 10.12	218.2 ± 93.2	0.44 ± 0.12	3.41 ± 1.03
G	0.428	0.392	0.770	0.705	0.125	0.138
trans/ analysis	log	log	log	KW	log	KW

Table 5.3. Arbuscular mycorrhizal fungi (AMF) hyphae presence in cereal (annual wheat, perennial wheat, and Kernza) roots in monoculture and in biculture with alfalfa. The hyphal presence is represented in proportions ranging from 0 to 1, with 1 being when all root sections inspected have been infected with AMF hyphae. Data shown in mean ± standard error. The bottom section lists p-values associated with genotype effect obtained via mixed effect linear model, with significant values (< 0.05) denoted in italics. The last row indicates what transformation, if any, was taken place to meet the assumptions for ANOVA.

Genotype	Cropping system	Hyphal presence
Annual wheat	Mono	0.34 ± 0.08
	Bi	0.38 ± 0.12
Perennial wheat	Mono	0.46 ± 0.14
	Bi	0.43 ± 0.09
Kernza	Mono	0.19 ± 0.10
	Bi	0.12 ± 0.03
	G	*< 0.001*
	S	0.750
	G x C	0.939
	trans	sqrt

5.4. Discussion

5.4.1. Total C and N dynamics in plant biomass and soil

We hypothesized that annual wheat would have the greatest biomass, but that Kernza would display the greatest change between the cropping systems. Contrary to our expectations, biomass data did not show any evidence of a genotype effect or a genotype x cropping system interaction (Table 5.1). However, we found a cropping system effect wherein individual cereal plants were much larger when grown next to alfalfa than in pots with the same genotype (Table 5.1). This may be caused by greater N availability in cereal-legume biculture, driven by biological N fixation (BNF) in the legume rhizosphere. However, we must note that the benefit BNF in cereal-legume biculture is not necessarily limited to N transfer between legume and cereal. N gained via BNF may remain in legume but this could

reduce competition for the native soil N, leading to greater overall N availability (Xing *et al.*, 2023). Furthermore, N dynamic is not solely responsible for the positive effect of intercropping. For example, legumes and cereals have been shown to take advantage of different P fractions allowing for greater mass accrual in per-mass basis (Li *et al.*, 2003; Cu *et al.*, 2005).

Increased biomass in biculture also had belowground C and N ramifications. We saw a slightly reduced amount of TDN and total soil N in the cereal rhizosphere when they were grown with alfalfa (Fig 5.1c). Larger plants likely contributed to this with a greater rate of uptake of available N into its biomass. We also observed highly elevated levels of DOC in the cereal rhizosphere in biculture (Fig 5.1a). This trend may also have been caused by greater biomass, as root biomass has been shown to be positively correlated with rhizodeposition (Remus and Augustin, 2016). Similarly, in a recent metanalysis by Sun *et al*. (2024), the authors found that intercropping increased DOC by nearly 20% across 107 different studies performed in various soil conditions, also concluding that this was likely the result of larger root biomass. Though the increase in DOC was much greater than that in root biomass, this would be expected if root biomass increase was associated with greater fine root growth (Table 5.1, Fig 5.1a). Therefore, we believe larger root system made possible by cereal-alfalfa biculture was at least in part responsible for the greater DOC in the rhizosphere.

Interestingly, within biculture treatment, we also observed a genotype effect on DOC level in which annual wheat's rhizosphere DOC was higher than that of perennial wheat (Fig 5.1a). Furthermore, this was accompanied by lower MBC level in annual wheat rhizosphere

compared to the perennial genotypes, only in biculture (Fig 5.1b). These data suggest that, in biculture, the DOC from the annual wheat rhizosphere is not being assimilated into microbial pools and is instead remaining in the dissolved pool. This trend may be driven by microbial substrate preference. It is possible that the perennial varieties are exuding a suite of substrates that are preferentially taken up by their rhizosphere microbes, leading to greater MBC and lower DOC levels, while annual wheat's exudates were less "catered" to its microbial community (Zhalnina *et al.*, 2018). While C dynamic between dissolved and microbial pools can typically have significant influence on N dynamics, we did not observe any genotype effect on TDN or MBN (Figs 5.1c, d). Increased MBC without commensurate increase in MBN could also lead to greater investment of C from microbes into N mineralization (i.e. N-degrading enzyme production; Sun *et al.*, 2021). This would lead to greater N availability for the perennial cereals, though the TDN levels in the rhizosphere did not reflect this explanation.

5.4.2. Estimation of N transfer using ^{15}N leaf feeding technique

We used ^{15}N leaf-feeding method to assess the N transfer from legume to cereal. The leaf labeling process was successful as we found elevated ^{15}N signals in legume, soil, and cereal pools. We hypothesized that the greatest proportion of legume-derived N will be found in Kernza, followed by perennial wheat. While we did observe this general trend for mean legume-derived N in the cereals, we did not find significant genotype or cropping system effects in any of our cereal associated pools in biculture, either in terms of proportion or absolute amount of legume derived N (Table 5.2).

It should be noted that ^{15}N data had considerable variability. While we succeeded in introducing ^{15}N to the alfalfa, enrichment levels within the plants were inconsistent. For instance, legume roots had a greater amount of ^{15}N than legume shoots in two experimental units (data not shown). In five experimental units, either cereal shoots or roots contained a greater amount of ^{15}N than the neighboring legume's roots (data not shown). Such a large variability is not uncommon in ^{15}N leaf feeding experiments (Rasmussen et al., 2019a). Recently, McNeil and Unkovich (2024) found that leaf feeding method led to incomplete uptake of ^{15}N material more often than stem feeding method. If the alfalfa plants were taking up ^{15}N at varying rate, it could have led to inconsistent distribution of ^{15}N throughout the cereal-alfalfa biculture after 8 days.

Another potential culprit is the short-term passive leakage of ^{15}N from alfalfa. Many studies report a large wave of ^{15}N in legume rhizosphere only a short period of time (1-3 days) after labeling, which some view as passive leakage caused by labeling process *per se* (Gasser *et al.*, 2015; Araujo *et al.*, 2023). In our study, passive leakage may explain why certain legume roots contained less ^{15}N than neighboring cereals. In case of passive leakage, legume roots would be acting as conduit for, rather than source of ^{15}N materials (Araujo *et al.*, 2023). In summation, we note that there are many sources of variability in this method and that methods for estimating N transfer must be further optimized or much greater replication be used to distinguish clear patterns in legume-cereal transfer.

5.4.3. Microbial community response to cereal genotype and cropping system

We hypothesized that 16S profiles of the cereals would differ across genotypes and cropping systems. In partial support of our hypothesis, we found that 16S profiles of Kernza

and perennial wheat differed significantly from those of annual wheat across both cropping systems (Fig 5.3). This result was consistent with our previous findings where Kernza and perennial wheat had distinct 16S profiles from annual wheat. Furthermore, Cui *et al*. (2022) found that the hybrid between an annual wheat and another species of perennial wheatgrass (*Thinopyrum elongatum*) differed significantly from its annual parent in 16S profiles.

We also hypothesized that Kernza would show the biggest shift between cropping systems followed by perennial wheat. Our results revealed that all cereals harbored distinct 16S profiles across two cropping systems, though we did not observe genotype x cropping system interaction as hypothesized (Fig 5.3). Past studies have suggested various explanations for shifts in microbial communities in biculture vs in monoculture. One study by Cavalieri *et al*. (2020) suggested top-down control of microbial communities mediated by plant-plant competition. The authors suggested that the less competitive species in the mixture shifted its 16S profiles in order to diversify its microbial function and better withstand competitive pressure from the more competitive species. This explanation is further bolstered by other studies showing that plants' root exudate composition, main mechanism by which plants assemble their microbial communities (Zhalnina *et al*., 2018), shifted based on neighbor context (Badri *et al*., 2012; Kong *et al*., 2018).

Another explanation for shifts in 16S profiles across cropping system is "microbial spillover", wherein microbial communities of one plant end up colonizing the neighboring plant's rhizosphere. This phenomenon is documented by Hortal *et al*. (2017) who found that microbial communities of the less competitive plant species shifted to resemble those

of the more competitive neighbor. They postulated that being able to establish microbial communities specifically beneficial to oneself is a part of the competitive advantage displayed by the better competitive species (Hortal *et al*., 2017). Ulbrich *et al*. (2022) also documented the case of microbial spillover, but in their study, two microbial communities of the plants simply converged when grown together, perhaps implying bidirectional microbial spillover.

Our 16S data seem to be driven by microbial spillover than by top-down shift. The 16S profiles of the bicultured cereals seemed to overlap with those of the neighboring legumes on the NMDS plot (Fig 5.3), suggesting an instance of microbial spillover. Interestingly, the three cereals maintained their genotype effect in biculture despite being grown next to the same species of legume as evidenced by the lack of genotype x cropping system interaction (Fig 5.3). This result suggests that even with microbial spillover, a microbiome driven by the genotype effect may remain in the cereal rhizosphere. We note however that we did not observe this trend in our analogous field experiment, where we also planted all three genotypes in monoculture and biculture (Hwang *et al*., in prep). In that study, we found that the genotype effect was no longer evident in biculture treatment (Hwang *et al*., in prep). We cannot confirm whether this was also the result of microbial spillover as we did not collect rhizosphere microbial data of alfalfa in the field. The discrepancies between our field experiment and the present study may stem from the fact that our field experiment went on for two growing seasons (Hwang *et al*., in prep). If the present study had gone on beyond 18 weeks, we could have observed 16S profiles of all three genotypes in biculture converge, presumably to resemble that of alfalfa.

Despite being likely driven by microbial spillover, our 16S profile trends deviated from those seen in either Hortal *et al*. (2017) or Ulbrich *et al*. (2022). Our result differed from Hortal *et al*. (2017) in that we did not observe any competitive pressure. In fact, our cereals in biculture, likely harboring microbes from legume rhizosphere, were larger than their counter parts in monoculture (Table 5.1). Our results also differed from Ulbrich *et al*. (2022) in that the microbial spillover seemed largely unidirectional (Fig 5.3). Even though 16S profiles of the cereals shifted to resemble that of alfalfa, the 16S profiles of alfalfa did not vary between cereal-alfalfa biculture and alfalfa monoculture (Fig 5.3). Therefore, we postulate that alfalfa microbial communities unidirectionally spilled over to cereal rhizosphere but either had a neutral impact on cereal's growth or played a facilitative role (rather than competitive role).

5.4.4. AMF presence and effect

We also measured the rate of AMF infection in cereal roots. We hypothesized that Kernza would have the highest infection rate followed by perennial wheat, especially so in biculture where CMN could act as an N transfer path. Contrary to our expectations, we found that Kernza had the lowest infection rate compared to the other two genotypes (Table 5.3). This finding also goes against Hetrick *et al*. (1992) who found that root fibrousness and AMF colonization rate was negatively correlated. In our previous greenhouse study, we had found that Kernza preferentially grew thicker roots compared to annual wheat and perennial wheat (Hwang *et al*., in prep). From these two studies, we would expect greater AMF colonization rate in Kernza root, which is the opposite of what we observed.

It must be noted that greater AMF infection does not necessarily lead to greater benefits. In fact, Hetrick *et al*. (1992) has found that one cultivar of durum wheat had negative growth response to AMF inoculation. In another study, Jansa *et al*. (2008) inoculated *Medicago truncatula* with various AMF strains and found that two strains with equal hyphal presence resulted in vastly different host biomass. The relationship between genotype, cropping system, and AMF could potentially be explored further in future studies by using sterilized soil and AMF inoculation.

5.4.5. Conclusion

Perennial biculture of cereal and legumes have the potential to reduce soil disturbance and synthetic N input in agroecosystem. However, ensuring that cereals are benefiting from their neighboring legumes can be a challenging task. In the present study we found alfalfa indeed benefits neighboring cereal's growth. Furthermore, we found that perennial varieties' rhizospheres foster greater levels of microbial biomass. In our estimation of N transfer from legume to cereal, perennial wheat had the greatest absolute amount of legume derived N in its shoot, while Kernza had the greatest amount in the overall plant biomass (shoots + roots), but high variability prohibited the detection of significant differences. We also observed microbial spillover effect in biculture systems, where cereal 16S profiles shifted to resemble those of neighboring alfalfa. Interestingly, Kernza had the lowest rate of AMF hyphae in its roots, though number of hyphae did not correspond to total N transfer. We believe that this study demonstrates certain unique properties of both perennial crops (MBC, 16S profiles) that warrant further exploration. The interaction between C and N dynamics in annuals vs perennials has considerable implications on N

mineralization and C sequestration. Future studies should employ other techniques to estimate N movement in cereal-legume biculture. Stable isotope probing via stem feeding shows promise, but natural abundance methods or labelling with N_2 gas also offer viable alternative to study this phenomenon. How perennial cereals react to neighboring legumes and what impact that has on legume N transfer can have lasting impact on how we design more sustainable agricultural systems.

BIBLIOGRAPHY

Abdalla, M., Hastings, A., Cheng, K., Yue, Q., Chadwick, D., Espenberg, M., Truu, J., Rees, R.M., Smith, P., 2019. A critical review of the impacts of cover crops on nitrogen leaching, net greenhouse gas balance and crop productivity. Global Change Biology 25, 2530–2543. doi:10.1111/gcb.14644

Abdel-Lateif, K., Bogusz, D., Hocher, V., 2012. The role of flavonoids in the establishment of plant roots endosymbioses with arbuscular mycorrhiza fungi, rhizobia and Frankia bacteria. Plant Signaling & Behavior 7, 636–641. doi:10.4161/psb.20039

Abdullaeva, Y., Ratering, S., Rosado-Porto, D., Ambika Manirajan, B., Glatt, A., Schnell, S., Cardinale, M., 2024. Domestication caused taxonomical and functional shifts in the wheat rhizosphere microbiota, and weakened the natural bacterial biocontrol against fungal pathogens. Microbiological Research 281, 127601. doi:10.1016/j.micres.2024.127601

An, T., Schaeffer, S., Li, S., Fu, S., Pei, J., Li, H., Zhuang, J., Radosevich, M., Wang, J., 2015. Carbon fluxes from plants to soil and dynamics of microbial immobilization under plastic film mulching and fertilizer application using 13C pulse-labeling. Soil Biology and Biochemistry 80, 53–61. doi:10.1016/j.soilbio.2014.09.024

Araujo, K.E.C., Vergara, C., dos Santos, R.C., Santos, W. de M., de Freitas Souza, R., de Farias Silva, C., Guimarães, A.P., Jantalia, C.P., Urquiaga, S., Araujo, E.S., Alves, B.J.R., Boddey, R.M., 2023. Can 15N leaf-labelling reliably quantify rhizodeposited nitrogen remaining after a nodulated legume crop? Nutrient Cycling in Agroecosystems 125, 235–260. doi:10.1007/s10705-022-10238-w

Aulakh, M.S., Wassmann, R., Bueno, C., Kreuzwieser, J., Rennenberg, H., 2004. Characterization of Root Exudates at Different Growth Stages of Ten Rice (Oryza sativa L.) Cultivars. Plant Biology 3, 139–148. doi:10.1055/s-2001-12905

Badri, D.V., De-la-Peña, C., Lei, Z., Manter, D.K., Chaparro, J.M., Guimarães, R.L., Sumner, L.W., Vivanco, J.M., 2012. Root Secreted Metabolites and Proteins Are Involved in the Early Events of Plant-Plant Recognition Prior to Competition. PLOS ONE 7, e46640. doi:10.1371/journal.pone.0046640

Bajgain, P., Zhang, X., Jungers, J.M., DeHaan, L.R., Heim, B., Sheaffer, C.C., Wyse, D.L., Anderson, J.A., 2020. 'MN-Clearwater', the first food-grade intermediate wheatgrass (Kernza perennial grain) cultivar. Journal of Plant Registrations 14, 288–297. doi:10.1002/plr2.20042

Baldauf, J.A., Hochholdinger, F., 2023. Molecular dissection of heterosis in cereal roots and their rhizosphere. Theoretical and Applied Genetics 136, 173. doi:10.1007/s00122-023-04419-6

Bates, D., Mächler, M., Bolker, B., Walker, S., 2015. Fitting Linear Mixed-Effects Models Using lme4. Journal of Statistical Software 67, 1–48. doi:10.18637/jss.v067.i01

Benjamini, Y., Hochberg, Y., 1995. Controlling the False Discovery Rate: A Practical and Powerful Approach to Multiple Testing. Journal of the Royal Statistical Society. Series B (Methodological) 57, 289–300.

Blanco-Canqui, H., Shaver, T.M., Lindquist, J.L., Shapiro, C.A., Elmore, R.W., Francis, C.A., Hergert, G.W., 2015. Cover Crops and Ecosystem Services: Insights from Studies in Temperate Soils. Agronomy Journal 107, 2449–2474. doi:10.2134/agronj15.0086

Bobbink, R., Hicks, K., Galloway, J., Spranger, T., Alkemade, R., Ashmore, M., Bustamante, M., Cinderby, S., Davidson, E., Dentener, F., Emmett, B., Erisman, J.-W., Fenn, M., Gilliam, F., Nordin, A., Pardo, L., De Vries, W., 2010. Global assessment of nitrogen deposition effects on terrestrial plant diversity: a synthesis. Ecological Applications 20, 30–59. doi:10.1890/08-1140.1

Bolyen, E., Rideout, J.R., Dillon, M.R., Bokulich, N.A., Abnet, C.C., Al-Ghalith, G.A., Alexander, H., Alm, E.J., Arumugam, M., Asnicar, F., Bai, Y., Bisanz, J.E., Bittinger, K., Brejnrod, A., Brislawn, C.J., Brown, C.T., Callahan, B.J., Caraballo-Rodríguez, A.M., Chase, J., Cope, E.K., Da Silva, R., Diener, C., Dorrestein, P.C., Douglas, G.M., Durall, D.M., Duvallet, C., Edwardson, C.F., Ernst, M., Estaki, M., Fouquier, J., Gauglitz, J.M., Gibbons, S.M., Gibson, D.L., Gonzalez, A., Gorlick, K., Guo, J., Hillmann, B., Holmes, S., Holste, H., Huttenhower, C., Huttley, G.A., Janssen, S., Jarmusch, A.K., Jiang, L., Kaehler, B.D., Kang, K.B., Keefe, C.R., Keim, P., Kelley, S.T., Knights, D., Koester, I., Kosciolek, T., Kreps, J., Langille, M.G.I., Lee, J., Ley, R., Liu, Y.-X., Loftfield, E., Lozupone, C., Maher, M., Marotz, C., Martin, B.D., McDonald, D., McIver, L.J., Melnik, A.V., Metcalf, J.L., Morgan, S.C., Morton, J.T., Naimey, A.T., Navas-Molina, J.A., Nothias, L.F., Orchanian, S.B., Pearson, T., Peoples, S.L., Petras, D., Preuss, M.L., Pruesse, E., Rasmussen, L.B., Rivers, A., Robeson, M.S., Rosenthal, P., Segata, N., Shaffer, M., Shiffer, A., Sinha, R., Song, S.J., Spear, J.R., Swafford, A.D., Thompson, L.R., Torres, P.J., Trinh, P., Tripathi, A., Turnbaugh, P.J., Ul-Hasan, S., Van Der Hooft, J.J.J., Vargas, F., Vázquez-Baeza, Y., Vogtmann, E., Von Hippel, M., Walters, W., Wan, Y., Wang, M., Warren, J., Weber, K.C., Williamson, C.H.D., Willis, A.D., Xu, Z.Z., Zaneveld, J.R., Zhang, Y., Zhu, Q., Knight, R., Caporaso, J.G., 2019. Reproducible, interactive, scalable and extensible microbiome data science using QIIME 2. Nature Biotechnology 37, 852–857. doi:10.1038/s41587-019-0209-9

Boot, C.M., Broeckling, C.D., Wallenstein, M.D., Schimel, J.P., 2022. Ecosystem metabolomics of dissolved organic matter from arctic soil pore water across seasonal transitions, in: Applied Environmental Metabolomics. Elsevier, pp. 91–106. doi:10.1016/B978-0-12-816460-0.00008-3

Bourke, P.M., Evers, J.B., Bijma, P., van Apeldoorn, D.F., Smulders, M.J.M., Kuyper, T.W., Mommer, L., Bonnema, G., 2021. Breeding Beyond Monoculture: Putting the "Intercrop" Into Crops. Frontiers in Plant Science 12. doi:10.3389/fpls.2021.734167

Brisson, V.L., Schmidt, J.E., Northen, T.R., Vogel, J.P., Gaudin, A.C.M., 2019. Impacts of Maize Domestication and Breeding on Rhizosphere Microbial Community Recruitment from a Nutrient Depleted Agricultural Soil. Scientific Reports 9, 15611. doi:10.1038/s41598-019-52148-y

Callahan, B.J., McMurdie, P.J., Rosen, M.J., Han, A.W., Johnson, A.J.A., Holmes, S.P., 2016. DADA2: High-resolution sample inference from Illumina amplicon data. Nature Methods 13, 581–583. doi:10.1038/nmeth.3869

Calvo-Baltanás, V., Wang, J., Chae, E., 2021. Hybrid Incompatibility of the Plant Immune System: An Opposite Force to Heterosis Equilibrating Hybrid Performances. Frontiers in Plant Science 11. doi:10.3389/fpls.2020.576796

Cao, Y., Qu, R., Tang, X., Sun, L., Chen, Q., Miao, Y., 2020. UPLC-Triple TOF-MS/MS based metabolomics approach to reveal the influence of nitrogen levels on Isatis indigotica seedling leaf. Scientia Horticulturae 266, 109280. doi:10.1016/j.scienta.2020.109280

Cavalieri, A., Bak, F., Garcia-Lemos, A.M., Weiner, J., Nicolaisen, M.H., Nybroe, O., 2020. Effects of Intra- and Interspecific Plant Density on Rhizosphere Bacterial Communities. Frontiers in Microbiology 11. doi:10.3389/fmicb.2020.01045

Cavani, L., Mimmo, T., 2007. Rhizodeposition of *Zea mays* L. as affected by heterosis. Archives of Agronomy and Soil Science 53, 593–604. doi:10.1080/03650340701630912

Chairi, F., Elazab, A., Sanchez-Bragado, R., Araus, J.L., Serret, M.D., 2016. Heterosis for water status in maize seedlings. Agricultural Water Management, Enhancing plant water use efficiency to meet future food production 164, 100–109. doi:10.1016/j.agwat.2015.08.005

Chalk, P.M., Peoples, M.B., McNeill, A.M., Boddey, R.M., Unkovich, M.J., Gardener, M.J., Silva, C.F., Chen, D., 2014. Methodologies for estimating nitrogen transfer between legumes and companion species in agro-ecosystems: A review of 15N-enriched techniques. Soil Biology and Biochemistry 73, 10–21. doi:10.1016/j.soilbio.2014.02.005

Chang, J., Sun, Y., Tian, L., Ji, L., Luo, S., Nasir, F., Kuramae, E.E., Tian, C., 2021. The Structure of Rhizosphere Fungal Communities of Wild and Domesticated Rice: Changes in Diversity and Co-occurrence Patterns. Frontiers in Microbiology 12.

Chapman, N., Miller, A.J., Lindsey, K., Whalley, W.R., 2012. Roots, water, and nutrient acquisition: let's get physical. Trends in Plant Science 17, 701–710. doi:10.1016/j.tplants.2012.08.001

Cheng, W., Coleman, D.C., Carroll, C.R., Hoffman, C.A., 1993. In situ measurement of root respiration and soluble C concentrations in the rhizosphere. Soil Biology and Biochemistry 25, 1189–1196. doi:10.1016/0038-0717(93)90214-V

Colorado Agricultural Meteorological Network, USDA ARS, 2024. Homepage - CoAgMET [WWW Document]. CoAgMET. URL https://coagmet.colostate.edu/ (accessed 6.18.24).

Coskun, D., Britto, D.T., Shi, W., Kronzucker, H.J., 2017. Nitrogen transformations in modern agriculture and the role of biological nitrification inhibition. Nature Plants 3, 1–10. doi:10.1038/nplants.2017.74

Cox, T.S., Van Tassel, D.L., Cox, C.M., DeHaan, L.R., 2010. Progress in breeding perennial grains. Crop and Pasture Science 61, 513. doi:10.1071/CP09201

Crews, T.E., Blesh, J., Culman, S.W., Hayes, R.C., Jensen, E.S., Mack, M.C., Peoples, M.B., Schipanski, M.E., 2016. Going where no grains have gone before: From early to mid-succession. Agriculture, Ecosystems & Environment 223, 223–238. doi:10.1016/j.agee.2016.03.012

Crews, T.E., Carton, W., Olsson, L., 2018. Is the future of agriculture perennial? Imperatives and opportunities to reinvent agriculture by shifting from annual monocultures to perennial polycultures. Global Sustainability 1, e11. doi:10.1017/sus.2018.11

Crews, T.E., Kemp, L., Bowden, J.H., Murrell, E.G., 2022. How the Nitrogen Economy of a Perennial Cereal-Legume Intercrop Affects Productivity: Can Synchrony Be Achieved? Frontiers in Sustainable Food Systems 6, 755548. doi:10.3389/fsufs.2022.755548

Crews, T.E., Peoples, M.B., 2004. Legume versus fertilizer sources of nitrogen: ecological tradeoffs and human needs. Agriculture, Ecosystems & Environment 102, 279–297. doi:10.1016/j.agee.2003.09.018

Cu, S.T.T., Hutson, J., Schuller, K.A., 2005. Mixed culture of wheat (Triticum aestivum L.) with white lupin (Lupinus albus L.) improves the growth and phosphorus nutrition of the wheat. Plant and Soil 272, 143–151. doi:10.1007/s11104-004-4336-8

Cui, M.-H., Chen, X.-Y., Yin, F.-X., Xia, G.-M., Yi, Y., Zhang, Y.-B., Liu, S.-W., Li, F., 2022. Hybridization affects the structure and function of root microbiome by altering gene expression in roots of wheat introgression line under saline-alkali stress. Science of The Total Environment 835, 155467. doi:10.1016/j.scitotenv.2022.155467

Dabney, S.M., Delgado, J.A., Reeves, D.W., 2001. USING WINTER COVER CROPS TO IMPROVE SOIL AND WATER QUALITY. Communications in Soil Science and Plant Analysis 32, 1221–1250. doi:10.1081/CSS-100104110

Daly, A.B., Jilling, A., Bowles, T.M., Buchkowski, R.W., Frey, S.D., Kallenbach, C.M., Keiluweit, M., Mooshammer, M., Schimel, J.P., Grandy, A.S., 2021. A holistic framework integrating plant-microbe-mineral regulation of soil bioavailable nitrogen. Biogeochemistry 154, 211–229. doi:10.1007/s10533-021-00793-9

de Graaff, M.-A., Van Kessel, C., Six, J., 2009. Rhizodeposition-induced decomposition increases N availability to wild and cultivated wheat genotypes under elevated CO2. Soil Biology and Biochemistry 41, 1094–1103. doi:10.1016/j.soilbio.2009.02.015

de Oliveira, G., Brunsell, N.A., Sutherlin, C.E., Crews, T.E., DeHaan, L.R., 2018. Energy, water and carbon exchange over a perennial Kernza wheatgrass crop. Agricultural and Forest Meteorology 249, 120–137. doi:10.1016/j.agrformet.2017.11.022

DeHaan, L., Christians, M., Crain, J., Poland, J., 2018. Development and Evolution of an Intermediate Wheatgrass Domestication Program. Sustainability 10, 1499. doi:10.3390/su10051499

DeHaan, L.R., Anderson, J.A., Bajgain, P., Basche, A., Cattani, D.J., Crain, J., Crews, T.E., David, C., Duchene, O., Gutknecht, J., Hayes, R.C., Hu, F., Jungers, J.M., Knudsen, S., Kong, W., Larson, S., Lundquist, P.-O., Luo, G., Miller, A.J., Nabukalu, P., Newell, M.T., Olsson, L., Palmgren, M., Paterson, A.H., Picasso, V.D., Poland, J.A., Sacks, E.J., Wang, S., Westerbergh, A., 2023. Discussion: Prioritize perennial grain development for sustainable food production and environmental benefits. Science of The Total Environment 895, 164975. doi:10.1016/j.scitotenv.2023.164975

Doebley, J., 2004. The Genetics of Maize Evolution. Annual Review of Genetics 38, 37–59. doi:10.1146/annurev.genet.38.072902.092425

Doebley, J., 1990. Molecular Evidence and the Evolution of Maize. Economic Botany 44, 6–27. doi:10.1007/BF02860472

Dührkop, K., Fleischauer, M., Ludwig, M., Aksenov, A.A., Melnik, A.V., Meusel, M., Dorrestein, P.C., Rousu, J., Böcker, S., 2019. SIRIUS 4: a rapid tool for turning tandem mass spectra into metabolite structure information. Nature Methods 16, 299–302. doi:10.1038/s41592-019-0344-8

Dumigan, C.R., Muileboom, J., Gregory, J., Shrestha, A., Hewedy, O.A., Raizada, M.N., 2021. Ancient Relatives of Modern Maize From the Center of Maize Domestication and Diversification Host Endophytic Bacteria That Confer Tolerance to Nitrogen Starvation. Frontiers in Plant Science 12.

Eissenstat, D.M., 1997. Trade-offs in Root Form and Function, in: Ecology in Agriculture. Elsevier, pp. 173–199. doi:10.1016/B978-012378260-1/50007-5

Food and Agriculture Organization, 2018. Emissions due to agriculture: Global, reigonal and country trends 200-2018. FAOSTAT Analytical Brief 18.

Furneaux, B., Song, Z., 2021. FUNGuildR: Look Up Guild Information for Fungi.

Galindo-Castañeda, T., Hartmann, M., Lynch, J.P., 2024. Location: root architecture structures rhizosphere microbial associations. Journal of Experimental Botany 75, 594–604. doi:10.1093/jxb/erad421

Galloway, J.N., Townsend, A.R., Erisman, J.W., Bekunda, M., Cai, Z., Freney, J.R., Martinelli, L.A., Seitzinger, S.P., Sutton, M.A., 2008. Transformation of the Nitrogen Cycle: Recent Trends, Questions, and Potential Solutions. Science 320, 889–892. doi:10.1126/science.1136674

Gasser, M., Hammelehle, A., Oberson, A., Frossard, E., Mayer, J., 2015. Quantitative evidence of overestimated rhizodeposition using 15N leaf-labelling. Soil Biology and Biochemistry 85, 10–20. doi:10.1016/j.soilbio.2015.02.002

Gaudin, A.C.M., McClymont, S.A., Raizada, M.N., 2011. The Nitrogen Adaptation Strategy of the Wild Teosinte Ancestor of Modern Maize, *Zea mays* subsp. *parviglumis*. Crop Science 51, 2780–2795. doi:10.2135/cropsci2010.12.0686

Gioia, T., Nagel, K.A., Beleggia, R., Fragasso, M., Ficco, D.B.M., Pieruschka, R., De Vita, P., Fiorani, F., Papa, R., 2015. Impact of domestication on the phenotypic architecture of durum wheat

under contrasting nitrogen fertilization. Journal of Experimental Botany 66, 5519–5530. doi:10.1093/jxb/erv289
Glover, J.D., Culman, S.W., DuPont, S.T., Broussard, W., Young, L., Mangan, M.E., Mai, J.G., Crews, T.E., DeHaan, L.R., Buckley, D.H., 2010. Harvested perennial grasslands provide ecological benchmarks for agricultural sustainability. Agriculture, Ecosystems & Environment 137, 3–12. doi:10.1016/j.agee.2009.11.001
Grace, J.B., 1995. On the Measurement of Plant Competition Intensity. Ecology 76, 305–308. doi:10.2307/1940651
Grandy, A.S., Daly, A.B., Bowles, T.M., Gaudin, A.C.M., Jilling, A., Leptin, A., McDaniel, M.D., Wade, J., Waterhouse, H., 2022. The nitrogen gap in soil health concepts and fertility measurements. Soil Biology and Biochemistry 175, 108856. doi:10.1016/j.soilbio.2022.108856
Grossman, J.D., Rice, K.J., 2012. Evolution of root plasticity responses to variation in soil nutrient distribution and concentration. Evolutionary Applications 5, 850–857. doi:10.1111/j.1752-4571.2012.00263.x
Hafner, S., Unteregelsbacher, S., Seeber, E., Lena, B., Xu, X., Li, X., Guggenberger, G., Miehe, G., Kuzyakov, Y., 2012. Effect of grazing on carbon stocks and assimilate partitioning in a Tibetan montane pasture revealed by 13CO2 pulse labeling. Global Change Biology 18, 528–538. doi:10.1111/j.1365-2486.2011.02557.x
Hayes, R., Wang, S., Newell, M., Turner, K., Larsen, J., Gazza, L., Anderson, J., Bell, L., Cattani, D., Frels, K., Galassi, E., Morgounov, A., Revell, C., Thapa, D., Sacks, E., Sameri, M., Wade, L., Westerbergh, A., Shamanin, V., Amanov, A., Li, G., 2018. The Performance of Early-Generation Perennial Winter Cereals at 21 Sites across Four Continents. Sustainability 10, 1124. doi:10.3390/su10041124
He, X.-H., Critchley, C., Bledsoe, C., 2003. Nitrogen Transfer Within and Between Plants Through Common Mycorrhizal Networks (CMNs). Critical Reviews in Plant Sciences 22, 531–567. doi:10.1080/713608315
Hetrick, B.A.D., Wilson, G.W.T., Cox, T.S., 1992. Mycorrhizal dependence of modern wheat varieties, landraces, and ancestors. Canadian Journal of Botany 70, 2032–2040. doi:10.1139/b92-253
Hitaj, C., Suttles, S., 2016. Trends in U.S. Agriculture's Consumption and Production of Energy: Renewable Power, Shale Energy, and Cellulosic Biomass. EIB-159, USDA ERS.
Høgh-Jensen, H., 2006. The Nitrogen Transfer Between Plants: An Important but Difficult Flux to Quantify. Plant and Soil 282, 1–5. doi:10.1007/s11104-005-2613-9
Høgh-Jensen, H., Schjoerring, J.K., 2000. Below-ground nitrogen transfer between different grassland species: Direct quantification by 15N leaf feeding compared with indirect dilution of soil 15N 13.
Hortal, S., Lozano, Y.M., Bastida, F., Armas, C., Moreno, J.L., Garcia, C., Pugnaire, F.I., 2017. Plant-plant competition outcomes are modulated by plant effects on the soil bacterial community. Scientific Reports 7, 17756. doi:10.1038/s41598-017-18103-5
Huang, X., Yang, S., Gong, J., Zhao, Y., Feng, Q., Gong, H., Li, W., Zhan, Q., Cheng, B., Xia, J., Chen, N., Hao, Z., Liu, K., Zhu, C., Huang, T., Zhao, Q., Zhang, L., Fan, D., Zhou, C., Lu, Y., Weng, Q., Wang, Z.-X., Li, J., Han, B., 2015. Genomic analysis of hybrid rice varieties reveals numerous superior alleles that contribute to heterosis. Nature Communications 6, 6258. doi:10.1038/ncomms7258
Iannucci, A., Fragasso, M., Beleggia, R., Nigro, F., Papa, R., 2017. Evolution of the Crop Rhizosphere: Impact of Domestication on Root Exudates in Tetraploid Wheat (Triticum turgidum L.). Frontiers in Plant Science 8, 2124. doi:10.3389/fpls.2017.02124

Isaac, M.E., Nimmo, V., Gaudin, A.C.M., Leptin, A., Schmidt, J.E., Kallenbach, C.M., Martin, A., Entz, M., Carkner, M., Rajcan, I., Boyle, T.D., Lu, X., 2021. Crop Domestication, Root Trait Syndromes, and Soil Nutrient Acquisition in Organic Agroecosystems: A Systematic Review. Frontiers in Sustainable Food Systems 5.

Jackson, L.E., Calderon, F.J., Steenwerth, K.L., Scow, K.M., Rolston, D.E., 2003. Responses of soil microbial processes and community structure to tillage events and implications for soil quality. Geoderma, The assessment of soil quality 114, 305–317. doi:10.1016/S0016-7061(03)00046-6

Jacquiod, S., Raynaud, T., Pimet, E., Ducourtieux, C., Casieri, L., Wipf, D., Blouin, M., 2022. Wheat Rhizosphere Microbiota Respond to Changes in Plant Genotype, Chemical Inputs, and Plant Phenotypic Plasticity. Frontiers in Ecology and Evolution 10. doi:10.3389/fevo.2022.903008

Jansa, J., Smith, F.A., Smith, S.E., 2008. Are there benefits of simultaneous root colonization by different arbuscular mycorrhizal fungi? New Phytologist 177, 779–789. doi:10.1111/j.1469-8137.2007.02294.x

Jilling, A., Keiluweit, M., Contosta, A.R., Frey, S., Schimel, J., Schnecker, J., Smith, R.G., Tiemann, L., Grandy, A.S., 2018. Minerals in the rhizosphere: overlooked mediators of soil nitrogen availability to plants and microbes. Biogeochemistry 139, 103–122. doi:10.1007/s10533-018-0459-5

Johnson, I.R., 1990. Plant respiration in relation to growth, maintenance, ion uptake and nitrogen assimilation. Plant, Cell and Environment 13, 319–328. doi:10.1111/j.1365-3040.1990.tb02135.x

Keeling, C.D., 1960. The Concentration and Isotopic Abundances of Carbon Dioxide in the Atmosphere. Tellus 12, 200–203. doi:10.3402/tellusa.v12i2.9366

Kelly, C., Haddix, M.L., Byrne, P.F., Cotrufo, M.F., Schipanski, M., Kallenbach, C.M., Wallenstein, M.D., Fonte, S.J., 2022a. Divergent belowground carbon allocation patterns of winter wheat shape rhizosphere microbial communities and nitrogen cycling activities. Soil Biology and Biochemistry 165, 108518. doi:10.1016/j.soilbio.2021.108518

Kelly, C., Haddix, M.L., Byrne, P.F., Cotrufo, M.F., Schipanski, M.E., Kallenbach, C.M., Wallenstein, M.D., Fonte, S.J., 2022b. Long-term compost amendment modulates wheat genotype differences in belowground carbon allocation, microbial rhizosphere recruitment and nitrogen acquisition. Soil Biology and Biochemistry 172, 108768. doi:10.1016/j.soilbio.2022.108768

Kong, C.-H., Zhang, S.-Z., Li, Y.-H., Xia, Z.-C., Yang, X.-F., Meiners, S.J., Wang, P., 2018. Plant neighbor detection and allelochemical response are driven by root-secreted signaling chemicals. Nature Communications 9, 3867. doi:10.1038/s41467-018-06429-1

Kuznetsova, A., Brockhoff, P.B., Christensen, R.H.B., 2017. lmerTest Package: Tests in Linear Mixed Effects Models. Journal of Statistical Software 82, 1–26. doi:10.18637/jss.v082.i13

Kuzyakov, Y., 2006. Sources of CO2 efflux from soil and review of partitioning methods. Soil Biology and Biochemistry 38, 425–448. doi:10.1016/j.soilbio.2005.08.020

Lai, H., Gao, F., Su, H., Zheng, P., Li, Y., Yao, H., 2022. Nitrogen Distribution and Soil Microbial Community Characteristics in a Legume–Cereal Intercropping System: A Review. Agronomy 12, 1900. doi:10.3390/agronomy12081900

Leff, J.W., Lynch, R.C., Kane, N.C., Fierer, N., 2017. Plant domestication and the assembly of bacterial and fungal communities associated with strains of the common sunflower, *Helianthus annuus*. New Phytologist 214, 412–423. doi:10.1111/nph.14323

Lenth, R., 2020. emmeans: Estimated Marginal Means, aka Least-Squares Means.

Li, L., Tang, C., Rengel, Z., Zhang, F., 2003. Chickpea facilitates phosphorus uptake by intercropped wheat from an organic phosphorus source. Plant and Soil 248, 297–303. doi:10.1023/A:1022389707051

Liu, Y.-X., Zhang, W.-P., Sun, J.-H., Li, X.-F., Christie, P., Li, L., 2015. High morphological and physiological plasticity of wheat roots is conducive to higher competitive ability of wheat than maize in intercropping systems. Plant and Soil 397, 387–399. doi:10.1007/s11104-015-2654-7

Lynch, L.M., Machmuller, M.B., Cotrufo, M.F., Paul, E.A., Wallenstein, M.D., 2018. Tracking the fate of fresh carbon in the Arctic tundra: Will shrub expansion alter responses of soil organic matter to warming? Soil Biology and Biochemistry 120, 134–144. doi:10.1016/j.soilbio.2018.02.002

Mallick, H., Rahnavard, A., McIver, L.J., Ma, S., Zhang, Y., Nguyen, L.H., Tickle, T.L., Weingart, G., Ren, B., Schwager, E.H., Chatterjee, S., Thompson, K.N., Wilkinson, J.E., Subramanian, A., Lu, Y., Waldron, L., Paulson, J.N., Franzosa, E.A., Bravo, H.C., Huttenhower, C., 2021. Multivariable association discovery in population-scale meta-omics studies. PLOS Computational Biology 17, e1009442. doi:10.1371/journal.pcbi.1009442

Mammadov, J., Buyyarapu, R., Guttikonda, S.K., Parliament, K., Abdurakhmonov, I.Y., Kumpatla, S.P., 2018. Wild Relatives of Maize, Rice, Cotton, and Soybean: Treasure Troves for Tolerance to Biotic and Abiotic Stresses. Frontiers in Plant Science 9. doi:10.3389/fpls.2018.00886

Mårtensson, L.-M.D., Barreiro, A., Li, S., Jensen, E.S., 2022. Agronomic performance, nitrogen acquisition and water-use efficiency of the perennial grain crop Thinopyrum intermedium in a monoculture and intercropped with alfalfa in Scandinavia. Agronomy for Sustainable Development 42, 21. doi:10.1007/s13593-022-00752-0

Matesanz, S., Milla, R., 2018. Differential plasticity to water and nutrients between crops and their wild progenitors. Environmental and Experimental Botany 145, 54–63. doi:10.1016/j.envexpbot.2017.10.014

McGonigle, T.P., Miller, M.H., Evans, D.G., Fairchild, G.L., Swan, J.A., 1990. A new method which gives an objective measure of colonization of roots by vesicular—arbuscular mycorrhizal fungi. New Phytologist 115, 495–501. doi:10.1111/j.1469-8137.1990.tb00476.x

McLaughlin, S., Zhalnina, K., Kosina, S., Northen, T.R., Sasse, J., 2023. The core metabolome and root exudation dynamics of three phylogenetically distinct plant species. Nature Communications 14, 1649. doi:10.1038/s41467-023-37164-x

McNeill, A.M., Unkovich, M.J., 2024. Estimates of N accumulated below-ground by grain legumes derived using leaf or stem 15N-feeding: in search of a practical method for potential use at remote field locations. Plant and Soil 500, 721–741. doi:10.1007/s11104-024-06515-y

Mead, R., Willey, R.W., 1980. The Concept of a 'Land Equivalent Ratio' and Advantages in Yields from Intercropping. Experimental Agriculture 16, 217–228. doi:10.1017/S0014479700010978

Meier, I.C., Finzi, A.C., Phillips, R.P., 2017. Root exudates increase N availability by stimulating microbial turnover of fast-cycling N pools. Soil Biology and Biochemistry 106, 119–128. doi:10.1016/j.soilbio.2016.12.004

Menegat, S., Ledo, A., Tirado, R., 2022. Greenhouse gas emissions from global production and use of nitrogen synthetic fertilisers in agriculture. Scientific Reports 12, 14490. doi:10.1038/s41598-022-18773-w

Mizuno, N., Hosogi, N., Park, P., Takumi, S., 2010. Hypersensitive Response-Like Reaction Is Associated with Hybrid Necrosis in Interspecific Crosses between Tetraploid Wheat and Aegilops tauschii Coss. PLOS ONE 5, e11326. doi:10.1371/journal.pone.0011326

Morris, E.K., Buscot, F., Herbst, C., Meiners, T., Obermaier, E., Wäschke, N.W., Wubet, T., Rillig, M.C., 2013. Land use and host neighbor identity effects on arbuscular mycorrhizal fungal community composition in focal plant rhizosphere. Biodiversity and Conservation 22, 2193–2205. doi:10.1007/s10531-013-0527-z

Näsholm, T., Kielland, K., Ganeteg, U., 2009. Uptake of organic nitrogen by plants. New Phytologist 182, 31–48. doi:10.1111/j.1469-8137.2008.02751.x

Nelson, A.R., Fegel, T.S., Danczak, R.E., Caiafa, M.V., Roth, H.K., Dunn, O.I., Turvold, C.A., Borch, T., Glassman, S.I., Barnes, R.T., Rhoades, C.C., Wilkins, M.J., 2024. Soil microbiome feedbacks during disturbance-driven forest ecosystem conversion. The ISME Journal 18, wrae047. doi:10.1093/ismejo/wrae047

Nguyen, N.H., Song, Z., Bates, S.T., Branco, S., Tedersoo, L., Menke, J., Schilling, J.S., Kennedy, P.G., 2016. FUNGuild: An open annotation tool for parsing fungal community datasets by ecological guild. Fungal Ecology 20, 241–248. doi:10.1016/j.funeco.2015.06.006

Oksanen, J., Simpson, G.L., Blanchet, F.G., Kindt, R., Legendre, P., Minchin, P.R., O'Hara, R.B., Solymos, P., Stevens, M.H.H., Szoecs, E., Wagner, H., Barbour, M., Bedward, M., Bolker, B., Borcard, D., Carvalho, G., Chirico, M., Caceres, M.D., Durand, S., Evangelista, H.B.A., FitzJohn, R., Friendly, M., Furneaux, B., Hannigan, G., Hill, M.O., Lahti, L., McGlinn, D., Ouellette, M.-H., Cunha, E.R., Smith, T., Stier, A., Braak, C.J.F.T., Weedon, J., 2022. vegan: Community Ecology Package.

Osiru, D.S.O., Willey, R.W., 1972. Studies on mixtures of dwarf sorghum and beans (Phaseolus vulgaris) with particular reference to plant population. The Journal of Agricultural Science 79, 531–540. doi:10.1017/S0021859600025910

Parr, M., Grossman, J.M., Reberg-Horton, S.C., Brinton, C., Crozier, C., 2011. Nitrogen Delivery from Legume Cover Crops in No-Till Organic Corn Production. Agronomy Journal 103, 1578–1590. doi:10.2134/agronj2011.0007

Patti, G.J., Yanes, O., Siuzdak, G., 2012. Metabolomics: the apogee of the omics trilogy. Nature Reviews Molecular Cell Biology 13, 263–269. doi:10.1038/nrm3314

Pausch, J., Kuzyakov, Y., 2018. Carbon input by roots into the soil: Quantification of rhizodeposition from root to ecosystem scale. Global Change Biology 24, 1–12. doi:10.1111/gcb.13850

Pausch, J., Tian, J., Riederer, M., Kuzyakov, Y., 2013. Estimation of rhizodeposition at field scale: upscaling of a 14C labeling study. Plant and Soil 364, 273–285. doi:10.1007/s11104-012-1363-8

Peralta, A.L., Sun, Y., McDaniel, M.D., Lennon, J.T., 2018. Crop rotational diversity increases disease suppressive capacity of soil microbiomes. Ecosphere 9, e02235. doi:10.1002/ecs2.2235

Pérez-Jaramillo, J.E., Carrión, V.J., Bosse, M., Ferrão, L.F.V., de Hollander, M., Garcia, A.A.F., Ramírez, C.A., Mendes, R., Raaijmakers, J.M., 2017. Linking rhizosphere microbiome composition of wild and domesticated Phaseolus vulgaris to genotypic and root phenotypic traits. The ISME Journal 11, 2244–2257. doi:10.1038/ismej.2017.85

Pérez-Jaramillo, J.E., Mendes, R., Raaijmakers, J.M., 2016. Impact of plant domestication on rhizosphere microbiome assembly and functions. Plant Molecular Biology 90, 635–644. doi:10.1007/s11103-015-0337-7

Post, D.M., 2002. Using Stable Isotopes to Estimate Trophic Position: Models, Methods, and Assumptions. Ecology 83, 703–718. doi:10.1890/0012-9658(2002)083[0703:USITET]2.0.CO;2

R Core Team, 2020. R: A Language and Environment for Statistical Computing. R Foundation for Statistical Computing, Vienna, Austria.

Raghothama, K.G., Karthikeyan, A.S., 2005. Phosphate Acquisition. Plant and Soil 274, 37–49. doi:10.1007/s11104-004-2005-6
Ranum, P., Peña-Rosas, J.P., Garcia-Casal, M.N., 2014. Global maize production, utilization, and consumption. Annals of the New York Academy of Sciences 1312, 105–112. doi:10.1111/nyas.12396
Rasmussen, J., Gylfadóttir, T., Dhalama, N.R., De Notaris, C., Kätterer, T., 2019a. Temporal fate of 15N and 14C leaf-fed to red and white clover in pure stand or mixture with grass – Implications for estimation of legume derived N in soil and companion species. Soil Biology and Biochemistry 133, 60–71. doi:10.1016/j.soilbio.2019.02.011
Rasmussen, J., Gylfadóttir, T., Dhalama, N.R., De Notaris, C., Kätterer, T., 2019b. Temporal fate of 15N and 14C leaf-fed to red and white clover in pure stand or mixture with grass – Implications for estimation of legume derived N in soil and companion species. Soil Biology and Biochemistry 133, 60–71. doi:10.1016/j.soilbio.2019.02.011
Reich, P.B., Tjoelker, M.G., Pregitzer, K.S., Wright, I.J., Oleksyn, J., Machado, J.-L., 2008. Scaling of respiration to nitrogen in leaves, stems and roots of higher land plants. Ecology Letters 11, 793–801. doi:10.1111/j.1461-0248.2008.01185.x
Reilly, E.C., Gutknecht, J.L., Tautges, N.E., Sheaffer, C.C., Jungers, J.M., 2022. Nitrogen transfer and yield effects of legumes intercropped with the perennial grain crop intermediate wheatgrass. Field Crops Research 286, 108627. doi:10.1016/j.fcr.2022.108627
Remus, R., Augustin, J., 2016. Dynamic linking of 14C partitioning with shoot growth allows a precise determination of plant-derived C input to soil. Plant and Soil 408, 493–513. doi:10.1007/s11104-016-3006-y
Renzi, J.P., Coyne, C.J., Berger, J., von Wettberg, E., Nelson, M., Ureta, S., Hernández, F., Smýkal, P., Brus, J., 2022. How Could the Use of Crop Wild Relatives in Breeding Increase the Adaptation of Crops to Marginal Environments? Frontiers in Plant Science 13. doi:10.3389/fpls.2022.886162
Rinkes, Z.L., Weintraub, M.N., DeForest, J.L., Moorhead, D.L., 2011. Microbial substrate preference and community dynamics during decomposition of Acer saccharum. Fungal Ecology 4, 396–407. doi:10.1016/j.funeco.2011.01.004
RStudio Team, 2020. RStudio: Integrated Development Environment for R. RStudio, PBC, Boston, MA.
Schmid, R., Heuckeroth, S., Korf, A., Smirnov, A., Myers, O., Dyrlund, T.S., Bushuiev, R., Murray, K.J., Hoffmann, N., Lu, M., Sarvepalli, A., Zhang, Z., Fleischauer, M., Dührkop, K., Wesner, M., Hoogstra, S.J., Rudt, E., Mokshyna, O., Brungs, C., Ponomarov, K., Mutabdžija, L., Damiani, T., Pudney, C.J., Earll, M., Helmer, P.O., Fallon, T.R., Schulze, T., Rivas-Ubach, A., Bilbao, A., Richter, H., Nothias, L.-F., Wang, M., Orešič, M., Weng, J.-K., Böcker, S., Jeibmann, A., Hayen, H., Karst, U., Dorrestein, P.C., Petras, D., Du, X., Pluskal, T., 2023. Integrative analysis of multimodal mass spectrometry data in MZmine 3. Nature Biotechnology 41, 447–449. doi:10.1038/s41587-023-01690-2
Schmidt, J.E., 2020. Impacts of directed evolution and soil management legacy on the maize rhizobiome. Soil Biology and Biochemistry 13.
Schmidt, J.E., Poret-Peterson, A., Lowry, C.J., Gaudin, A.C.M., 2020. Has agricultural intensification impacted maize root traits and rhizosphere interactions related to organic N acquisition? AoB PLANTS 12, plaa026. doi:10.1093/aobpla/plaa026
Scholze, P., Krämer, R., Ryschka, U., Klocke, E., Schumann, G., 2010. Somatic hybrids of vegetable brassicas as source for new resistances to fungal and virus diseases. Euphytica 176, 1–14. doi:10.1007/s10681-010-0205-0

Seethepalli, A., Dhakal, K., Griffiths, M., Guo, H., Freschet, G.T., York, L.M., 2021. RhizoVision Explorer: open-source software for root image analysis and measurement standardization. AoB PLANTS 13, plab056. doi:10.1093/aobpla/plab056
Seethepalli, A., York, L.M., 2020. RhizoVision Explorer - Interactive software for generalized root image analysis designed for everyone. doi:10.5281/ZENODO.4095629
Smil, V., 2001. Enriching the earth: Fritz Haber, Carl Bosch, and the transformation of world food production. MIT Press, Cambridge, Mass.
Soil Survey Staff, U.S.D. of A., Natural Resources Conservation Service, 2019. Web soil survey [WWW Document]. URL http://websoilsurvey.sc.egov.usda.gov/ (accessed 3.20.24).
Spor, A., Roucou, A., Mounier, A., Bru, D., Breuil, M.-C., Fort, F., Vile, D., Roumet, P., Philippot, L., Violle, C., 2020. Domestication-driven changes in plant traits associated with changes in the assembly of the rhizosphere microbiota in tetraploid wheat. Scientific Reports 10, 12234. doi:10.1038/s41598-020-69175-9
Sugiyama, A., Ueda, Y., Zushi, T., Takase, H., Yazaki, K., 2014. Changes in the Bacterial Community of Soybean Rhizospheres during Growth in the Field. PLOS ONE 9, e100709. doi:10.1371/journal.pone.0100709
Sun, L., Ataka, M., Kominami, Y., Yoshimura, K., Kitayama, K., 2021. A constant microbial C/N ratio mediates the microbial nitrogen mineralization induced by root exudation among four co-existing canopy species. Rhizosphere 17, 100317. doi:10.1016/j.rhisph.2021.100317
Sun, T., Zhou, J., Fu, Y., Wu, L., Zhang, T., 2024. Soil nitrogen availability mediates the positive effects of intercropping on soil organic carbon at global scales. Soil and Tillage Research 239, 106063. doi:10.1016/j.still.2024.106063
Taylor, H.H. (Ed.), 1994. Fertilizer Use and Price Statistics, 1960-93, SB 893. doi:10.22004/ag.econ.154834
The Inkscape Project, 2023. Inkscape.
Thilakarathna, M.S., McElroy, M.S., Chapagain, T., Papadopoulos, Y.A., Raizada, M.N., 2016. Belowground nitrogen transfer from legumes to non-legumes under managed herbaceous cropping systems. A review. Agronomy for Sustainable Development 36, 58. doi:10.1007/s13593-016-0396-4
Thompson, L.R., Sanders, J.G., McDonald, D., Amir, A., Ladau, J., Locey, K.J., Prill, R.J., Tripathi, A., Gibbons, S.M., Ackermann, G., Navas-Molina, J.A., Janssen, S., Kopylova, E., Vázquez-Baeza, Y., González, A., Morton, J.T., Mirarab, S., Zech Xu, Z., Jiang, L., Haroon, M.F., Kanbar, J., Zhu, Q., Jin Song, S., Kosciolek, T., Bokulich, N.A., Lefler, J., Brislawn, C.J., Humphrey, G., Owens, S.M., Hampton-Marcell, J., Berg-Lyons, D., McKenzie, V., Fierer, N., Fuhrman, J.A., Clauset, A., Stevens, R.L., Shade, A., Pollard, K.S., Goodwin, K.D., Jansson, J.K., Gilbert, J.A., Knight, R., 2017. A communal catalogue reveals Earth's multiscale microbial diversity. Nature 551, 457–463. doi:10.1038/nature24621
Tian, B., Pei, Y., Huang, W., Ding, J., Siemann, E., 2021. Increasing flavonoid concentrations in root exudates enhance associations between arbuscular mycorrhizal fungi and an invasive plant. The ISME Journal 15, 1919–1930. doi:10.1038/s41396-021-00894-1
Townsend, A.R., Howarth, R.W., Bazzaz, F.A., Booth, M.S., Cleveland, C.C., Collinge, S.K., Dobson, A.P., Epstein, P.R., Holland, E.A., Keeney, D.R., Mallin, M.A., Rogers, C.A., Wayne, P., Wolfe, A.H., 2003. Human Health Effects of a Changing Global Nitrogen Cycle. Frontiers in Ecology and the Environment 1, 240–246. doi:10.2307/3868011
Ulbrich, T.C., Rivas-Ubach, A., Tiemann, L.K., Friesen, M.L., Evans, S.E., 2022. Plant root exudates and rhizosphere bacterial communities shift with neighbor context. Soil Biology and Biochemistry 172, 108753. doi:10.1016/j.soilbio.2022.108753
USDA National Agricultural Statistics Service, 2024. NASS - Quick Stats.

USDA National Agricultural Statistics Service, 2017. NASS - Quick Stats.
van der Pol, L.K., Nester, B., Schlautman, B., Crews, T.E., Cotrufo, M.F., 2022. Perennial grain Kernza® fields have higher particulate organic carbon at depth than annual grain fields. Canadian Journal of Soil Science 102, 1005–1009. doi:10.1139/cjss-2022-0026
Van Tassel, D.L., Albrecht, K.A., Bever, J.D., Boe, A.A., Brandvain, Y., Crews, T.E., Gansberger, M., Gerstberger, P., González-Paleo, L., Hulke, B.S., Kane, N.C., Johnson, P.J., Pestsova, E.G., Picasso Risso, V.D., Prasifka, J.R., Ravetta, D.A., Schlautman, B., Sheaffer, C.C., Smith, K.P., Speranza, P.R., Turner, M.K., Vilela, A.E., von Gehren, P., Wever, C., 2017. Accelerating Silphium Domestication: An Opportunity to Develop New Crop Ideotypes and Breeding Strategies Informed by Multiple Disciplines. Crop Science 57, 1274–1284. doi:10.2135/cropsci2016.10.0834
Van Tassel, D.L., DeHaan, L.R., Diaz-Garcia, L., Hershberger, J., Rubin, M.J., Schlautman, B., Turner, K., Miller, A.J., 2022. Re-imagining crop domestication in the era of high throughput phenomics. Current Opinion in Plant Biology 65, 102150. doi:10.1016/j.pbi.2021.102150
Vitousek, P.M., Aber, J.D., Howarth, R.W., Likens, G.E., Matson, P.A., Schindler, D.W., Schlesinger, W.H., Tilman, D.G., 1997. Human Alteration of the Global Nitrogen Cycle: Sources and Consequences. Ecological Applications 7, 737–750. doi:10.1890/1051-0761(1997)007[0737:HAOTGN]2.0.CO;2
Wang, R., Bicharanloo, B., Shirvan, M.B., Cavagnaro, T.R., Jiang, Y., Keitel, C., Dijkstra, F.A., 2021. A novel 13C pulse-labelling method to quantify the contribution of rhizodeposits to soil respiration in a grassland exposed to drought and nitrogen addition. New Phytologist 230, 857–866. doi:10.1111/nph.17118
Wang, Z., Ni, Z., Wu, H., Nie, X., Sun, Q., 2006. Heterosis in root development and differential gene expression between hybrids and their parental inbreds in wheat (Triticum aestivum L.). Theoretical and Applied Genetics 113, 1283–1294. doi:10.1007/s00122-006-0382-3
Weintraub, M.N., Scott-Denton, L.E., Schmidt, S.K., Monson, R.K., 2007. The effects of tree rhizodeposition on soil exoenzyme activity, dissolved organic carbon, and nutrient availability in a subalpine forest ecosystem. Oecologia 154, 327–338. doi:10.1007/s00442-007-0804-1
Wickham, H., 2016. ggplot2: Elegant Graphics for Data Analysis. Springer-Verlag New York.
Wickham, H., Averick, M., Bryan, J., Chang, W., McGowan, L., François, R., Grolemund, G., Hayes, A., Henry, L., Hester, J., Kuhn, M., Pedersen, T., Miller, E., Bache, S., Müller, K., Ooms, J., Robinson, D., Seidel, D., Spinu, V., Takahashi, K., Vaughan, D., Wilke, C., Woo, K., Yutani, H., 2019. Welcome to the Tidyverse. Journal of Open Source Software 4, 1686. doi:10.21105/joss.01686
Williams, A., Langridge, H., Straathof, A.L., Fox, G., Muhammadali, H., Hollywood, K.A., Xu, Y., Goodacre, R., de Vries, F.T., 2021. Comparing root exudate collection techniques: An improved hybrid method. Soil Biology and Biochemistry 161, 108391. doi:10.1016/j.soilbio.2021.108391
Williams, A., Langridge, H., Straathof, A.L., Muhamadali, H., Hollywood, K.A., Goodacre, R., de Vries, F.T., 2022. Root functional traits explain root exudation rate and composition across a range of grassland species. Journal of Ecology 110, 21–33. doi:10.1111/1365-2745.13630
Xing, Y., Yu, R.-P., An, R., Yang, N., Wu, J.-P., Ma, H.-Y., Zhang, J.-D., Bao, X.-G., Lambers, H., Li, L., 2023. Two pathways drive enhanced nitrogen acquisition via a complementarity effect in long-term intercropping. Field Crops Research 293, 108854. doi:10.1016/j.fcr.2023.108854
Yang, Z., Chen, X., Huang, Y., Song, J., Shi, T., Li, Y., Tang, X., Yi, Y., Li, F., 2022. Distant somatic hybridization alters the structure of wheat root bacterial microbiota. Agronomy Journal 114, 1952–1962. doi:10.1002/agj2.20952

York, L.M., Galindo-Castaneda, T., Schussler, J.R., Lynch, J.P., 2015. Evolution of US maize (Zea mays L.) root architectural and anatomical phenes over the past 100 years corresponds to increased tolerance of nitrogen stress. Journal of Experimental Botany 66, 2347–2358. doi:10.1093/jxb/erv074

Zai, X., Luo, W., Bai, W., Li, Y., Xiao, X., Gao, X., Wang, E., Wei, G., Chen, W., 2021. Effect of Root Diameter on the Selection and Network Interactions of Root-Associated Bacterial Microbiomes in Robinia pseudoacacia L. Microbial Ecology 82, 391–402. doi:10.1007/s00248-020-01678-4

Zhalnina, K., Louie, K.B., Hao, Z., Mansoori, N., da Rocha, U.N., Shi, S., Cho, H., Karaoz, U., Loqué, D., Bowen, B.P., Firestone, M.K., Northen, T.R., Brodie, E.L., 2018. Dynamic root exudate chemistry and microbial substrate preferences drive patterns in rhizosphere microbial community assembly. Nature Microbiology 3, 470–480. doi:10.1038/s41564-018-0129-3

Zhang, M., Wang, Y., Hu, Y., Wang, H., Liu, Y., Zhao, B., Zhang, J., Fang, R., Yan, Y., 2023. Heterosis in root microbiota inhibits growth of soil-borne fungal pathogens in hybrid rice. Journal of Integrative Plant Biology 65, 1059–1076. doi:10.1111/jipb.13416

Zhang, Y., Sun, Z., Su, Z., Du, G., Bai, W., Wang, Q., Wang, R., Nie, J., Sun, T., Feng, C., Zhang, Z., Yang, N., Zhang, X., Evers, J.B., van der Werf, W., Zhang, L., 2022. Root plasticity and interspecific complementarity improve yields and water use efficiency of maize/soybean intercropping in a water-limited condition. Field Crops Research 282, 108523. doi:10.1016/j.fcr.2022.108523

Supplemental Table 3.1. List of all identified features from the LC-MSMS analysis of exudate samples. Non exudate features refer to those features not significantly elevated in intensity in sample vs blanks. No MS2 spectra refers to those exudate features that did not have MS2 spectra, and therefore no structural/formula annotation. SIRIUS only offered substructure annotation for certain features without full compound identity. Italicized lines denote those features appearing in Fig 3.3. Bolded line denotes the one feature in this list that showed significant genotype effect.

Ionization	Type of feature	Number of features	Compound Number	Molecular formula	m/z	Sirius Score	Metabolic pathway	Class	Pubchem number
Positive	Compound ID	5	*Pos.C71*	*C17H35O2*	*272.27*	*20.6*	*Fatty acids*	*Unsaturated fatty acids*	*102280231*
			Pos.C25	*C23H46N8O7*	*320.12*	*27.3*	*Carbohydrates*	*Polyamines*	*11387242*
			Pos.C209	C24H54N4O6	512.44	17.5	Amino acids and Peptides	Linear peptides	138736421
			Pos.C22	*C25H46N2O8*	*520.36*	*34.3*	*Terpenoids*	*Open-chain polyketides*	*124189880*
			Pos.C357	C29H58N2O5	532.47	25.8	Terpenoids	Ceramides	10118579
	Substructure annotation only	4	Pos.C114	C7H30N12O3	295.24	7.2	Alkaloids	Polyamines	*NA*
			Pos.C41	C26H36N14O5	625.31	28.1	Carbohydrates	Purine nucleos(t)ides	
			Pos.C171	C7H28N12O	279.25	1.7	Alkaloids	Polyamines	
			Pos.C179	C9H30N9O2	297.26	11.1	Alkaloids	Polyamines	
	Formula only	10	Pos.C295	C22H38	303.31	11.0		*NA*	
			Pos.C156	C24H22O2	365.15	5.2			
			Pos.C42	C17H18O	261.12	5.0			
			Pos.C34	C13H29N3O	244.24	0.4			
			Pos.C44	C10H16N5O2	239.14	5.4			
			Pos.C10	C6H17N7O3S	268.12	2.8			
			Pos.C32	C17H35O3	288.27	1.4			
			Pos.C101	C14H34N3O6	341.25	9.8			
			Pos.C211	C25H55N3O3	468.41	17.3			
			Pos.C40	C44H42O3	641.30	3.2			
	No MS2 spectra	*39*	*Pos.C1*		*162.12*				
			Pos.C100		*149.07*				
			...						
	Non exudate feature	*260*							
	TOTAL	**318**							

Negative	Compound ID	5	*Neg.C2*	*C12H6O*	*201.01*	*16.4*	*Shikimates and Phenylpropanoids*	*Phenanthrenes*	*86087506*
			Neg.C33	C9H16N4O2	211.12	11.0	Amino acids and Peptides	Amino acids	65611665
			Neg.G.C5.C7	***C15H10N2O7***	***367.01***	***6.5***	***Alkaloids***	***Anthranilic acid derivatives***	***745724***
			Neg.C18	C13H26N2O3	293.16	23.4	Amino acids and Peptides	Dipeptides	49864736
			Neg.C24	C10H16N4O3	239.12	12.7	Amino acids and Peptides	Dipeptides	9942822
	Formula only	4	Neg.C3	C5H2O6	156.98	4.8			
			Neg.C51	*C16H30O5*	*301.20*	*5.3*		*NA*	
			Neg.C17	*C11H18N4O3*	*253.13*	*11.4*			
			Neg.C43	*C16H28O5*	*299.19*	*3.3*			
	No MS2 spectra	*8*	*Neg.C29*		*416.00*				
			Neg.C39		*297.23*				
			Neg.C40		*199.16*				
			Neg.C42		*250.13*				
			...						
	Non exudate feature	*101*							
	TOTAL	**118**							

Supplemental Table 5.1. Biomass and N concentrations of alfalfa in monoculture and in biculture with three cereals (AW = annual wheat, PW = perennial wheat, K= Kernza) and root:shoot ratio (R:S). Dry mass and N concentration are given for shoots, roots, and total plant. Data shown in mean ± standard error. The bottom section lists p-values associated with each response variable obtained via mixed effect linear model, with significant values (< 0.05) denoted in italics. G = genotype effect, S = cropping system effect. Note that genotype effect tests only those alfalfa in biculture and cropping system effect compares all biculture alfalfa against the monoculture alfalfa.

Crop genotype	Cropping system	Cereal genotype	Biomass						
			Shoots		Roots		Total		
			g plant $^{-1}$	%N	g plant $^{-1}$	%N	g plant $^{-1}$	%N	R:S
Alfalfa	Bi	AW	4.79 ± 0.93	2.66 ± 0.18	3.01 ± 0.59	1.59 ± 0.39	7.80 ± 1.49	2.26 ± 0.2	0.62 ± 0.05
		PW	6.46 ± 0.83	2.93 ± 0.56	3.95 ± 0.78	2.10 ± 0.33	10.61 ± 1.7	2.61 ± 0.36	0.57 ± 0.04
		K	5.20 ± 1.35	3.36 ± 0.35	3.53 ± 0.92	2.25 ± 0.37	8.74 ± 2.24	2.93 ± 0.35	0.65 ± 0.08
	Mono	NA	7.33 ± 1.09	3.12 ± 0.1	4.37 ± 0.65	2.05 ± 0.12	11.69 ± 1.74	2.72 ± 0.06	0.60 ± 0.01
		G	0.539	0.466	0.735	0.351	0.627	0.269	0.712
		S	0.150	0.734	0.300	0.847	0.206	0.694	0.743

Supplemental Table 5.2. Labile N soil pool in rhizosphere of alfalfa grown in biculture with cereals (AW = annual wheat, PW = perennial wheat, K= Kernza) or in monoculture. Data shown in mean ± standard error. TDN = Total dissolved N, MBN = microbial biomass. Labile C information can be found in Fig 2. The bottom section lists p-values associated with each response variable obtained via mixed effect linear model, with significant values (< 0.05) denoted in italics. G = genotype effect, S = cropping system effect. Note that genotype effect tests only those alfalfa in biculture and cropping system effect compares all biculture alfalfa against the monoculture alfalfa.

			Soil N (ug N g soil^{-1})		
			TDN	MBN	Total
Alfalfa	Bi	AW	0.82 ± 0.08	0.72 ± 0.08	821.5 ± 30.5
		PW	0.74 ± 0.04	0.89 ± 0.10	774.8 ± 74.8
		K	0.71 ± 0.05	0.63 ± 0.08	767 ± 44.9
	Mono	NA	0.80 ± 0.10	0.88 ± 0.10	823 ± 44.1
		G	0.389	0.170	0.551
		S	0.593	0.266	0.546

Supplemental Table 5.3. Diversity indices for both cereals (annual wheat, perennial wheat, and Kernza) and alfalfa rhizosphere 16S profiles. Shannon's index was used as the evenness index. The bottom section lists p-values associated with each response variable obtained via mixed effect linear model, with significant values (< 0.05) denoted in italics. G = genotype, T = crop type (cereal in monoculture, cereal in biculture, and alfalfa in biculture), and S = cropping system. Note that in this context, cropping system effect compares all biculture alfalfa against the monoculture alfalfa.

			Diversity	
Genotype	Cropping system	Crop type	ASV richness	Shannon's index
Annual wheat	Mono	-	1170 ± 82	6.46 ± 0.06
	Bi	Cereal	1176 ± 95	6.46 ± 0.06
		Legume	1088 ± 73	6.38 ± 0.07
Perennial wheat	Mono	-	1035 ± 123	6.32 ± 0.11
	Bi	Cereal	899 ± 107	6.17 ± 0.1
		Legume	1204 ± 94	6.44 ± 0.06
Kernza	Mono	-	1055 ± 149	6.33 ± 0.13
	Bi	Cereal	1084 ± 109	6.37 ± 0.1
		Legume	1280 ± 63	6.52 ± 0.06
Alfalfa	Mono	-	1214 ± 146	6.42 ± 0.12
		G	0.484	0.283
		T	0.276	0.302
		G x T	0.395	0.363
		S	0.837	0.755

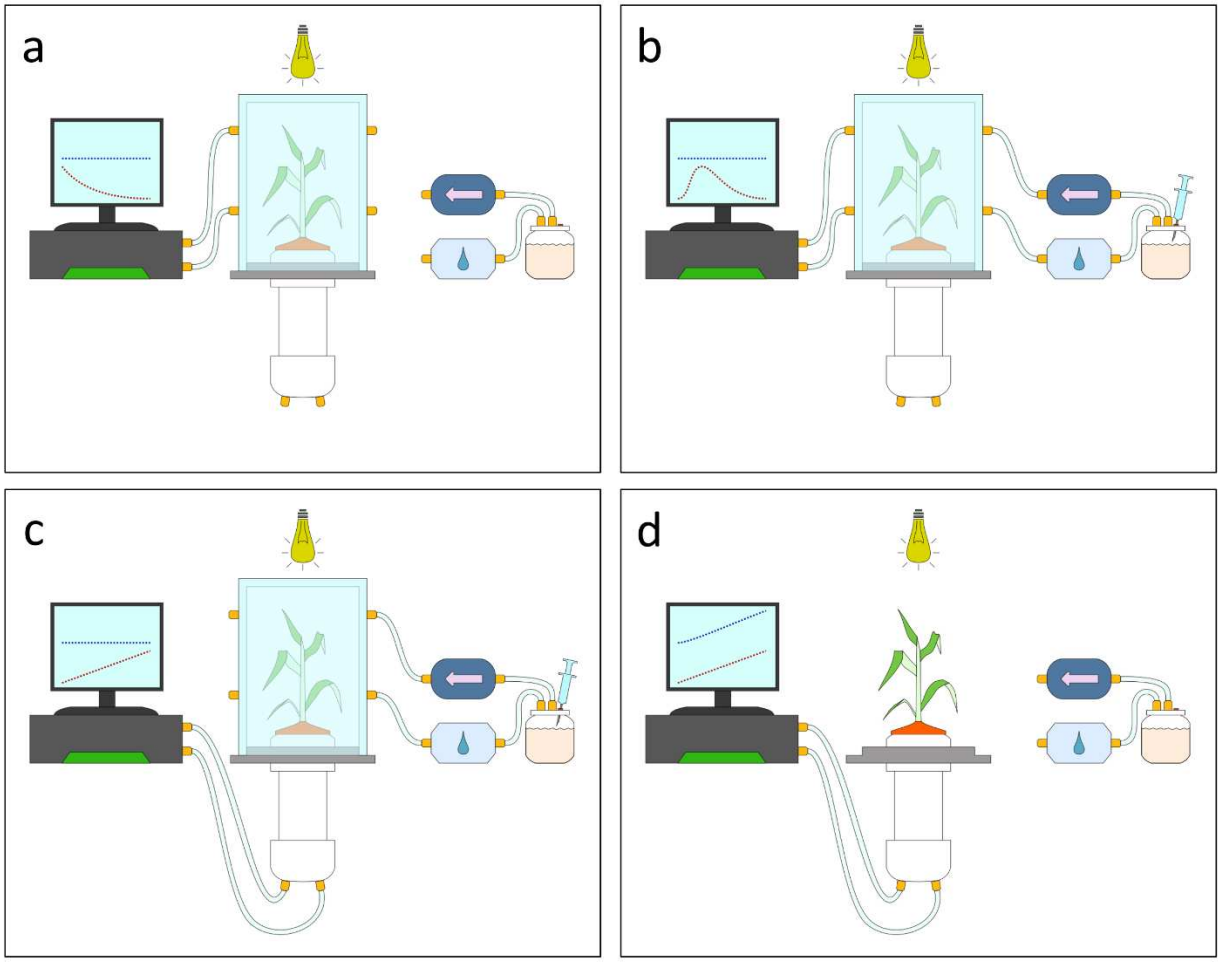

Supplemental Figure 2.1. Each panel **(a – d)** shows four distinct phases of pulse labeling procedure. Blue dotted line on the monitor approximates the $\delta^{13}C$ value and the red dotted line approximates CO_2 concentration. Briefly, **(a)** ambient CO_2 taken up by the plant to prepare the chamber for a controlled amount of CO_2 injection. **(b)** A set amount of natural abundance carbonate is injected into the HCl container, releasing CO_2 into the chamber. The plant takes up the CO_2 and the time elapsed between the carbonate injection and full ($[CO_2] < 50$ ppm) drawdown is noted. **(c)** Enriched carbonate solution is injected this time, with the gas analyzer now monitoring the soil column CO_2 efflux. **(d)** Once we estimate that the plant has taken up all the given CO_2 we remove the chamber from the top. We terminate the labeling process once we observe a concurrent increase in CO_2 concentration and $\delta^{13}C$ signature.

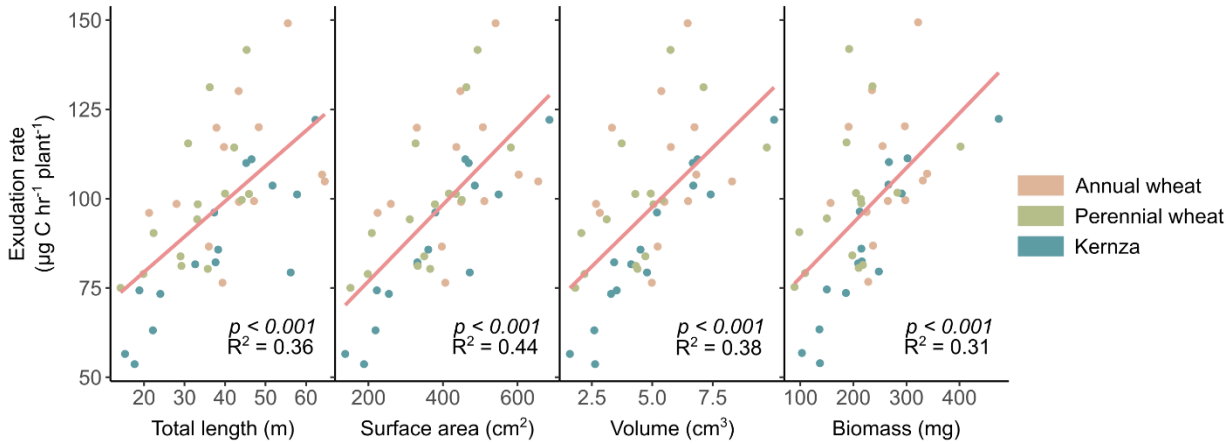

Supplemental Figure 3.1. Correlation between four root parameters (length, surface area, volume, and mass) and exudation rate. The *p*-values for the correlation are denoted within each panel and significant values ($p < 0.05$) are italicized. Corresponding adjusted R^2 values are denoted under the *p*-values.

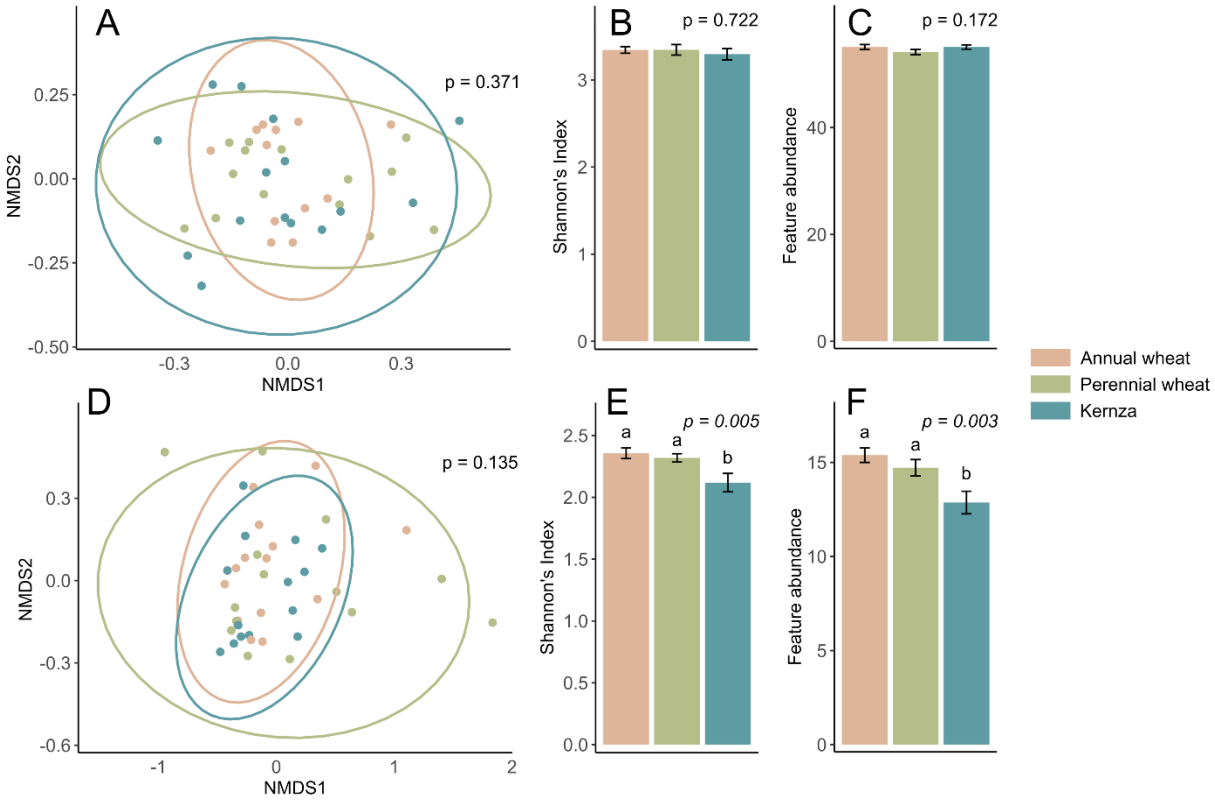

Supplemental Figure 3.2. Root exudate chemical composition and diversity for positive ionization mode (top row) and negative ionization mode (bottom row). (A, D) Chemical composition of the root exudate samples was ordinated using nonmetric multidimensional scaling (NMDS) based on Bray-Curtis dissimilarity index. The *p*-value in panels (A, D) were obtained from permutational multivariate analysis of variance (PERMANOVA) of genotype effect on root exudate composition. Alpha diversity of the root exudate chemistry was evaluated in both evenness (B, E) and richness (C, F; values shown in mean ± SE). (B, C, E, F) The *p*-values for the genotype effect are denoted within each panel and significant values ($p < 0.05$) are italicized. Lower-case letters above the bars in panels (E, F) denote significant ($p < 0.05$) pairwise difference between the genotypes (Tukey's post-hoc).

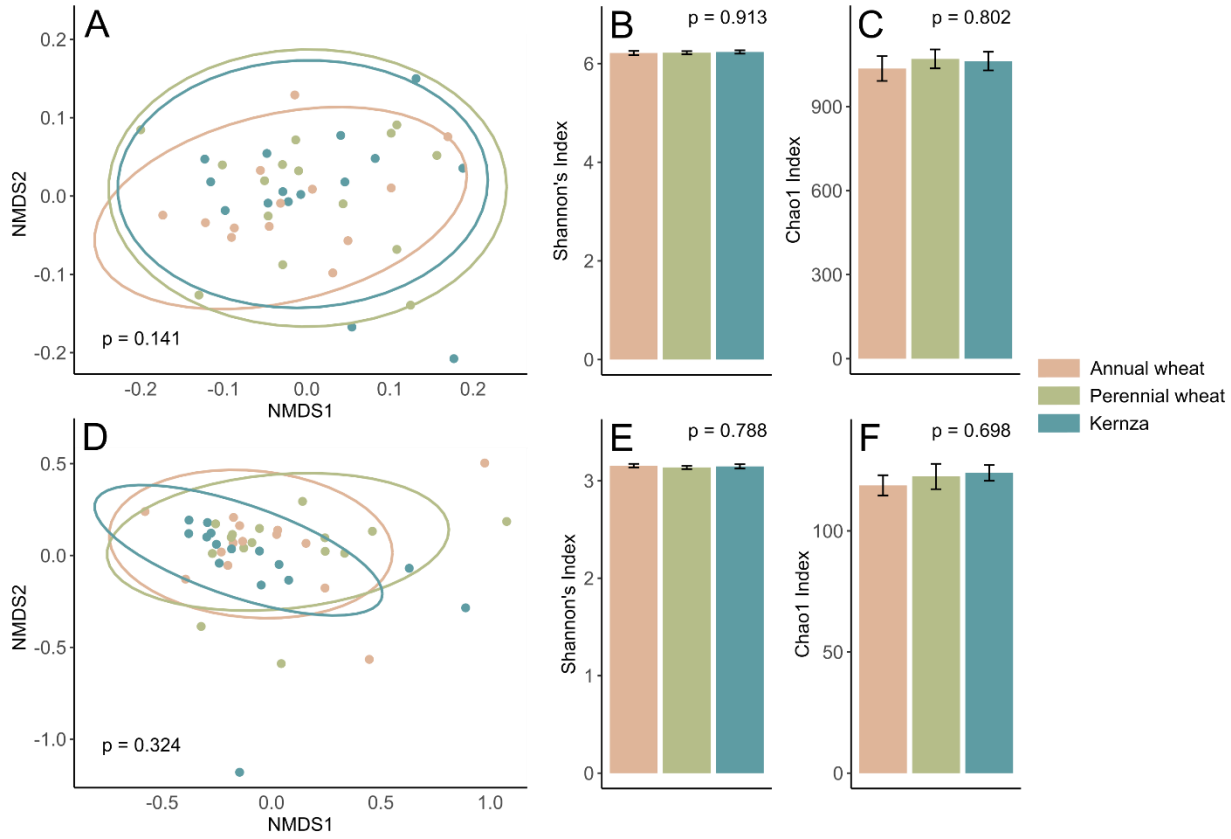

Supplemental Figure 3.3. Rhizosphere bacterial/archaeal (top) and fungal (bottom) composition and diversity. (A, D) Microbial community composition was ordinated using nonmetric multidimensional scaling (NMDS) based on Bray-Curtis dissimilarity index. The *p*-values in panels (A, D) were obtained from permutational multivariate analysis of variance (PERMANOVA) of genotype effect on the microbial community composition. Alpha diversity of the microbial community was evaluated in both evenness (B, E) and richness (C, F; values shown in mean ± SE). (B, D, C, F) The *p*-values for the genotype effect denoted within each panel.

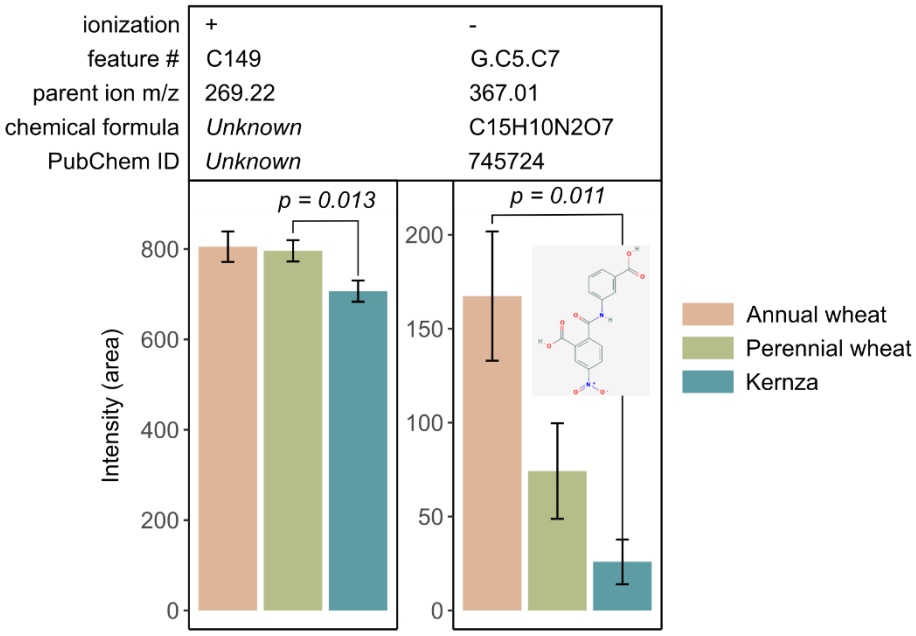

Supplemental Figure 3.4. Mean intensity of the two exudate features that showed significant effect among genotypes (annual wheat, perennial wheat, Kernza; error bars represent the standard error). Only 2-[(3-Carboxyanilino)carbonyl]-5-nitrobenzoic acid (G.C5.C7) had MS2 spectra and compound annotation from SIRIUS. The structure of the compound is inlaid in the right panel. Significant differences ($p < 0.05$) are noted with upside down brackets above the columns, with the corresponding *p*-values. Note that the *p*-values are for pairwise-comparisons only.

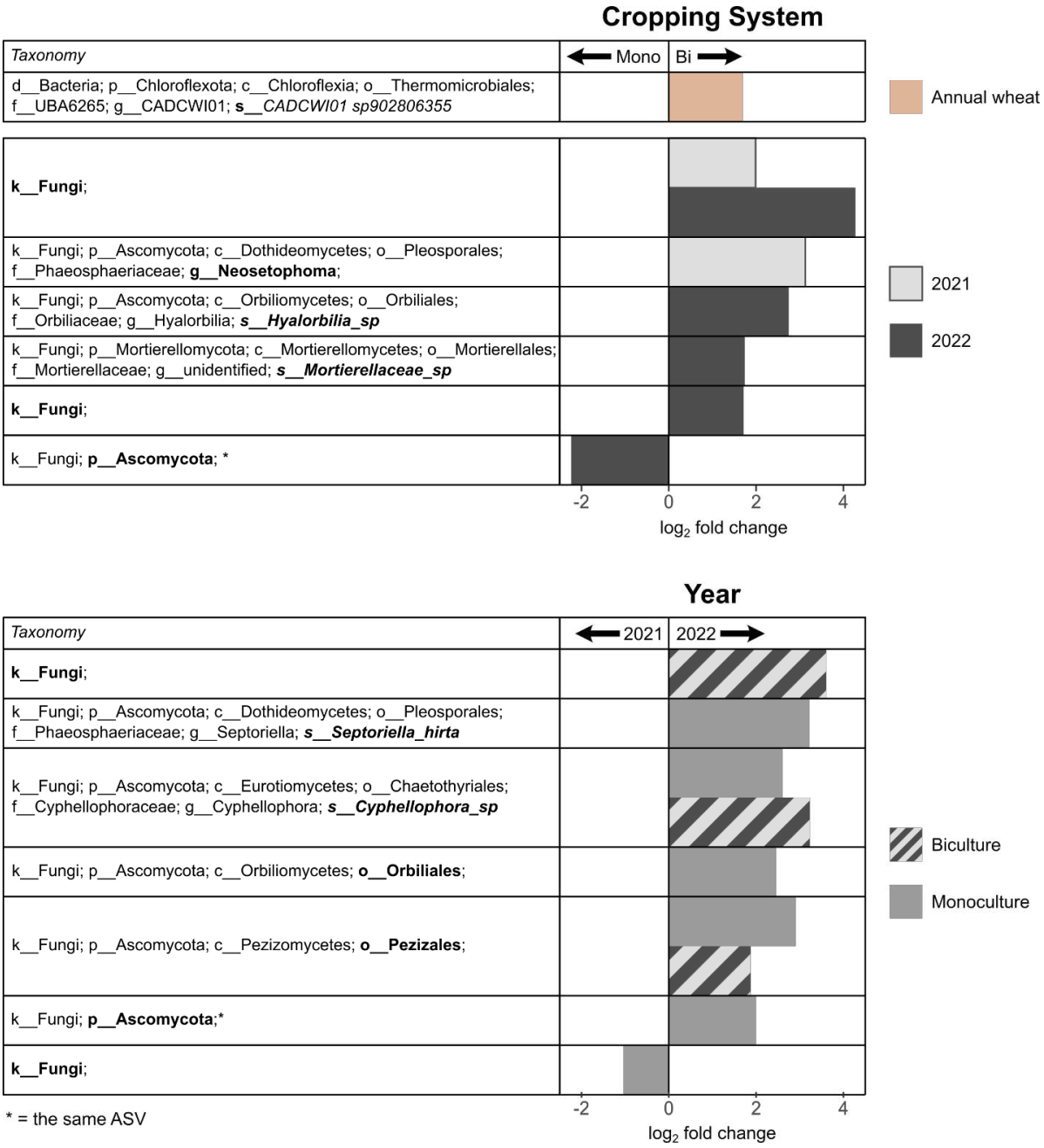

Supplemental Figure 4.1. List of 16S and ITS ASVs and their fold change in cropping systems (monoculture vs biculture) and year (2021 vs 2022) according to Maaslin2 results. Horizontal bars indicate $\log_2$ fold change in the direction of the bars (i.e., if <0 in under "cropping system", greater abundance is found in monoculture than in biculture). Legend accompanying each panel denotes levels of another factor in which this effect is found. In the first column, full taxonomic information is given when applicable. The lowest level of taxonomy with known identity is highlighted in bold. All bars shown were significant at p = 0.05 level.

Supplemental Figure 5.1. Ordination plot (NMDS) showing prokaryote (16S) community composition in rhizospheres of alfalfa in monoculture or in biculture with three crop genotypes (annual wheat, perennial wheat, Kernza). The distances were calculated using the Bray-Curtis Dissimilarity Index. The small box inside the panel indicates p-values for effects obtained with PERMANOVA. G = genotype effect, S = cropping system effect. Note that genotype effect tests only those alfalfa in biculture and cropping system effect compares all biculture alfalfa against the monoculture alfalfa. Those values significant at 0.05 level are highlighted in italics.